

## ***the sonar equations***

The many phenomena and effects peculiar to underwater sound produce a variety of quantitative effects on the design and operation of sonar equipment. These diverse effects can be conveniently and logically grouped together quantitatively in a small number of units called the *sonar parameters*, which, in turn, are related by the *sonar equations*. These equations are the working relationships that tie together the effects of the medium, the target, and the equipment; they are among the design and prediction tools available to the engineer for underwater sound applications.

The sonar equations were first formulated during World War II (1) as the logical basis for calculations of the maximum range of sonar equipments. In recent years, they have seen increasing use in the optimum design of sonars for new applications. Essentially the same relationships are employed in radar (2), though with linear instead of logarithmic units and with slightly different definitions of the parameters.

The essentially simple sonar equations serve two important practical functions. One is the *prediction of performance* of sonar equipments of known or existing design. In this application the design characteristics of the sonar set are known or assumed, and what is desired is an estimate of performance in some meaningful terms such as detection probability or search rate. This is achieved in the sonar equations by a prediction of range through the parameter transmission loss. The equations are solved for transmission loss, which is

then converted to range through some assumption concerning the propagation characteristics of the medium.

The other general application of the equations is in *sonar design*, where a preestablished range is required for the operation of the equipment being designed. In this case the equation is solved for the particular troublesome parameter whose practical realization is likely to cause difficulty. An example would be the directivity required, along with other probable values of sonar parameters, to yield a desired range of detection in a detection sonar or the range of actuation by a passing ship of an acoustic mine mechanism. After the directivity needed to obtain the desired range has been found, the design continues through the "trade-offs" between directivity index and other parameters. The design is finally completed through several computations using the equations and the design engineer's intuition and experience.

## 2.1 Basic Considerations

The equations are founded on a basic equality between the desired and undesired portions of the received signal at the instant when some function of the sonar set is just performed. This function may be detection of an underwater target, or it may be the homing of an acoustic torpedo at the instant when it just begins to acquire its target. These functions all involve the reception of acoustic energy occurring in a natural acoustic background. Of the total acoustic field at the receiver, a portion may be said to be *desired* and is called the *signal*. The remainder of the acoustic field is *undesired* and may be called the *background*. In sonar the background is either *noise*, the essentially steady-state portion not due to one's own echo ranging, or *reverberation*, the slowly decaying portion of the background representing the return of one's own acoustic output by scatterers in the sea. The design engineer's objective is to find means for *increasing* the overall response of the sonar system to the signal and for *decreasing* the response of the system to the background—in other words, to *increase* the signal-to-background ratio.

Let us imagine a sonar system serving a practical purpose such as *detection*, *classification* (determining the nature of a target), *torpedo homing*, *communication*, or *fish finding*. For each of these purposes there will be a certain signal-to-background ratio that will depend on the functions being performed and on the performance level that is desired in terms of percentages of successes and "false alarms," such as an apparent detection of a target when no target is present. If the signal is imagined to be slowly increasing in a constant background, the desired purpose will be accomplished when the *signal level equals the level of the background which just masks it*. That is to say, when the sonar's purpose is just accomplished,

$$\text{Signal level} = \text{background masking level}$$

The term "masking" implies that not all the background interferes with the signal, but only a portion of it—usually that portion lying in the frequency band of the signal. The word "masking" is borrowed from the theory of

audition, where it refers to that part of a broadband noise background that masks out a pure tone or a narrow-band signal presented to a human listener.

We should note that the equality just stated will exist at only *one* instant of time when a target approaches, or recedes from, a sonar receiver. At short ranges, its signal level will exceed the background masking level; at long ranges, the reverse will occur. But the instant of equality is the moment of greatest interest to the sonar engineer or designer, for it is at this instant that the sonar system *just* performs its assigned function. It is this instant to which the engineer or designer will often focus attention in a sonar calculation.

## **2.2 The Active and Passive Equations**

The next step is to expand the basic equality in terms of the *sonar parameters* determined by the *equipment*, the *medium*, and the *target*. We will denote these parameters by two-letter symbols in order to avoid Greek and subscripted symbols as much as possible in the writing of the equations. These parameters are levels in units of decibels relative to the standard reference intensity of a 1- $\mu$ Pa plane wave. They are as follows:

### Parameters Determined by the *Equipment*

Projector Source Level: SL

Self-Noise Level: NL

Receiving Directivity Index: DI

Detection Threshold: DT

### Parameters Determined by the *Medium*

Transmission Loss: TL

Reverberation Level: RL

Ambient-Noise Level: NL

### Parameters Determined by the *Target*

Target Strength: TS

Target Source Level: SL

Two pairs of the parameters are given the same symbol because they are essentially identical. It should be mentioned in passing that this set of parameters is not unique. Others, which could be employed equally well, might be more fundamental or might differ by a constant. For example, sound velocity could be adopted as a parameter, and TS could be replaced by the parameter "backscattering cross section" expressed in decibels, as is done in radar. The chosen parameters are therefore arbitrary; those employed here are the ones conventionally used in underwater sound.\* It should also be noted that they may all be expanded in terms of fundamental quantities like frequency, ship speed, and bearing—a subject that will be of dominant importance in the descriptions of the parameters that will follow. The units of the parameters are decibels, and they are added together in forming the sonar equations.

\* There is, however, no conventional symbolism for many of the parameters.

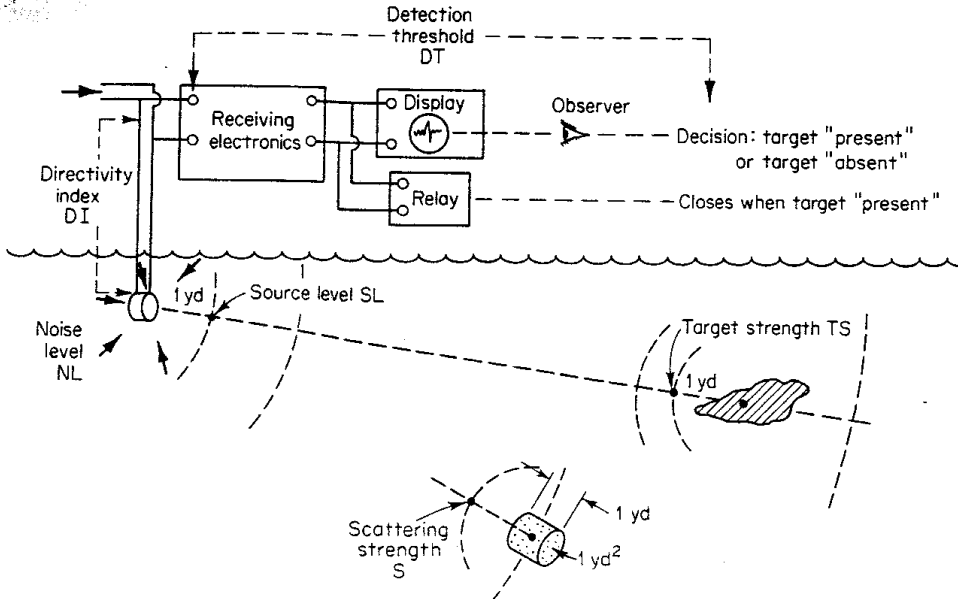


**fig. 2.1** Diagrammatic view of echo ranging, illustrating the sonar parameters.

The meaning of these quantities can best be illustrated through some simple considerations for an active (echo-ranging) sonar (Fig. 2.1). A sound source acting also as a receiver (a *transducer*) produces by some means a *source level* of SL decibels at a unit distance (1 yd) on its axis. When the radiated sound reaches the target (if the axis of the sound source points toward the target), its level will be reduced by the *transmission loss*, and becomes  $SL - TL$ . On reflection or scattering by the target of target strength  $TS$ , the reflected or backscattered level will be  $SL - TL + TS$  at a distance of 1 yd from the acoustic center of the target in the direction back toward the source. In traveling back toward the source, this level is again attenuated by the *transmission loss* and becomes  $SL - 2TL + TS$ . This is the echo level at the transducer. Turning now to the background and assuming it to be isotropic noise rather than reverberation, we find that the *background level* is simply  $NL$ . This level is reduced by the *directivity index* of the transducer acting as a receiver or *hydrophone* so that at the terminals of the transducer the relative noise power is  $NL - DI$ . Since the axis of the transducer is pointing in the direction from which the echo is coming, the relative echo power is unaffected by the transducer directivity. At the transducer terminals, therefore, the echo-to-noise ratio is

$$SL - 2TL + TS - (NL - DI)$$

Let us now assume that the function that this sonar is called upon to perform is *detection*, that is, that its principal purpose is to give an indication of some sort on its *display* whenever an echoing target is present. When the input signal-to-noise ratio is above a certain detection threshold fulfilling certain

probability criteria, a decision will be made by a human observer that a target is *present*\*; when the input signal-to-noise ratio is less than the detection threshold, the decision will be made that the target is *absent*. When the target is *just* being detected, the signal-to-noise ratio *equals* the detection threshold, and we have

$$SL - 2TL + TS - (NL - DI) = DT$$

We have here the active-sonar equation as an equality in terms of the *detection threshold*, called in audition and in much of the older underwater sound literature . In terms of the basic equality described above, we could equally well consider that only that part of the noise power lying above the detection threshold masks the echo, and we would then have

$$SL - 2TL + TS = NL - DI + DT$$

a more convenient arrangement of the parameters, since the echo level occurs on the left-hand side and the noise-masking background level occurs on the right.

This is the active-sonar equation for the *monostatic case* in which the source and receiving hydrophone are coincident and in which the acoustic return of the target is back toward the source. In some sonars, a separated source and receiver are employed and the arrangement is said to be *bistatic*; in this case, the two transmission losses to and from the target are not, in general, the same. Also in some modern sonars, it is not possible to distinguish between DI and DT, and it becomes appropriate to refer to DI - DT as the increase in signal-to-background ratio produced by the entire receiving system of transducer, electronics, display, and observer (if one is used).

A modification is required when the background is reverberation instead of noise. In this case, the parameter DI, defined in terms of an isotropic background, is inappropriate, inasmuch as reverberation is by no means isotropic. For a reverberation background we will replace the terms  $NL - DI$  by an *equivalent plane-wave reverberation level* RL observed at the hydrophone terminals. The active-sonar equation then becomes

$$SL - 2TL + TS = RL + DT$$

where the parameter DT for reverberation has in general a different value than DT for noise.

In the passive case, the target itself produces the signal by which it is detected, and the parameter source level now refers to the level of the radiated noise of the target at the unit distance of 1 yd. Also, the parameter target strength becomes irrelevant, and one-way instead of two-way transmission is involved. With these changes, the *passive-sonar equation* becomes

\* If the human observer is replaced by a relay at the output of the detector, then the detection threshold is the input signal-to-background ratio at the transducer terminals which *just* closes the relay to indicate "target present."

$$SL - TL = NL - DI + DT$$

Table 2.1 is a list of parameters, reference locations, and short definitions in the form of ratios. More complete definitions of the parameters will be given near the beginnings of the chapters dealing with the parameters.

### **2.3 Names for Various Combinations of Parameters**

In practical work it is convenient to have separate names for different combinations of the terms in the equations. Methods exist for measuring some of these on shipboard sonars as a check on system operation. Table 2.2 is a listing of these names and the combination of terms that each represents. Of these, *the figure of merit* is the most useful, because it combines together the various equipment and target parameters so as to yield a quantity significant for the performance of the sonar. Since it equals the transmission loss at the instant when the sonar equation is satisfied, the figure of merit gives an immediate indication of the range at which a sonar can detect its target, or more generally, perform its function. However, when the background is reverberation instead of noise, the figure of merit is not constant, but varies with range and so fails to be a useful indicator of sonar performance.

**table 2.1 The Sonar Parameters, Their Definitions, and Reference Locations**

Parameter symbol	Reference	Definition
Source level	SL      1 yd from source on its acoustic axis	10 log — intensity of source reference intensity*
Transmission loss	TL      1 yd from source and at target or receiver	10 log — signal intensity at 1 yd signal intensity at target or receiver
Target strength	TS      1 yd from acoustic center of target	10 log — echo intensity at 1 yd from target incident intensity
Noise level	NL      At hydrophone location	10 log — noise intensity reference intensity*
Receiving directivity index	DI      At hydrophone terminals	10 log — noise power generated by an equivalent nondirectional hydrophone noise power generated by actual hydrophone
Reverberation level	RL      At hydrophone terminals	10 log — reverberation power at hydrophone terminals power generated by signal of reference intensity*
Detection threshold	DT      At hydrophone terminals	10 log — signal power to just perform a certain function noise power at hydrophone terminals

\* The reference intensity is that of a plane wave of rms pressure 1  $\mu\text{Pa}$ .

**table 2.2 Terminology of Various Combinations of the Sonar Parameters**

Name	Parameters	Remarks
Echo level	$SL - 2TL + TS$	The intensity of the echo as measured in the water at the hydrophone
Noise-masking level	$NL - DI + DT$	Another name for these two combinations is <i>minimum detectable echo level</i>
Reverberation-masking level	$RL + DT$	
Echo excess	$SL - 2TL + TS - (NL - DI + DT)$	Detection just occurs, under the probability conditions implied in the term DT, when the echo excess is zero
Performance figure	$SL - (NL - DI)$	Difference between the source level and the noise level measured at the hydrophone terminals
Figure of merit	$SL - (NL - DI + DT)$	Equals the maximum allowable one-way transmission loss in passive sonars, or the maximum allowable two-way loss for $TS = 0$ dB in active sonars

#### 2.4 The Parameters in Metric Units

Some of the parameters of Table 2.1 have 1 yard as their reference distance. These are SL, TL, TS, and (as a determining quantity for RL) the scattering strength S. If, instead, 1 meter is taken as the reference distance, and it is desired to use metric units in a calculation involving the sonar equations, these quantities should be *decreased* by the amount  $20 \log (1 \text{ meter}/1 \text{ yard}) = 0.78$  dB. In addition, the attenuation coefficient, commonly expressed in English units in decibels per kiloyard, must be multiplied by 1.094 to convert it to decibels per kilometer. No other sonar quantities are affected by a choice of units; nor are the quantities echo level, noise-masking level, and echo excess (defined in Table 2.2). For finding sonar ranges in metric units, it is often more convenient to find the range first in kiloyards, and then to divide by the factor 1.094 to obtain the range in kilometers.

#### 2.5 Echo, Noise, and Reverberation Level as Functions of Range

The sonar equations just written are no more than a statement of an equality between the desired portion of the acoustic field called the *signal*—either an echo or a noise from a target—and an undesired portion, called the *background* of noise or reverberation. This equality, in general, will hold at only one range; at other ranges, one or the other will be the greater, and the equality will no longer exist.

This is illustrated in Fig. 2.2, where curves of echo level, noise-masking level, and reverberation-masking level are shown as a function of range. Both the echo and reverberation fall off with range, whereas the noise remains

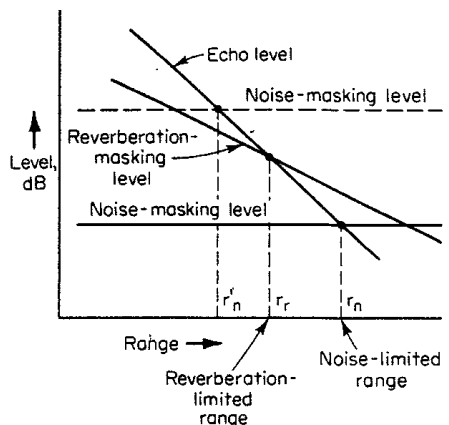


**fig. 2.2** Echo, noise, and reverberation as functions of range.

constant. The echo-level curve will generally fall off more rapidly with range than the reverberation-masking level curve and will intersect it at the *reverberation-limited range*  $r_r$ , given by the sonar equation for reverberation. The curve of echo level will also intersect the noise-masking level at the range of the sonar equation for noise  $r_n$ . If the reverberation is high, the former will be less than the latter, and the range will be said to be *reverberation-limited*. If for any reason the noise-masking level rises to the level shown by the dashed line in the figure, the echoes will then die away into a background of noise rather than reverberation. The new noise-limited range  $r_n'$  will then be less than the reverberation-limited range  $r_n$ , and the range will become *noise-limited*. Both ranges are given by the appropriate form of the sonar equation.

A knowledge of whether a sonar will be noise- or reverberation-limited is necessary for both the sonar predictor and the sonar designer. In general, the curves for echo and reverberation will not be straight lines because of complications in propagation and in the distribution of reverberation-producing scatterers. For a new sonar system, such curves should always be drawn from the best information available for the conditions most likely to be encountered in order to demonstrate visually to the design engineer the behavior of the signals and background with range.

For passive sonars, a convenient graphical way of solving the sonar equations is called SORAP, denoting "sonar overlay range prediction." It consists of two plots that are laid one upon the other (Fig. 2.3). The overlay (solid lines) is a plot of SL versus frequency for a particular passive target or class of targets; the underlay (dashed lines) is a plot of the sum of the parameters TL + NL - DI + DT for a particular passive sonar and for a number of different ranges. The range and frequency at which the target can be detected can be readily read off by inspection. In Fig. 2.3, where the two plots are superposed, the target will be detected first at a range of 10 miles by means of the line component at frequency  $f_1$ . However, if the criterion is adopted that *three* spectral lines must appear on the display, whatever it may be, before a detec-

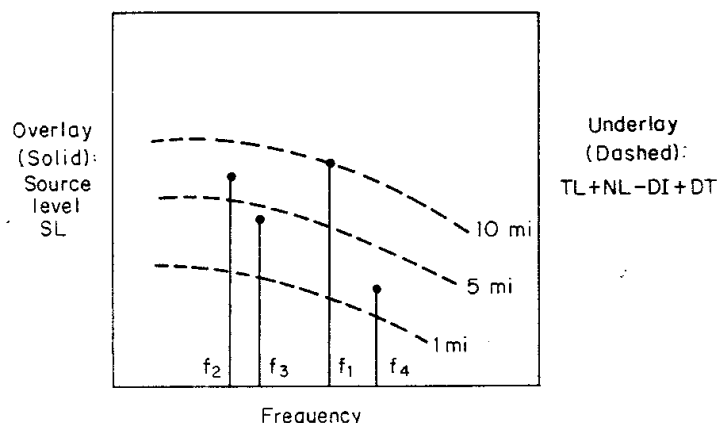


**fig. 2.3** SORAP: a graphical way to solve the passive sonar equation.

tion is called, the range would be reduced to 4 miles, and the display would show the lines at frequencies  $f_1, f_2$ , and  $f_3$ . The method is particularly useful for separating the target parameter SL from the equipment parameters and medium parameters at the location where it is used, while at the same time accommodating a wide range of frequencies. Thus, targets can be compared for the same equipment and locations, or, alternatively, locations can be compared for the same target, and so forth.

## 2.6 Transient Form of the Sonar Equations

The equations thus far have been written in terms of *intensity*, or the average acoustic power per unit area of the sound emitted by the source or received from the target. The word "average" implies a time interval over which the average is to be taken. This time interval causes uncertain results whenever short transient sources exist or, generally, whenever severe distortion is introduced by propagation in the medium or by scattering from the target.

A more general approach is to write the equations in terms of *energy flux density*, defined as the acoustic energy per unit area of wavefront (see Sec. 1.5). If a plane acoustic wave has a time-varying pressure  $p(t)$ , then the energy flux density of the wave is

$$E = \frac{1}{\rho c} \int_0^{\infty} p^2(t) dt$$

If the units of pressure are dynes per square centimeter and the acoustic impedance of the medium is in cgs units (for water,  $\rho c \approx 1.5 \times 10^5$ ), then  $E$  will be expressed in ergs per square centimeter. The intensity is the mean-square pressure of the wave divided by  $\rho c$  and averaged over an integral of time  $T$ , or

$$I = \frac{1}{T} \int_0^T \frac{p^2(t)}{\rho c} dt$$

so that over the time interval  $T$ ,

$$I = \frac{E}{T}$$

The quantity  $T$  is accordingly the time interval over which the energy flux density of an acoustic wave is to be averaged to form the intensity. For long-pulse active sonars, this time interval is the duration of the emitted pulse and is very nearly equal to the duration of the echo. For short transient sonars, however, the interval  $T$  is often ambiguous, and the duration of the echo is vastly different from the duration of the transient emitted from the source. Under these conditions, however, it can be shown (3) that the intensity form of the sonar equations can be used, provided that the source level is defined as

$$SL = 10 \log E - 10 \log \tau_e$$

where  $E$  is the energy flux density of the source at 1 yd and is measured in units of the energy flux density of a 1- $\mu$ Pa plane wave taken over an interval of 1 second, and  $\tau_e$  is the duration of the echo in seconds for an active sonar. For explosives,  $E$  is established by measurements for a given charge weight, depth, and type of explosive (Sec. 4.4). For pulsed sonars emitting a flat-topped pulse of constant source level  $SL'$  over a time interval  $\tau_0$ , then, since the energy density of a pulse is the product of the average intensity times its duration,

$$10 \log E = SL' + 10 \log \tau_0$$

By combining the last two equations, the effective source level  $SL$  for use in the sonar equations is therefore

$$SL = SL' + 10 \log \frac{\tau_0}{\tau_e}$$

Here  $\tau_0$  is the duration of the emitted pulse of source level  $SL'$ , and  $\tau_e$  is the echo duration. For long-pulse sonars,  $\tau_0 = \tau_e$  and  $SL = SL'$ . For short-pulse sonars,  $\tau_e > \tau_0$ , and the effective source level  $SL$  is less than  $SL'$  by the amount  $10 \log (\tau_0/\tau_e)$ . The effect of time stretching on source level may be visualized as shown in Fig. 2.4. A short pulse of duration  $\tau_0$  and source level  $SL'$  is replaced in a sonar calculation by an effective or equivalent pulse of longer duration  $\tau_e$  and lower source level  $SL$ . The two source levels are related so as to keep the energy flux-density source levels the same, namely:

$$SL + 10 \log \tau_e = SL' + 10 \log \tau_0$$

or

$$SL = SL' + 10 \log \frac{\tau_0}{\tau_e}$$

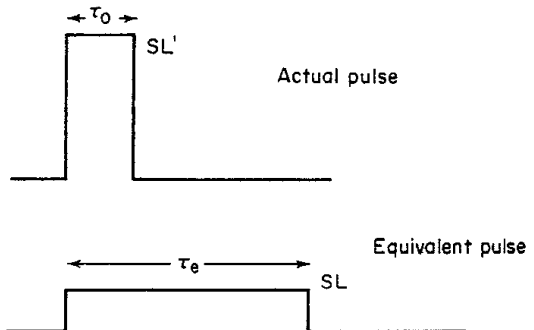


**fig. 2.4** Equivalent source level in short-pulse sonars.

In effect, the pulse emitted by the source is stretched out in time and thereby reduced in level by the multipath effects of propagation and by the processes of target reflection. The appropriate values of other sonar parameters in the equations, such as TS and TL, are those applying for long-pulse or CW conditions, in which the effects of multipaths in the medium and on the target are added up and accounted for.

For active short-pulse sonars, the echo duration  $\tau_e$  is, accordingly, a parameter in its own right. Figure 2.5 illustrates a pulse as a short exponential tran-

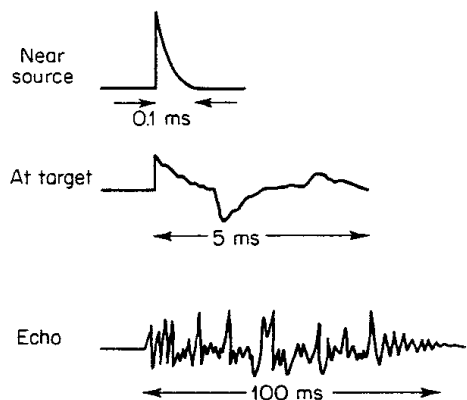


**fig. 2.5** Diagrams of the pressure of an explosive pulse near the source, on arrival at an extended target, and as an echo back in the vicinity of the source.

sient at the source, as a distorted pulse at the target, and as an echo received back in the vicinity of the source. An exponential pulse, similar in form to the shock wave from an explosion of about 1 lb of TNT and having an initial duration of 0.1 ms, becomes distorted into an echo 1,000 times as long. Two actual examples of explosive echoes are shown in Fig. 2.6.

The echo duration can be conceived as consisting of three components:  $\tau_0$ , the duration of the emitted pulse measured near the source;  $\tau_m$ , the additional duration imposed by the two-way propagation in the sea; and  $\tau_t$ , the additional duration imposed by the extension in range of the target. In this view, the echo duration is the sum of the three components, or

$$\tau_e = \tau_0 + \tau_t + \tau_m$$

Typical examples of the magnitude of these three components of the echo duration under different conditions are given in Table 2.3. Thus, with these

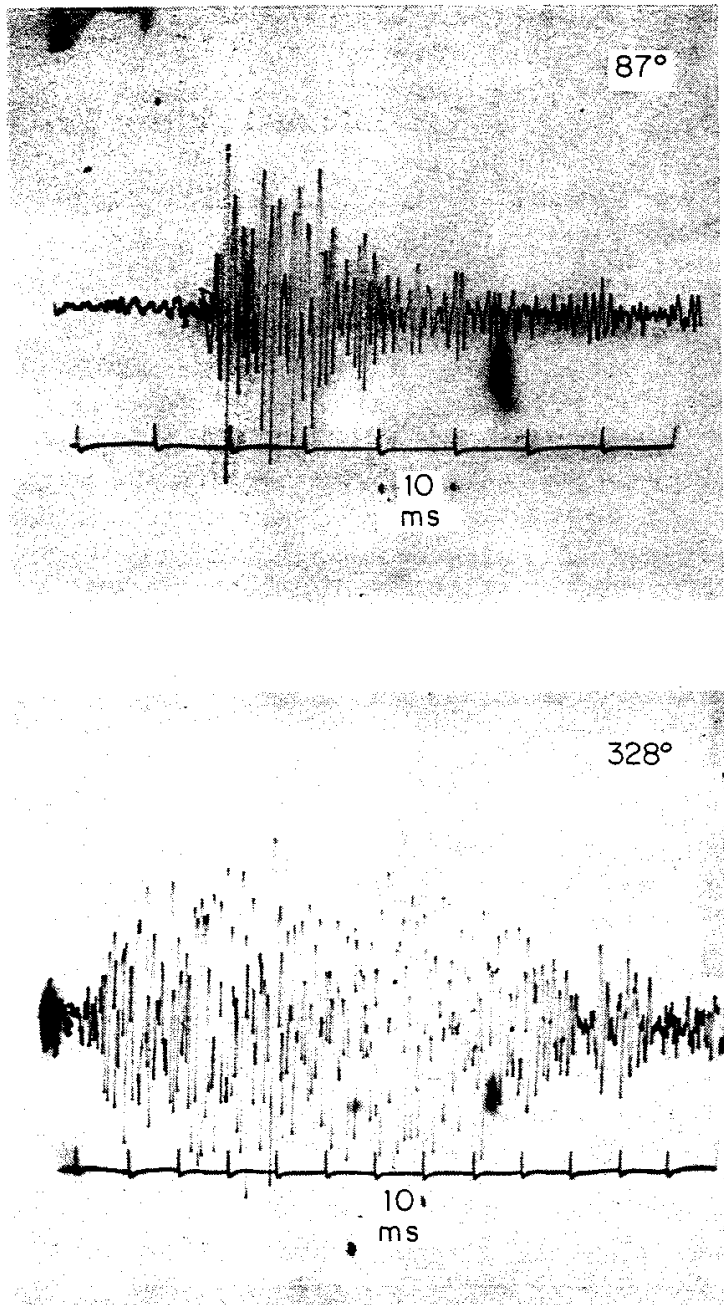


**fig. 2.6** Oscilloscope photographs of explosive echoes from a submarine at aspect angles  $87^\circ$  (near-beam aspect) and  $328^\circ$  (near-bow aspect). The time ticks are 10 ms apart.

**table 2.3 Components of Echo Duration**

Component	Typical values, ms
Duration of the emitted pulse at short ranges	Explosives: 0.1 Sonar: 100
Duration produced by multiple paths	Deep water: 1 Shallow water: 100
Duration produced by a submarine target	Beam aspect: 10 Bow-stern aspect: 100

values, the time duration of an explosive echo from a bow-stern aspect submarine in shallow water would be  $0.1 + 100 + 100 = 200.1$  ms.

### **2.7 Statement of the Equations**

A condensed statement of the equations is as follows.

Active sonars (monostatic):

Noise background

$$SL - 2TL + TS = NL - DI + DT$$

Reverberation background

$$SL - 2TL + TS = RL + DT_R$$

Passive sonars:

$$SL - TL = NL - DI + DT_N$$

where DT has been subscripted to make it clear that this parameter is quantitatively different for noise and for reverberation.

### **2.8 Limitations of the Sonar Equations**

The sonar equations written in terms of intensities are not always complete for some types of sonars. We have already seen how short-pulse sonars require the addition of another term, the echo duration, to account for the time-stretching produced by multipath propagation. Another such addition is a *correlation loss* in correlation sonars to account for the decorrelation of the signal relative to a stored replica; such decorrelation occurs on bottom reflection and scattering in bottom-bounce sonars. Other terms may be conceivably required for other sophisticated sonars whose operation does not depend on intensity alone.

A limitation of another kind is produced by the nature of the medium in which sonars operate. The sea is a moving medium containing inhomogeneities of various kinds, together with irregular boundaries, one of which is in motion. Multipath propagation is the rule. As a result, many of the sonar parameters fluctuate irregularly with time, while others change because of unknown changes in the equipment and the platform on which it is mounted. Because of these fluctuations, a "solution" of the sonar equations is no more than a best-guess time average of what is to be expected in a basically stochastic problem.

Precise calculations, to tenths of decibels, are futile; a predicted sonar range is an average quantity about which the observed values of range are likely to congregate. We can hope that as our knowledge of underwater sound and its fluctuations improves, the accuracy of the predictions of the sonar equations can be expected to increase.

**reflection and  
scattering by  
sonar targets:  
target  
strength**

This chapter is concerned with the subject of *catacoustics*. According to Webster's "New International Dictionary of the English Language," 2d edition, the word "catacoustics" is defined as "that part of acoustics which treats of reflected sounds or echoes."

In active sonar the parameter *target strength* refers to the echo returned by an underwater target. Such targets may be objects of military interest, such as submarines and mines, or they may be schools of fish sought by fish-finding sonars. Excluded from the category of "targets" are inhomogeneities in the sea of indefinite extent, such as scattering layers and the ocean surface and bottom, which, because of their indefinite size, return sound in the form of *reverberation* instead of as *echoes*.

In the context of the sonar equations, target strength is defined as 10 times the logarithm to the base 10 of the ratio of the intensity of the sound returned by the target, at a distance of 1 yd from its "acoustic center" in some direction, to the incident intensity from a distant source. In symbols,

$$TS = 10 \log \left. \frac{I_r}{I_i} \right|_{r=1}$$

where  $I_r$  = intensity of return at 1 yd

$I_i$  = incident intensity

Pictorially this is shown in Fig. 9.1, where  $P$  is the point at which  $I_r$  is imagined to be measured and  $C$  is the acoustic center of the target. This fictitious point,

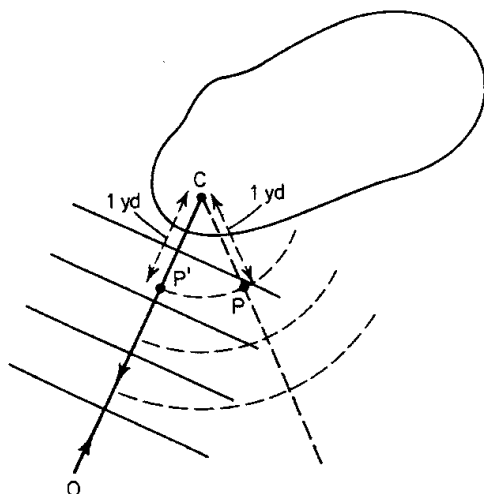


**Fig. 9.1** Geometry of target strength. A plane wave is incident on the target in the direction  $OC$ . Target strength refers to the points  $P$  and  $P'$  1 yd from the acoustic center  $C$ .

inside or outside of the target itself, is the point from which the returned sound appears to originate on the basis of measurements made at a distance. In "monostatic" sonars, having the same, or closely adjacent source and receiver, the point  $P$  lies in the direction back toward the source of sound. In "bistatic" sonars,  $P$  can lie in any direction relative to the target, and target strength then becomes a function of both the incident direction and the direction of the receiver, both relative to some axis of symmetry of the target. Because most sonars are "monostatic," we will restrict most of our discussion to "back reflection" and "backscattering," in which the reference point lies at  $P'$  back in the direction of the incident sound.

Target strength measurements are always at a long range—that is, in the "far field" (Fig. 4.2)—where the target reradiates as a point source of sound. This virtual point source is the acoustic center  $C$ .

Special mention should be made of the use of 1 yd as the reference distance for target strength. This arbitrary reference often causes many underwater objects to have *positive* values of target strength. Such positive values should not be interpreted as meaning that more sound is coming back from the target than is incident upon it; rather, they should be regarded as a consequence of the arbitrary reference distance. If, instead of 1 yd, 1 kyd was used, all customary targets would have a negative target strength. In metric units of length, where 1 meter is the reference distance instead of 1 yd, all target-strength values are *lower* by the amount  $20 \log 1.0936$  or 0.78 dB; in other words, when a 1-meter reference distance is used, all target-strength values referred to 1 yd must be *reduced* by 0.78 dB.

The meaning of target strength can be shown by computing the target strength of a sphere, large compared to a wavelength, on the assumption that the sphere is an isotropic reflector; that is, it distributes its echo equally in all directions. Let a large, perfect, rigid sphere (Fig. 9.2) be insonified by a plane

wave of sound of intensity  $I_i$ . If the sphere is of radius  $a$ , the power intercepted by it from the incident wave will be  $\pi a^2 I_i$ . On the assumption that the sphere reflects this power uniformly in all directions, the intensity of the reflected wave at a distance  $r$  yards from the sphere will be the ratio of this power to the area of a sphere of radius  $r$ , or

$$I_r = \frac{\pi a^2 I_i}{4\pi r^2} = I_i \frac{a^2}{4r^2}$$

where  $I_r$  is the intensity of the reflection at range  $r$ . At the reference distance of 1 yd, the ratio of the reflected intensity  $I_r$  to the incident intensity is

$$\left. \frac{I_r}{I_i} \right|_{r=1} = \frac{a^2}{4}$$

and the target strength of the sphere becomes

$$TS = 10 \log \left. \frac{I_r}{I_i} \right|_{r=1} = 10 \log \frac{a^2}{4}$$

It is therefore evident that an ideal sphere of radius 2 yd ( $a = 2$ ) has a target strength of 0 dB. In practical work, spheres make good reference targets for sonar when they can be used, because their target strengths are relatively independent of orientation.

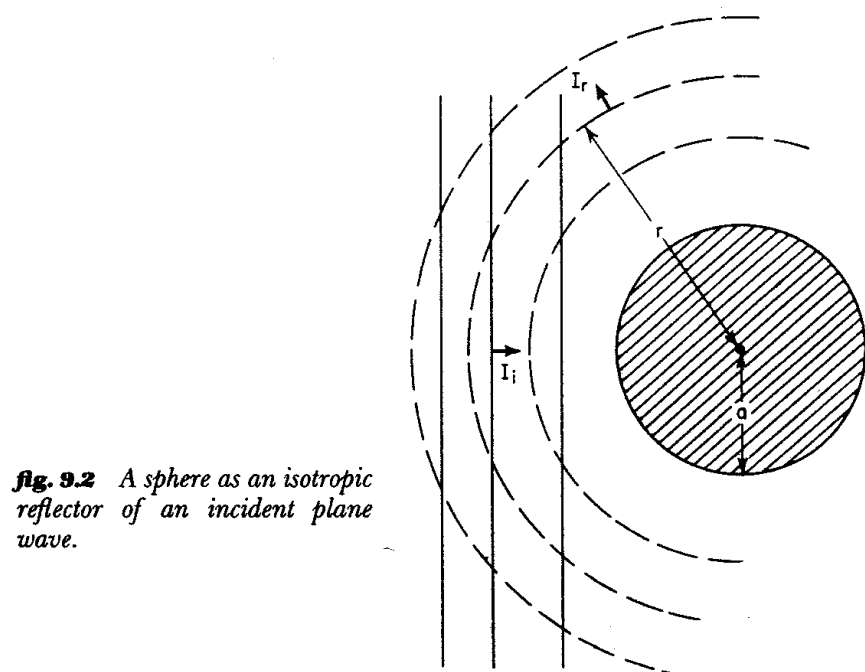


**fig. 9.2** A sphere as an isotropic reflector of an incident plane wave.

### 9.1 The Echo as the Sum of Backscattered Contributions

For radar it was shown by Kerr (1) that the backscattering cross section of a radar target in integral form is

$$\sigma = \frac{4\pi}{\lambda^2} \left| \int_{\alpha}^{\beta} \frac{dA}{dz} e^{2ikz} dz \right|^2$$

where  $\sigma$  = ratio of scattered power to incident intensity

$dA/dz$  = rate of change of cross-sectional area of body in direction of propagation  $z$

$k$  = wave number  $2\pi/\lambda$

$\lambda$  = incident wavelength

$z = \alpha, z = \beta$  are the range limits of the target

The return of an incident plane wave from the target can therefore be regarded as the sum of many wavelets, each originating at the changes in cross-sectional area of the target and added with respect to phase. The application of this expression to sonar is restricted to targets that are large, rigid, and immovable in the sound field, that is, to large targets that do not deform or move under the impact of the incident sound wave.

A thorough application of this approach to the backscattering of underwater sound targets has been made by Freedman (2). In his notation

$$TS = 10 \log |J|^2$$

where

$$J = \frac{1}{\lambda} \sum_{g=1} e^{-2ik(r_g - r_1)} \sum_{n=0}^{\infty} \frac{D_g^n(A)}{(2ik)^n}$$

and where the symbol  $D_g^n(A)$  denotes the magnitude of the discontinuity of the  $n$ th derivative of the cross-sectional area of the object at range  $r_g$ , and  $r_1$  is the range of the closest point of the target. The target-strength factor  $J$  is thus proportional to the sum of all the discontinuities of the derivatives of the cross-sectional area  $A$  of the object, measured at some range  $r_g - r_1$  from the point nearest the source, weighted by the factor  $1/(2ik)^n$ , and then summed over all points of the object after allowance for phase by means of the factor  $e^{-2ik(r_g - r_1)}$ . Freedman also showed experimentally that echo envelopes can be predicted from the various contributions of the derivatives of the cross-sectional-area function occurring at times corresponding to the location of the cross sections along the object in the direction of propagation. A summation method for finding the reflection from irregular bodies has also been the subject of a paper by Neubauer (3).

Figure 9.3, taken from Freedman's work, shows the wave theory echo from a sphere, where each discontinuity in the derivatives give rise to a component of the echo. Wave theory yields a diffracted echo from the edge of the geometrical shadow in addition to the echo from the front of the sphere.

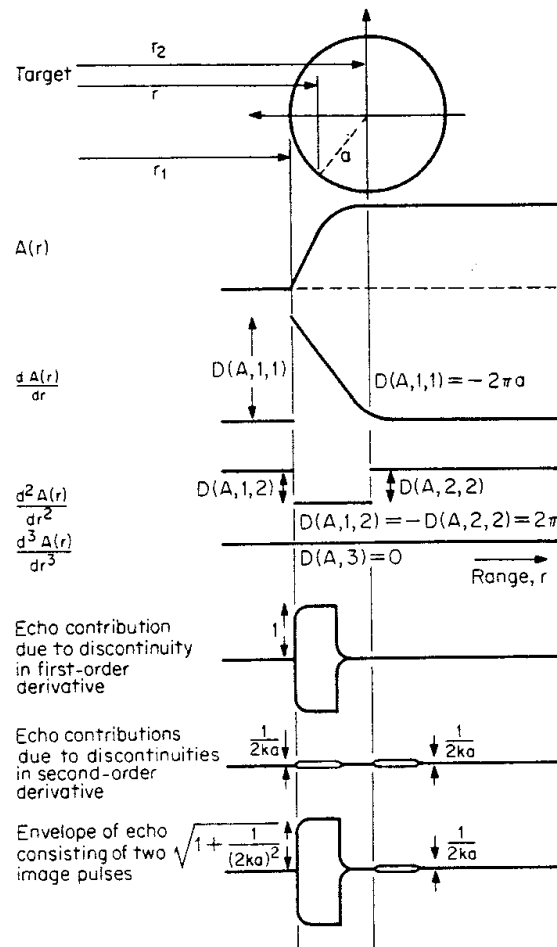


**fig. 9.3** Wave theory origin of the echo from a sphere. The echo is made up of contributions from the discontinuities in the derivatives of the cross-sectional area of the sphere. The theory applies only to objects that are smooth, large compared to  $\lambda$ , immovable, nondeformable, and impenetrable to sound. (Ref. 2.)

## 9.2 Geometry of Specular Reflection

For objects of radii of curvature large compared to a wavelength, the echo originates principally by *specular reflection*, in which those portions of the target in the neighborhood of the point at which sound is normally incident give rise to a coherent reflected echo. One way to find the magnitude of the specular reflection is to construct Fresnel, or quarter-wave zones, on the surface of the body and to add their contributions, as has been done for underwater targets by Steinberger (4). A heuristic intuitive approach is to consider target strength as a measure of the spreading of an incident plane wave induced by specular reflection from a curved surface. If the power or energy-density contained within a small area  $A_i$  of the incident sound beam is spread, on reflection, over the area  $A_r$  at unit distance, then the target strength is  $10 \log (A_i/A_r)$ . These areas can be determined by drawing rays. This geometric view of specular reflection will be illustrated by computing the target strength of a sphere and a general convex surface, both satisfying the requirement of large radii of curvature compared to a wavelength.

Figure 9.4 shows a perfect, large rigid sphere with a plane sound wave incident from the left. Adjacent incident rays intersect along the curve  $OQO'$ ,

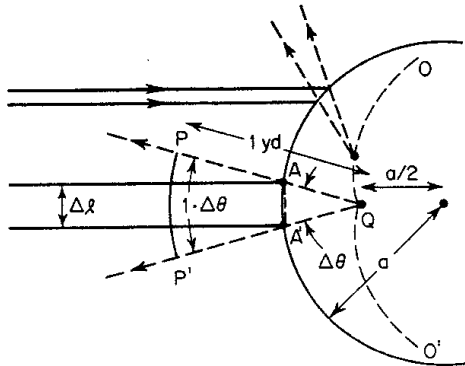


**fig. 9.4** Target strength of a sphere. The acoustic energy contained in the pencil of diameter  $\Delta l$  is spread on reflection over a portion  $PP'$  of a 1-yd sphere.

having a cusp at  $Q$  halfway from the surface to the center of the sphere. This *caustic* is the locus of the acoustic centers of the adjacent intersecting rays. Consider a small cylindrical bundle of parallel rays normally incident upon the sphere at  $AA'$  and of cross section  $\Delta l$ . If the intensity of the incident wave is  $I_i$ , the power contained in the bundle is  $I_i \pi (\Delta l)^2 / 4$ . This power will, in effect, be reradiated within an angle  $\Delta\theta$  from the acoustic center  $Q$  for these rays. At unit distance from  $Q$ , this power is distributed over a portion of a sphere  $PP'$  of area  $\pi (\Delta\theta \times 1)^2 / 4$  if  $\Delta\theta$  is small, and the intensity there becomes

$$I_r = \frac{I_i \pi (\Delta l)^2 / 4}{\pi (\Delta\theta \times 1)^2 / 4} = I_i \left( \frac{\Delta l}{\Delta\theta} \right)^2$$

But, referring to the triangle  $AQA'$ , it will be seen that

$$AA' = \Delta l = \frac{a}{2} \Delta\theta$$

for small  $\Delta\theta$ . Hence  $\Delta l/\Delta\theta = a/2$  and

$$TS = 10 \log \left. \frac{I_r}{I_i} \right|_{r=1} = 10 \log \frac{a^2}{4}$$

This is the same as before, and indicates that a large sphere reflects the incident plane wave in the backward direction *as though* it were a uniform, or isotropic, reflector of sound. For this simple expression to hold strictly, distances must be reckoned from the acoustic center of the sphere located halfway from the surface to the center. For practical purposes in sonar, where ranges much greater than the radius of the sphere are involved, the exact location of the acoustic center is not usually significant. It should be observed that we have considered a sphere that is (1) *perfect* in shape, without irregularities, depressions, or protuberances, (2) *rigid*, or nondeformable by the impinging sound beam, (3) *immovable*, or does not partake of the acoustic motion of the field in which it is embedded, and (4) *large* compared to a wavelength ( $2\pi a/\lambda \gg 1$ ).

This same method can be extended to the reflection at normal incidence from any convex surface having all radii of curvature large compared to a

wavelength. This requirement carries with it the absence of protuberances, corners, and angles, all of which involve small radii of curvature and which serve as scatterers instead of reflectors of sound. Such a large, smooth, convex object is shown in Fig. 9.5a, with sound normally incident at point  $P$  along the line  $OP$ . Imagine a series of planes through  $OP$  intersecting the object. Two of them lie at right angles to each other and intersect the object in the *principal normal sections* having a maximum and a minimum radius of curvature. Figure 9.5b is a plan view at  $P$  in which the principal normal sections are  $AA'$  and  $BB'$ ; Fig. 9.5c is a cross section through  $AA'$  in which  $R_1$  is the radius of curvature,  $O$  the center of curvature, and  $Q$  the acoustic center located half-way from  $O$  to  $P$ . Consider a small rectangular segment of the surface having one corner located at  $P$ , and of infinitesimal lengths  $dl_1$  and  $dl_2$  on each side.

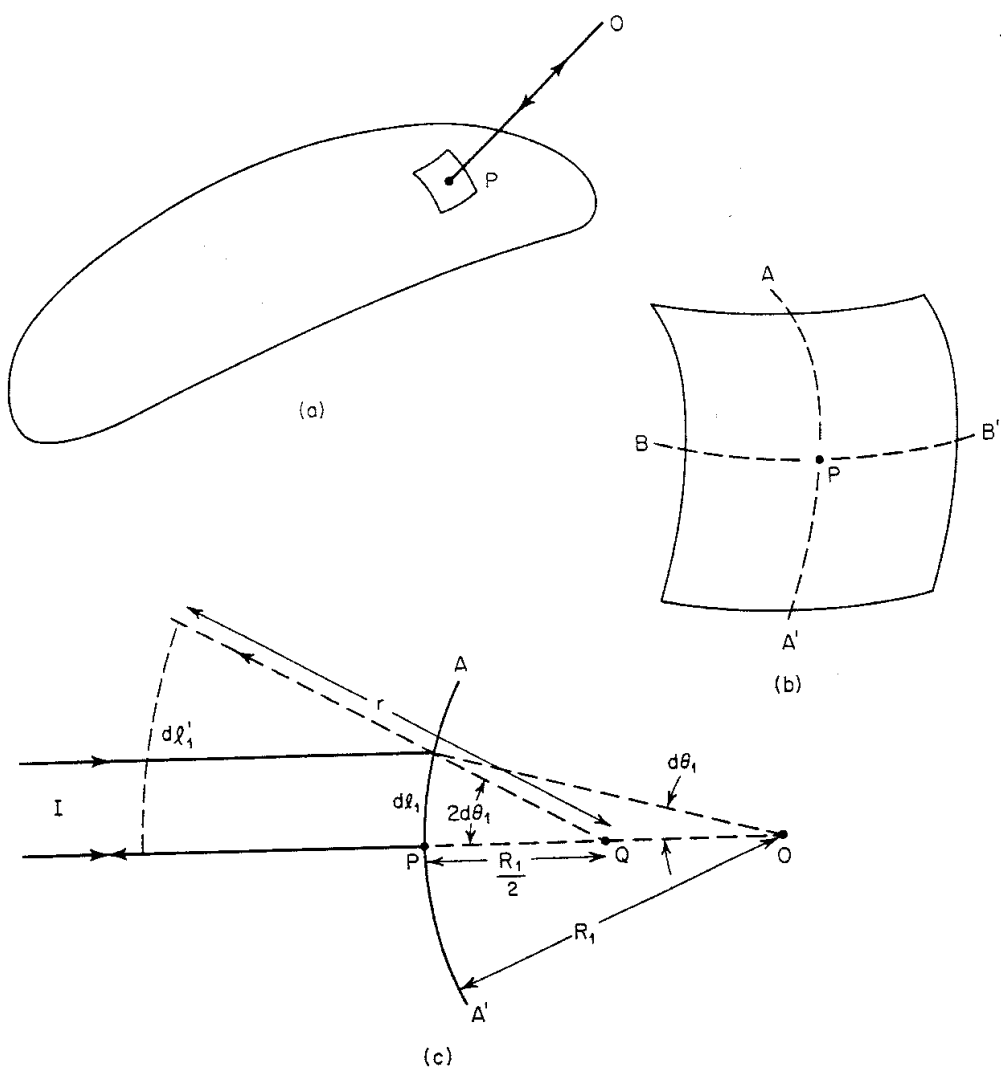


**Fig. 9.5** Target strength of a convex target of large radius of curvature: (a) A target with sound normally incident along  $OP$ . (b) Plan view of the vicinity of  $P$  with  $AA'$  and  $BB'$  in the principal normal sections. (c) Cross section through  $AA'$  of radius of curvature  $R_1$ .

If a plane wave of intensity  $I_i$  is incident on the surface, the power  $dP$  intercepted by the segment will be

$$dP = I_i dl_1 dl_2$$

But from the cross section of Fig. 9.5c, it is apparent that

$$dl_1 = R_1 d\theta_1$$

and similarly in the perpendicular plane containing  $BB'$  we would have

$$dl_2 = R_2 d\theta_2$$

so that the power intercepted will be

$$dP = I_i R_1 R_2 d\theta_1 d\theta_2$$

On reflection from the sphere, this power is distributed, at range  $r$  from the acoustic center  $C$ , over an area

$$dA = dl'_1 dl'_2 = 2r d\theta_1 2r d\theta_2$$

Hence the intensity at  $r$  will be

$$I_r = \frac{dP}{dA} = \frac{I_i R_1 R_2}{4r^2}$$

and the target strength will be

$$TS \equiv 10 \log \left. \frac{I_r}{I_i} \right|_{r=1} = 10 \log \frac{R_1 R_2}{4}$$

### **9.3 Target Strength of a Small Sphere**

We consider now the target strength of a small sphere, in which the return of sound back toward the source is a process of scattering instead of reflection.

The theory of sound scattering by a small, fixed, rigid sphere was first worked out by Rayleigh (5). By *small* is meant a sphere whose ratio of circumference to wavelength is much less than unity ( $ka = 2\pi a/\lambda \ll 1$ ); by *fixed*, a sphere that does not partake of the acoustic motion of particles of the fluid in which the sphere is embedded; by *rigid*, a sphere that is nondeformable by the incident acoustic waves and into which the sound field does not penetrate. Under these conditions, Rayleigh showed that the ratio of the scattered intensity  $I_r$  at a large distance  $r$  to the intensity  $I_i$  of the incident phase wave is

$$\frac{I_r}{I_i} = \frac{\pi^2 T^2}{r^2 \lambda^4} \left( 1 + \frac{3}{2} \mu \right)^2$$

where  $T$  = volume of sphere ( $\frac{4}{3}\pi a^3$ )

$\lambda$  = wavelength

$\mu$  = cosine of angle between scattering direction and reverse direction of incident wave

For backscattering  $\mu = +1$ . On reducing to  $r = 1$  and on taking 10 times the logarithm, we obtain

$$TS \equiv 10 \log \left| \frac{I_r}{I_i} \right|_{r=1} = 10 \log \frac{\pi^2 T^2}{\lambda^4} \left( \frac{5}{2} \right)^2 = 10 \log \left[ (1,082) \frac{a^6}{\lambda^4} \right]$$

where  $a$  and  $\lambda$  are in units of yards. Thus, the target strength of a small sphere varies as the sixth power of the radius and inversely as the fourth power of the wavelength.

If we define the backscattering cross section of the sphere as

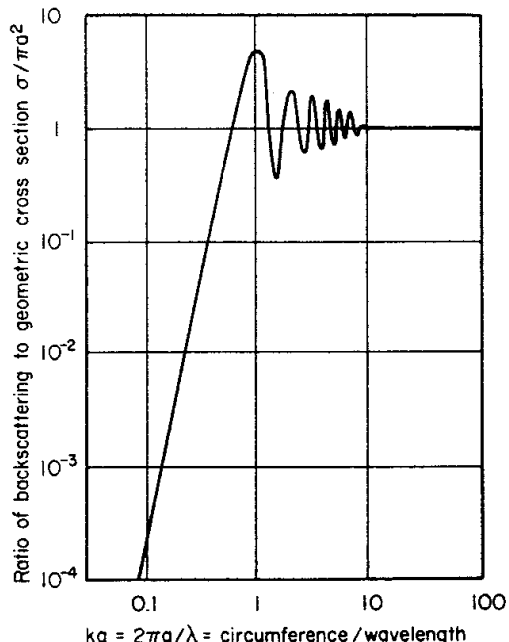
$$\sigma \equiv 4\pi \left| \frac{I_r}{I_i} \right|_{r=1}$$

the ratio of backscattering cross section to geometric cross section becomes

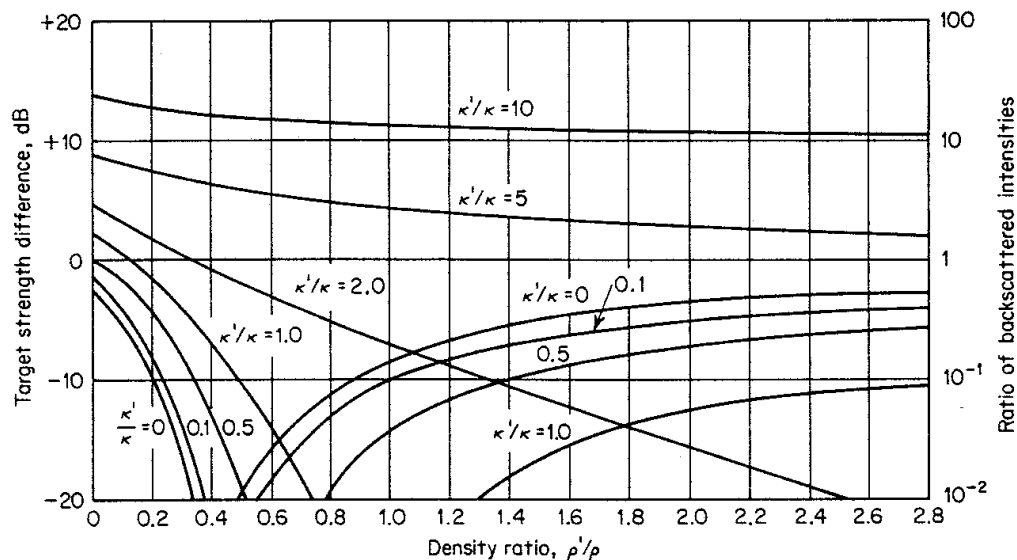
$$\frac{\sigma}{\pi a^2} = 2.8(ka)^4$$

Figure 9.6 is a plot of this normalized ratio against the nondimensional quantity  $ka = 2\pi a/\lambda$ . It is seen that this quantity varies as the fourth power of  $ka$ , or as the fourth power of the frequency, for  $ka$  less than about 0.5, and is unity for  $ka$  greater than 5.0. Oscillations occur in the intermediate region ( $ka \approx 1$ ).

Rayleigh also dealt with the scattering by small spheres, not fixed and rigid, but possessing a compressibility  $\kappa'$  and a density  $\rho'$  in a fluid of compressibility  $\kappa$  and density  $\rho$ . Fixed, rigid spheres are incompressible ( $\kappa'/\kappa \ll 1$ ) and very dense ( $\rho'/\rho \gg 1$ ) compared to the surrounding fluid; spheres having bulk moduli and densities comparable with those of the fluid oscillate to and fro in



**fig. 9.6** Ratio of acoustic to geometric cross sections of a fixed rigid sphere. The oscillations in the range  $1 < ka < 10$  are due to interference by the creeping wave. For small  $ka$  (low frequencies) the ratio varies as the fourth power of  $ka$ ; for large  $ka$  the ratio is unity.



**fig. 9.7** Corrections to the target strength of a fixed rigid sphere for compressibility and density. The sphere is of compressibility ratio  $\kappa'/\kappa$  and density ratio  $\rho'/\rho$  relative to the surrounding fluid.

the incident sound field. They also pulsate, or change their volume, in the compressions and rarefactions of the incident wave. These motions of the sphere modify the scattered wave. Rayleigh showed (6) that the term  $(1 + \frac{3}{2}\mu)^2$  in the expression for the ratio of intensities for a fixed, rigid sphere becomes

$$\left[ 1 - \frac{\kappa'}{\kappa} + \frac{3(\rho'/\rho - 1)}{1 + 2\rho'/\rho} \mu \right]^2$$

in terms of the ratios of compressibility  $\kappa'/\kappa$  and density  $\rho'/\rho$ . Figure 9.7 is a plot of the quantity

$$10 \log \left[ 1 - \frac{\kappa'}{\kappa} + \frac{3(\rho'/\rho - 1)}{1 + 2\rho'/\rho} \mu \right]^2 / \left( 1 + \frac{3}{2} \mu \right)^2$$

This is the “correction” for compressibility and density to be applied to the target strength of a fixed, rigid sphere. This correction is seen from Fig. 9.7 to be large in most instances. For a sand grain in water, for example, for which  $\rho'/\rho = 2.6$  and  $\kappa'/\kappa \approx 0.1$ , the target strength is seen to be 4 dB less than for the classic Rayleigh case of a fixed, rigid sphere. On the other hand, highly compressible spheres such as gas bubbles in water have enormously greater target strengths, even in the absence of resonance effects. For example, for a nonresonant air bubble in water at 1 atm,  $\kappa'/\kappa$  is approximately 19,000, and its backscattering is some 77 dB greater than that for classic Rayleigh scattering by a sphere of the same size.

A thorough theoretical treatment of sound scattering from a fluid sphere is given in a paper by Anderson (7).

#### 9.4 Complications for a Large Smooth Solid Sphere

When a sound wave impinges on a large, smooth solid sphere in water, the sphere does not remain inert, but reacts to the impinging wave in different ways. First, sound can enter the sphere as a compressional wave and be reflected from the back side, so as to produce a secondary echo occurring slightly later than the specularly reflected echo from the front of the sphere. Second, flexural waves can be excited on the surface of the sphere at the place where their wavelength and that of sound in water "match." These waves of deformation travel with their own velocity around the sphere and contribute to the echo in the backward direction. Finally, "creeping" waves predicted by wave theory have been observed experimentally (8, 9). These are diffracted waves that originate at the edge of the geometrical shadow and travel around the sphere with the velocity of sound in water. Both surface and creeping waves reradiate in all directions as they travel around the sphere and in so doing become attenuated. The creeping or diffracted waves are the cause of the oscillations in the backscattering cross-section plot of Fig. 9.6 in the region  $1 < ka < 10$ .

These waves are illustrated in Fig. 9.8. Although they are somewhat academic, they illustrate some of the complications that can occur in the echo from real sonar targets in water.

The penetration of sound into a sphere can be used to enhance its target strength. Marks and Mikeska (10) filled a thin-wall stainless steel sphere with a mixture of the liquids freon and  $\text{CCl}_4$ , having a sound velocity 0.56 that of water, and found target strengths higher by 20 dB over the theoretical value

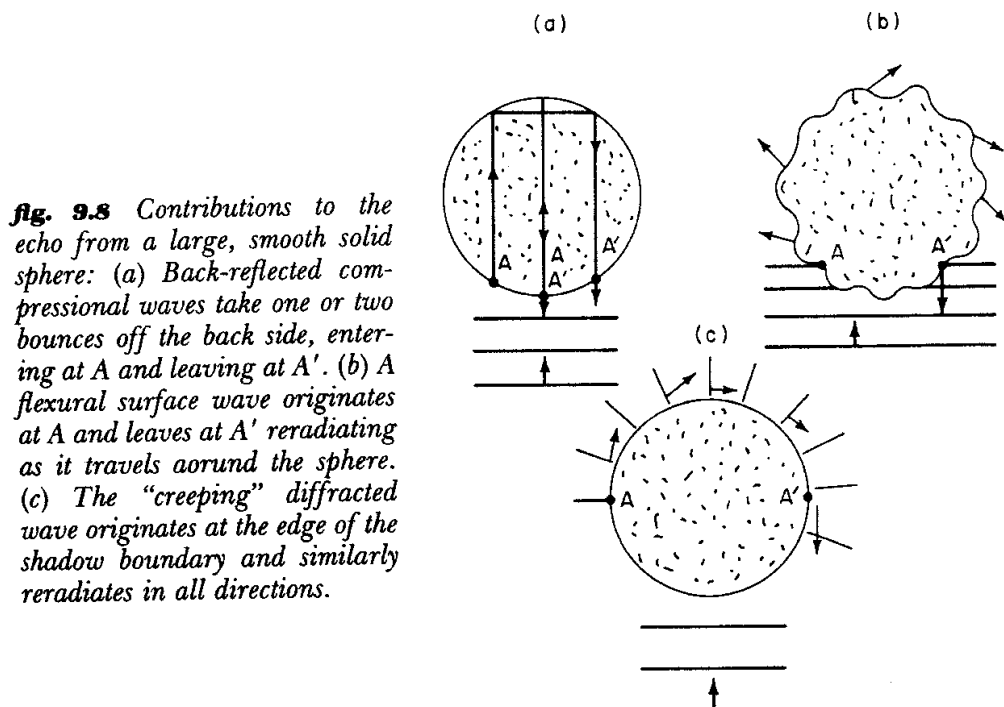


**Fig. 9.8** Contributions to the echo from a large, smooth solid sphere: (a) Back-reflected compressional waves take one or two bounces off the back side, entering at A and leaving at A'. (b) A flexural surface wave originates at A and leaves at A' reradiating as it travels around the sphere. (c) The "creeping" diffracted wave originates at the edge of the shadow boundary and similarly reradiates in all directions.

$10 \log a^2/4$  for an impenetrable sphere. In addition, the beamwidth of the returned sound was narrow—about the same as that of a circular piston of the same diameter as the sphere. The filling fluid served to focus the incident sound to the rear of the sphere and thereby produced stronger echoes than would occur if the sphere were either hollow or of solid steel.

### **9.5 Target Strength of Simple Forms**

The target strength of a number of geometric shapes and forms has been found theoretically, in most cases for applications to radar. Table 9.1 presents a list of a number of mathematical forms for which the target strength has been determined, together with the appropriate literature references. These idealized expressions should be viewed as no more than crude approximations for targets of complex internal construction for which penetration and scattering are suspected to occur. Moreover, the mobility and nonrigidity of sonar targets (unlike radar targets) cause them to have target strengths different from what they would have if they were fixed and rigid as theory requires. Yet the expressions will often be found useful for the prediction of the target strength of new and unusual objects for which no measured data are available and which, it is believed, can be approximated well enough by an ideal geometric shape. This use of these expressions will be illustrated later on for mines and torpedoes.

More complex targets can be modeled by breaking them up into elemental parts and replacing each part of one of the various simple forms. For example, a submarine can be modeled by a series of cylinders, wedges, plates, etc., each corresponding to some component of the hull structure. For a long-pulse sonar, the target strength can be found by adding up the contributions of the various simple forms into which the target has been divided. This technique appears to have been successfully employed in radar for estimating the target strength of targets as complex as an approaching jet bomber (11).

### **9.6 Bistatic Target Strength**

Because of the fact that in sonar, as in radar, the monostatic geometry has usually been employed, much less is known about the target strength of underwater objects in the “bistatic” arrangement, that is, when widely separated sources and receivers are used. A rule of thumb assumption that is commonly made is that the target is isotropic: that is, that its target strength is the same in all directions, except possibly in the “glint” directions where specular reflection might exist.

In radar, a method has been found for estimating the bistatic target strength when the monostatic value is known (12). The bistatic theorem states that for large smooth objects, the bistatic target strength is equal to the monostatic target strength, taken at the bisector of “bistatic angle” between the

**table 9.1 Target Strength of Simple Forms**

Form	Target strength $\frac{t}{r} = 10 \log t$	Symbols	Direction of incidence	Conditions	References
Any convex surface	$\frac{a_1 a_2}{4}$	$a_1 a_2 =$ principal radii of curvature $r =$ range $k = 2\pi/\text{wavelength}$	Normal to surface	$ka_1, ka_2 \gg 1$ $r > a$	1
Sphere Large	$\frac{a^2}{4}$	$a =$ radius of sphere	Any	$ka \gg 1$ $r > a$	1
Small	$61.7 \frac{V^2}{\lambda^4}$	$V =$ volume of sphere $\lambda =$ wavelength	Any	$ka \ll 1$ $kr \gg 1$	2
Cylinder Infinitely long Thick	$\frac{\alpha r}{2}$	$a =$ radius of cylinder	Normal to axis of cylinder	$ka \gg 1$ $r > a$	1
Thin	$\frac{9\pi^4 a^4}{\lambda^2} r$	$a =$ radius of cylinder	Normal to axis of cylinder	$ka \ll 1$	3
Finite	$aL^2/2\lambda$	$L =$ length of cylinder $a =$ radius of cylinder	Normal to axis of cylinder	$ka \gg 1$ $r > L^2/\lambda$	4
Plate Infinite (plane surface)	$\frac{r^2}{4}$	$a =$ radius of cylinder $\beta = kL \sin \theta$	At angle $\theta$ with normal	Normal to plane	

**table 9.1 Target Strength of Simple Forms (Continued)**

Form	$t$ Target strength $= 10 \log t$	Symbols	Direction of incidence	Conditions	Refer- ences
Finite Any shape	$\left(\frac{A}{\lambda}\right)^2$	$A = \text{area of plate}$ $L = \text{greatest linear di-}$ $\text{mension of plate}$ $l = \text{smallest linear di-}$ $\text{mension of plate}$	Normal to plate	$r > \frac{L^2}{\lambda}$ $kl \gg 1$	5
Rectangular	$\left(\frac{ab}{\lambda}\right)^2 \left(\frac{\sin \beta}{\beta}\right)^2 \cos^2 \theta$	$a, b = \text{side of rectangle}$ $\beta = ka \sin \theta$	At angle $\theta$ to normal in plane containing side $a$	$r > \frac{a^2}{\lambda}$ $kb \gg 1$ $a > b$	4
Circular	$\left(\frac{\pi a^2}{\lambda}\right)^2 \left(\frac{2I_1(\beta)}{\beta}\right)^2 \cos^2 \theta$	$a = \text{radius of plate}$ $\beta = 2ka \sin \theta$	At angle $\theta$ to normal	$r > \frac{a^2}{\lambda}$ $ka \gg 1$	4
Ellipsoid	$\left(\frac{bc}{2a}\right)^2$	$a, b, c = \text{semimajor}$ $\text{axes of ellip-}$ $\text{soid}$	Parallel to axis of $a$	$ka, kb, kc \gg 1$ $r \gg a, b, c$	6
Average over all aspects			Average over all direc- tions	$ka \gg 1$ $r > \frac{(2a)^2}{\lambda}$	5
Circular disk	$\frac{a^2}{8}$	$a = \text{radius of disk}$	At angle $\theta$ with axis of cone	$\theta < \psi$	7
Conical tip	$\left(\frac{\lambda}{8\pi}\right)^2 \tan^4 \psi \left(1 - \frac{\sin^2 \theta}{\cos^2 \psi}\right)^{-3}$	$\psi = \text{half angle of cone}$			

**Table 9.1 Target Strength of Simple Forms (Continued)**

Form	$t$ Target strength $= 10 \log t$	Symbols	Direction of incidence	Conditions	Refer- ences
Any smooth convex object	$\frac{S}{16\pi}$	$S =$ total surface area of object	Average over all direc- tions	All dimensions and radii of curvature large compared with $\lambda$	4 7
Triangular corner reflector	$\frac{L^4}{3\lambda^2} (1 - 0.00076\theta^2)^2$	$L =$ length of edge of reflector	At angle $\theta$ to axis of symmetry	Dimensions large compared with $\lambda$	5
Any elongated body of rev- olution	$\frac{16\pi^2 V^2}{\lambda^4}$	$V =$ body volume	Along axis of revolu- tion	All dimensions small compared to $\lambda$	8
Circular plate	$\left(\frac{4}{3\pi}\right)^2 k^4 a^6$	$a =$ radius $k = \frac{2\pi}{\lambda}$	Perpendicular to plate	$ka \ll 1$	8
Infinite plane strip	$\frac{1}{4\pi k} \left[ \frac{\cos \theta \sin (2ka \sin \theta)}{\sin \theta} \right]^2$ $\frac{ka^2}{\pi}$	$2a =$ width of strip $\theta =$ angle to normal	At angle $\theta$	$ka \gg 1$	8
			Perpendicular to strip	$\frac{ka}{\theta} \gg 1$ $\theta = 0$	

REFERENCES FOR TABLE 9.1

1. Physics of Sound in the Sea, pt. III, *Nat. Def. Res. Comm. Div. 6 Sum. Tech. Rep.* 8:358–362 (1946). (Note: Eqs. 49, 50, 53, and 56 in this reference are in error.)
2. Rayleigh, Lord: "Theory of Sound," vol. II, p. 277, Dover Publications, Inc., New York, 1945.
3. Rayleigh, Lord: "Theory of Sound," vol. II, p. 311, Dover Publications, Inc., New York, 1945.
4. Kerr, D. E. (ed.): "Propagation of Short Radio Waves," M.I.T. Radiation Laboratory Series, vol. 13, pp. 445–469, McGraw-Hill Book Company, New York, 1951.
5. Propagation of Radio Waves, Committee on Propagation, *Nat. Def. Res. Comm. Sum. Rep.*, 3:182 (1946).
6. Willis, H. F.: Unpublished (British) report, 1941.
7. Spencer, R. C.: Backscattering from Conducting Surfaces, RDB Committee on Electronics, Symposium on Radar Reflection Studies, September 1950.
8. Ruck, G. T., and others: "Radar Cross-Section Handbook," vols. I and II, Plenum Press, New York, 1970.

direction to source and receiver. This means, referring to Fig. 9.9, that the bistatic target strength with the source and receiver in the directions  $OS$  and  $OR$  from the target is the same as the monostatic target strength in the direction  $OP$  along the bisector of the angle  $SOR$ . This theorem, originating in physical optics, is said to be approximately true if the bistatic angle is considerably less than  $180^\circ$ . In the forward direction, where the bistatic angle equals  $180^\circ$ , physical optics also shows that the target strength of any large smooth object of projected area  $A$  equals  $10 \log A^2/\lambda^2$ , where  $\lambda$  is the acoustic wavelength, which must be small compared with all target dimensions. This is the same as the target strength of a flat plate of area  $A$  in the backward direction (Table 9.1).

Unfortunately, in the absence of measured data, it is not known how well these theoretical approximations apply, if they do at all, to the complex underwater targets of sonar.

### 9.7 Target-Strength Measurement Methods

The obvious and direct method of measuring the target strength of an underwater object is to place a hydrophone at a distance 1 yd from the object and to measure the ratio of the reflected (or scattered) intensity to the incident intensity. This method is impractical for a number of reasons. For many objects, it is difficult, if not impossible, to locate and place a hydrophone at this 1-yd point; even if it could be done, it would be difficult to separate the reflected sound from the incident sound at such a short distance. Moreover, the results would be invalid, in many cases, for use at longer ranges, since the target strength of objects like cylinders and submarines is different at short ranges than at long.

A more practical method is to use a reference target of known target strength, placed at the same range as the unknown, and to compare the levels of the echoes from the reference target and the target to be measured. The

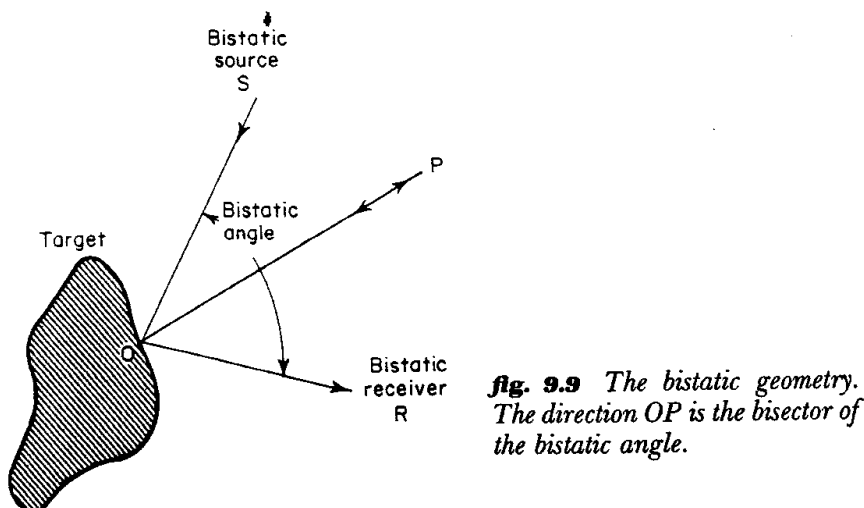
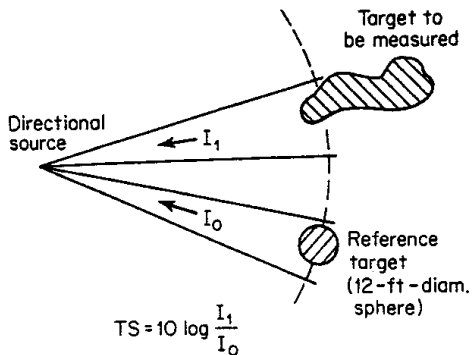


**fig. 9.9** The bistatic geometry.  
The direction  $OP$  is the bisector of  
the bistatic angle.

**fig. 9.10** Target-strength measurement using a reference sphere. A sphere of diameter 12 ft is placed at the same range as the target being measured. Using a directional active sonar, the intensities of the echoes are compared.



method is illustrated in Fig. 9.10. If the reference target is a sphere of diameter 4 yd, its target strength is 0 dB. Then the target strength of the target to be measured will be 10 times the logarithm of the ratio of the echo intensity of the unknown target to that of the 0-dB reference target. Suitable corrections can easily be made for differences in range and size of the reference target. This straightforward comparison method is particularly suited to measurements on small objects at short ranges. For large objects, such as submarines at longer ranges, the handling and the size requirements of the reference sphere make the method impractical. In all cases, the construction and dimensions of the reference target must be carefully controlled to make sure that its target strength approximates that of the ideal shape. Because of its ease of handling and its higher effective target strength, a calibrated transponder is a substitute for such a passive reference target.

Most target-strength measurements have been made by what may be called the conventional method, in which measurements of the peak or average intensity of the irregular echo envelope are made at some long range and then reduced to what they would be at 1 yd. This reduction requires, in effect, a knowledge of the transmission loss appropriate to the time and place the echoes were measured, together with the source level of the sound source producing the echoes. The method is illustrated in Fig. 9.11. A number of echo-level measurements of a sonar target are made at some range  $r$ . The average level of the echoes is reduced to 1 yd by adding the known or estimated transmission loss; the difference between the reduced 1-yd level and the known source level is the target strength desired. The method employs the active-sonar equation written in the form

$$EL = SL - 2TL + TS$$

where  $EL$  is the level of the echo. The equation is solved for the unknown,  $TS$ . This conventional method has the disadvantage of requiring an accurate knowledge of the transmission loss, which in turn requires either simple propagation conditions, or a special series of field measurements made for the purpose. Much of the scatter and diversity in existing target-strength data are doubtless attributable to erroneous transmission-loss assumptions and to

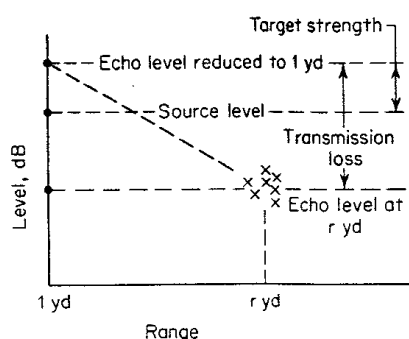


**fig. 9.11** Target-strength measurement using echo levels reduced to 1 yd. The range, source level, and transmission loss must be known.

indiscriminate use of peak and average levels of the echo. Nevertheless, the method is basically simple and straightforward and requires no special equipment or instrumentation.

A method requiring no knowledge of the transmission loss, but needing special instrumentation, was used by Urick and Pieper (13). A measurement hydrophone and a transponder located about 1 yd from it were installed on the target submarine. On the measuring vessel (a surface ship) a hydrophone was suspended near the sound source producing the echoes to be measured. The relative levels of echo and transponder pulses were recorded aboard the surface ship; the relative levels of the incoming pulse and the transponder pulse were recorded aboard the submarine. As will be evident from Fig. 9.12, the target strength of the submarine is simply the difference in level between the two level differences recorded on the two vessels. The transponder serves, in effect, to "calibrate out" the underwater transmission path between the two vessels. No absolute calibration of the transducers used is needed, and the range separating the vessels need not be known.

### 9.8 Target Strength of Submarines

The target strength of submarines, of all underwater targets, has had the earliest historical attention and has been relatively well known from work

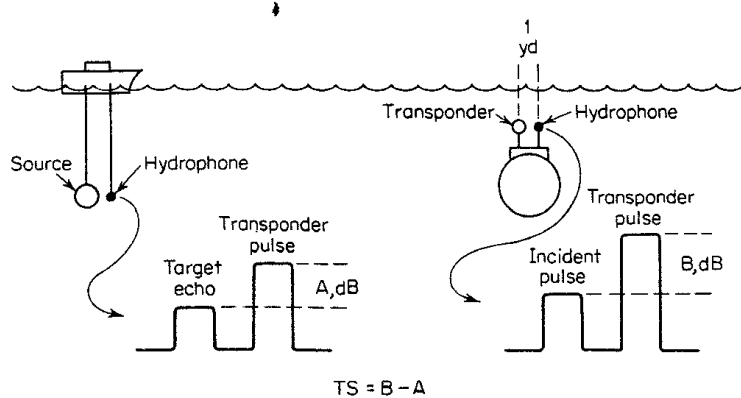


**fig. 9.12** A transponder method of target-strength measurement. No calibrations or knowledge of transmission loss are necessary.

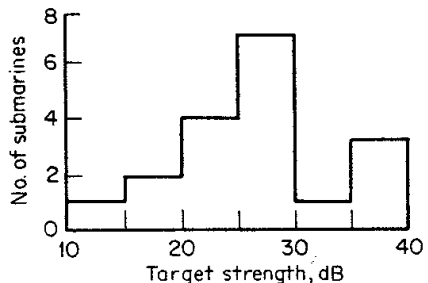


**fig. 9.13** Histogram showing the spread of the reported target strengths of 18 submarines at beam aspect, taken from the literature.

done during World War II. This work has been well summarized in the NDRC Summary Technical Reports (14, 15). The present treatment of the subject will center about the variations of target strength with aspect, frequency, ping duration, depth, and range. The submarines considered will be limited to fleet-type diesel-powered submarines.

It should be emphasized at the outset that submarine target strengths are perhaps most noteworthy for their variability. Not only do individual echoes vary greatly from echo to echo on a single submarine, but also average values from submarine to submarine, as measured by different workers at different times and reduced to target strength, are vastly different.

Figure 9.13 shows the distribution of target strengths at beam aspect of diesel-powered submarines as reported in 18 separate reports by different observers using different sonars. As a result, the following discussion of the subject will be concerned with trends and broad effects, with the exception that individual measurements will show great differences from the mean or average values.

**Variation with aspect** Figure 9.14 shows two examples of the variation of target strength with aspect around a submarine. Example A is a typical World War II determination (16) at 24 kHz with each point representing an average of about forty individual echoes in a  $15^\circ$  sector of aspect angle. Example B is the result of a postwar measurement (13) in which about five echoes were averaged in each  $5^\circ$  sector. Plots of this kind are based on measurements at sea of echoes from a submarine which runs in a tight circle at a distance from the source-receiver ship. Alternatively, the latter may circle a submarine running on a straight course at a slow speed.

The two examples of Fig. 9.14 illustrate the variability of target-strength measurements mentioned above. There is first a point-to-point variability with aspect that is due to the variability in level of individual echoes. There is also an average difference of about 10 dB between the two sets of measurements, with A being more typical of other determinations.

Nevertheless, when viewed in a broad fashion, the aspect dependence of target strength may be considered to have the pattern shown in Fig. 9.15. This "butterfly" pattern has the following characteristics:

1. "Wings" at beam aspect, extending up to about 25 dB and caused by specular reflection from the hull.
2. Dips at bow and stern aspects caused by shadowing of the hull and wake.
3. Lobes at about  $20^\circ$  from bow and stern, extending 1 or 2 dB above the general level of the pattern, perhaps caused by internal reflections in the tank structure of the submarine. These lobes do not appear in the aspect plots of nuclear-powered submarines not having ballast and fuel tanks outside the pressure hull.
4. A circular shape at other aspects due to a multiplicity of scattered returns from the complex structure of the submarine and its appendages.

All the characteristics of this idealized pattern are seldom seen in individual measurements. They may be absent entirely or lost in the scatter of the data. For example, Fig. 9.16 illustrates aspect plots of two submarines measured more recently at a frequency near 20 kHz with a pulse length of 80 ms while the submarines circled at a range of roughly 1,500 yd. Each plotted point

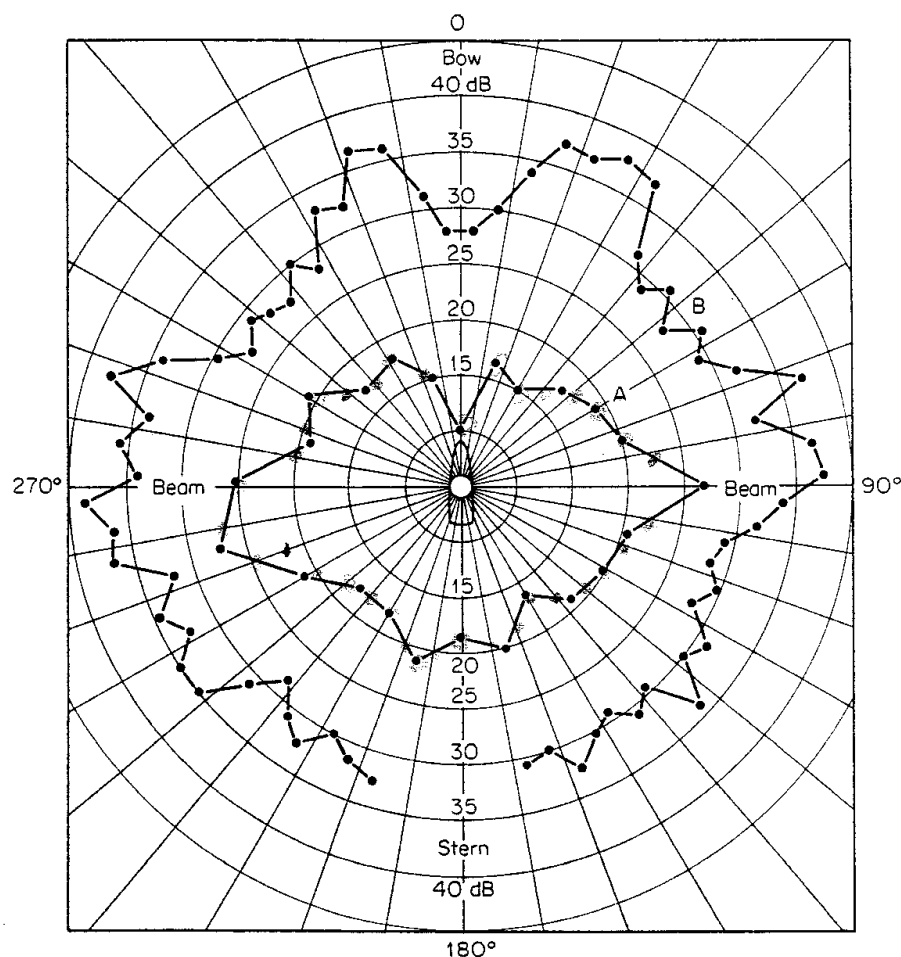


**fig. 9.14** Two determinations of the target strength of a submarine at various aspects. Example A (Ref. 15) is more typical of other determinations than B (Ref. 13).

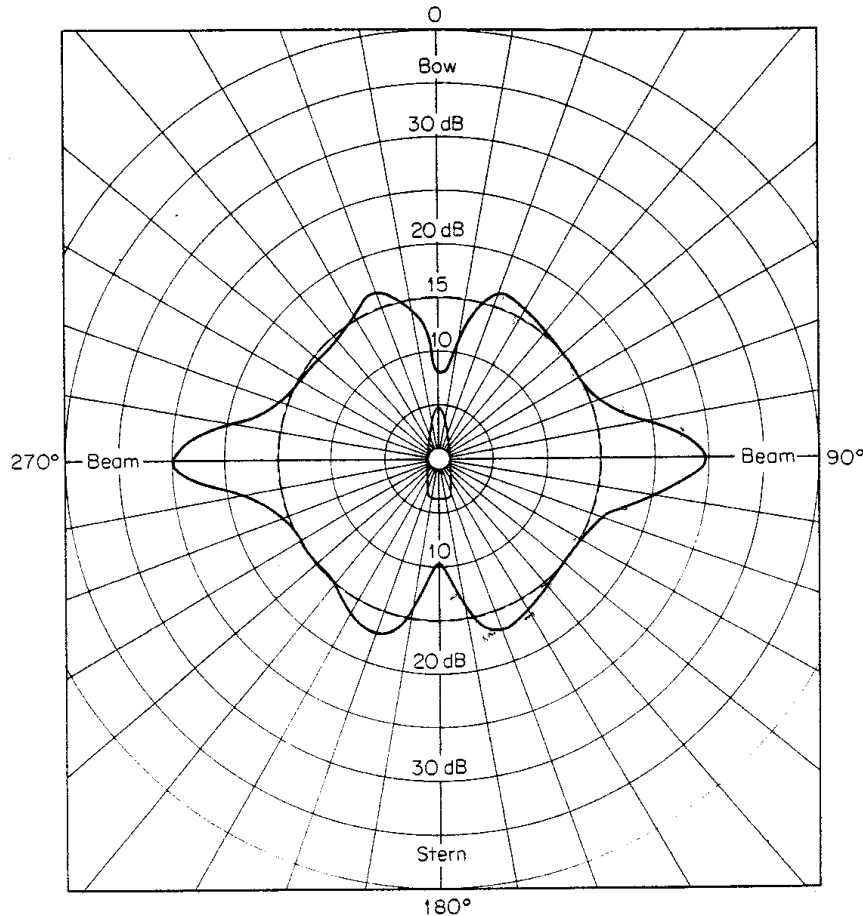


**fig. 9.15** The "butterfly" pattern of the aspect variation of submarine target strength.

represents a single echo. Particularly striking is the variability between echoes during the circling maneuver, as well as the difference of about 5 dB between the target strengths of the two submarines when averaged over all aspects. One is hard-pressed to see in these data any sign of the "butterfly" pattern just described. Aspect patterns showing wide echo-to-echo variability are well known in radar (17). The tremendous variability between echoes is caused by a changing phase relationship between the different scatterers and reflectors on the target; as the target aspect changes, the various contributions add up with different phase relationships so as to produce a variable echo amplitude. Echo fluctuations are observed even from a target at an apparently constant aspect, as a result of the small changes of heading that must be made by the helmsman, or by the pilot of an aircraft, attempting to steer a steady course.

**Variation with frequency** Target-strength data were obtained during World War II (18) at 12, 24, and 60 kHz in an attempt to determine the effect of frequency on target strength. This attempt was unsuccessful, and it was concluded at that time that, if any frequency dependence existed, it was lost in the

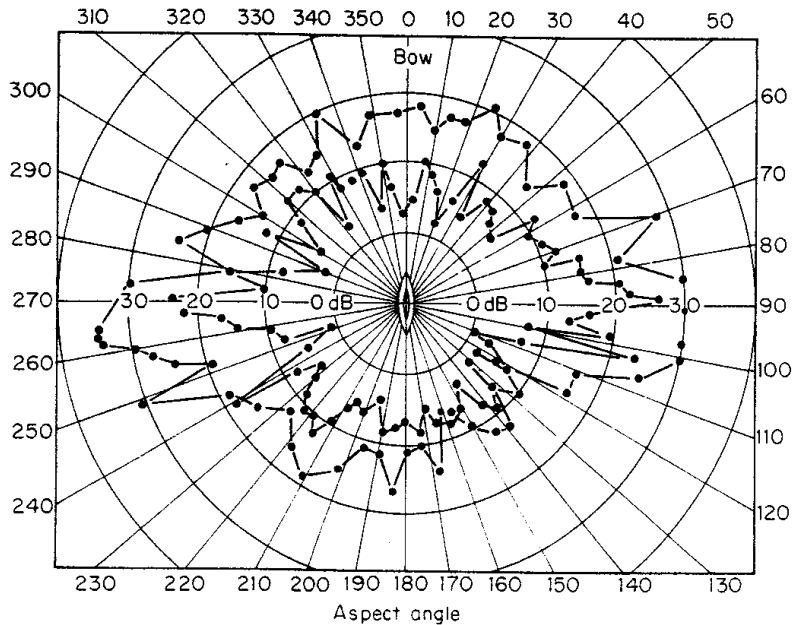


**fig. 9.16** Measurements of target strength versus aspect for two submarines. Each dot represents a single echo as the target circled at a distance.

uncertainties of the data. The cause of this apparent frequency independence must be the many processes and sources that govern the return of sound from a submarine.

**Variation with depth** Except for the contribution of sound returned from the submarine's wake, no effect of depth on target strength has been established or expected. Depth effects on the echo are more likely the result of changing sound propagation with changing depth in the sea, instead of a depth effect on the submarine itself.

**Variation with range** For two reasons, the target strength of submarines is likely to be less at short ranges than at long ranges. One is the failure of a directional sonar, if one is used for the target-strength measurement, to insinuate the entire target. The other is the fact that the echo of some geometrical forms does not fall off with range like the level from a point source. The solid curve in Fig. 9.17 shows the variation of echo intensity with range for a cylinder of length  $L$  at "beam" aspect. The intensity falls off like  $1/r$  at short ranges ("cylindrical spreading") and like  $1/r^2$  at long ranges ("spherical spreading") with a transition range approximately equal to  $L^2/\lambda$ . An echo at a short range  $r_1$ , when reduced to 1 yd by applying the transmission loss appropriate for a point source, would yield an apparent target strength  $TS_1$  that would be less than the value  $TS_0$  obtained with a long-range echo. Also, the target strength of an infinitely long cylinder, for which all points at a finite

distance are in the near field or Fresnel region of the cylinder, is seen in Table 9.1 to increase linearly with range. The former effect—that of failure to insonify all the target—would apply to conditions of aspect and frequency where scattering by numerous scatterers on or in the target is the dominant echo-producing process; the latter effect applies to specular reflection. Both effects cause the short-range target strength of submarines to be less than the long-range target strength.

**Variation with pulse length** The target strength of an extended target, such as a submarine, may be expected to fall off with decreasing pulse length, inasmuch as a short pulse must fail to insonify the entire target. Thus, Fig. 9.18 illustrates that the target strength of an extended target should increase with the pulse length (in logarithmic units) until the pulse length is just long enough for all points on the target to contribute to the echo simultaneously at some instant of time. This occurs when the ping duration  $\tau_0$  is such that

$$\tau_0 = \frac{2l}{c}$$

where  $l$  = extension in range of target

$c$  = velocity of sound

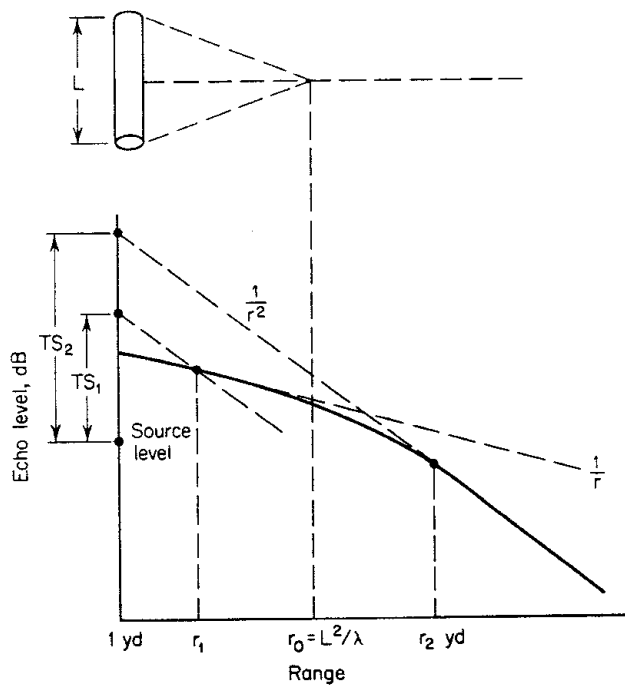


**Fig. 9.17** Target strength versus range for a beam-aspect cylinder. At ranges less than  $r_0$ , the echo level varies with range like  $1/r$  rather than  $1/r^2$ . This causes a lower target strength at short ranges than at long ranges ( $TS_1 < TS_2$ ) if a  $1/r^2$  transmission loss is used for the reduction to 1 yd.

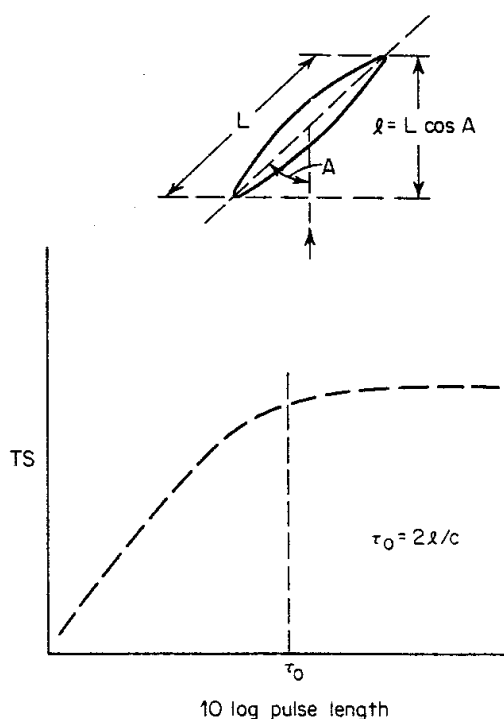


**Fig. 9.18** Variation with pulse length. The target strength increases until the pulse length is great enough for the entire target to contribute to the echo at some one instant of time. This occurs at pulse length  $\tau_0 = 2l/c$ .

If the target is of length  $L$ , then at aspect angle  $A$ ,

$$l = L \cos A$$

This theoretical effect of reduced ping duration is not noticeable in target-strength measurements at beam aspect, where the extension in range is small and where specular reflection is the principal echo formation process, nor in measurements of peak target strength where individual target highlights are being measured.

### 9.9. Target Strength of Surface Ships

Because surface ships are not important targets for active sonars, comparatively little data are available on their target strengths. Three series of measurements at frequencies from 20 to 30 kHz were made during World War II on a total of 17 naval and merchant ships (19). They yielded beam-aspect values of 37, 21, and 16 dB for the three different groups of measurements and values of 13, 17, and 14 dB for corresponding off-beam target strengths. Standard deviations between 5 and 16 dB are quoted for these values. The small amount of available data show similar effects of aspect and range, as for submarines.

### 9.10 Target Strength of Mines

Modern mines are quasi-cylindrical objects a few feet long and 1 to 2 ft in diameter, flat or rounded on one end, and containing protuberances, depres-

sions, and fins superposed on their generally cylindrical shape. Such targets should be expected to have a high target strength at "beam" aspect, as well as at aspects where some flat portion of the shape is normal to the direction of incidence; at other aspects, a relatively low target strength should be had. Measured target strengths range from about +10 dB within a few degrees of beam aspect, to much smaller values at intermediate aspects, with occasional lobes in the pattern attributable to reflections from flat facets of the mine shape. By Table 9.1, the target strength of a cylinder of length  $L$ , radius  $a$ , at wavelength  $\lambda$  is at long ranges

$$TS = 10 \log \frac{aL^2}{2\lambda}$$

If  $a$  be taken as 0.2 yd,  $L = 1.5$  yd, and  $\lambda = 0.03$  yd, corresponding to a frequency of 56 kHz, then

$$TS = 10 \log \frac{0.2 \times (1.5)^2}{2 \times 0.03} = 9 \text{ dB}$$

in approximate agreement with measurements on mines at beam aspect. The principal effects of frequency, aspect, range, and pulse length described for submarines apply for mines generally as well.

### **9.11 Target Strength of Torpedoes**

A torpedo is, like most mines, basically cylindrical in shape with a flat or rounded nose. When specular reflection can be presumed to be the principal echo formation process, the target strength of a torpedo can be approximated by the theoretical formulas. An approaching torpedo of diameter 20 in. (radius = 0.28 yd) and having a hemispherical nose with a diameter equal to that of the torpedo, would have a target strength equal to  $10 \log [(0.28)^2/4] = -17$  dB. At beam aspect its target strength could be approximated by the cylindrical formula illustrated for mines.

### **9.12 Target Strength of Fish**

Fish are the targets of fish-finding sonars. Their target strengths are of interest for the optimum design of such sonars and, ideally, might be used for acoustic fish classification—that is, for estimating the number, type, and size of fish when fish finders are employed at sea.

Extensive data on the target strengths of fish of different species have been reported by Love (20, 21), both for fish in dorsal aspect (looking down at the fish) and in side aspect (looking broadside). Echoes from live fish, anesthetized to keep them motionless, were measured in a test tank, and the measurements were reduced to target strength in the conventional way (Sec. 9.7). Eight frequencies over the range 12 to 200 kHz were used; the fish specimens ranged in length between 1.9 and 8.8 inches. The results showed a strong

dependence on the size of the fish, as measured by its length, and only a weak dependence on frequency or wavelength. When combined with older data reported by others, it was found that the measurements at dorsal aspect could be fitted by the empirical equation

$$TS = 19.1 \log_{10} L - 0.9 \log_{10} f - 54.3$$

where  $L$  is the fish length in inches, and  $f$  is the frequency of kilohertz. With  $L$  in centimeters, this equation becomes

$$TS = 19.1 \log_{10} L - 0.9 \log_{10} f - 62.0$$

The range of validity was  $0.7 < L/\lambda < 90$ ; over this range an individual fish had a target strength differing on the average by about 5 dB from that given by the equation. Figure 9.19 shows TS plotted against  $L$  for frequencies 10 and 100 kHz according to these expressions. At side aspect, the measured values were on the average 1 dB higher at  $L/\lambda = 1$  and 8 dB higher at  $L/\lambda = 100$  than those at dorsal aspect. Additional measurements at lower frequencies over the range 4 to 20 kHz have been reported by McCartney and Stubbs (22), with generally similar results. These investigators point out that, at least in their frequency range, the swim bladder of the fish is the major cause of the backscattered return. Fish without swim bladders, such as mackerel, have a target strength some 10 dB lower than those that do, such as cod (23).

Although it is biologically incorrect to speak of whales as "fish," we may note

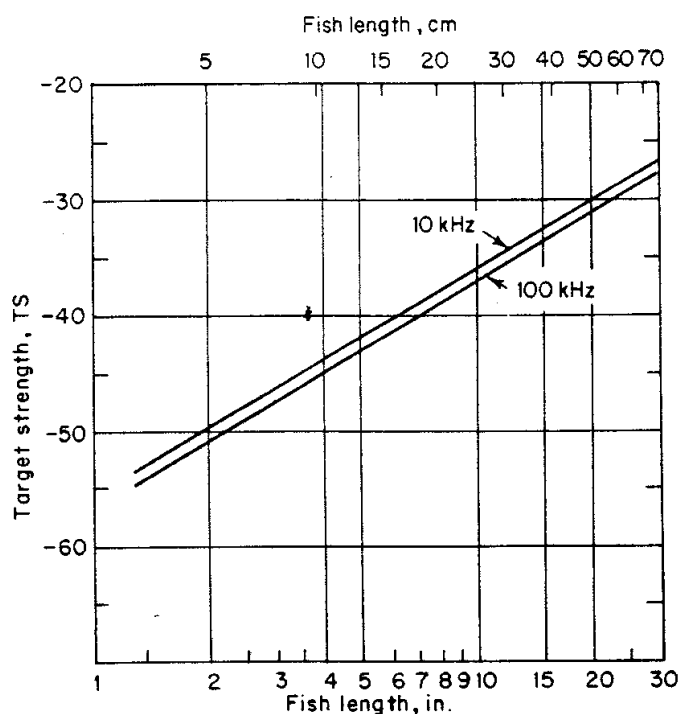


**Fig. 9.19** Target strength of fish as a function of fish length for two frequencies, according to expressions given in text.

here, if only as a curiosity, that the target strength of one species of whale in the open sea has been reported (24). Echoes were obtained from a number of humpback whales as they cavorted around the Argus Island oceanographic tower off Bermuda. At 20 kHz, two whales about 15 yd long were found to have a target strength of +7 at side aspect and -4 dB at head aspect; at 10 kHz, one smaller whale 10 yd long had a target strength of +2 dB at side aspect. These values are roughly what would be obtained by extrapolations in Fig. 9.19. Strange to say, they are not greatly different from what would be obtained from the expression  $TS = 10 \log R_1 R_2 / 4$  for the target strength of a large curved object of the same dimensions (Sec. 9.2).

### 9.13 Target Strength of Small Organisms

The target strength of various forms of zooplankton, such as squid, crabs, euphausiid shrimp, and copepods has been reported by a number of investigators. The results have been reviewed by Penrose and Kaye (25) who found, strangely enough, that the expression of Love given above fitted the measurements fairly well. Thus copepods 3 mm long were found to have a target strength of about -80 dB, crabs 30 mm in size, -60 dB; squid 100 mm in size, -45 dB. Little or no frequency dependence was found, although Greenlaw (26), using preserved specimens in the frequency range 200 to 1,000 kHz, observed a strong ( $20 \log f$ ) increase with frequency. The spread of measured data is large and the mechanism by which a small marine organism—which may or may not have a hard shell or contain a bubble of gas—interacts with sound is still not clear.

### 9.14 Echo Formation Processes

Complex underwater targets return sound back to the source by a number of processes. These processes will all occur, in general, for a complex target like a submarine, but only one or two will be dominant under any particular conditions of frequency and aspect angle.

**Specular reflection** The most simple and best understood echo formation process is *specular reflection*. It is illustrated by the return of sound from large spheres or convex surfaces, as described earlier in this chapter. In this process, the target remains stationary and does not move in the sound field and thereby generates a reflected wave having a *particle velocity* just sufficient, in wave theory, to cancel that of the incident wave over the surface of the object. Alternatively, the reflecting surface may be *soft* instead of *hard* or stationary, so as to form a reflection in which the *pressures* of the two waves will cancel. A specular reflection has a waveform that is a duplicate of the incident waveform and can be perfectly correlated with it. For submarines and mines, specular reflection appears to be the dominant process at beam aspects, where a much-enhanced return is observed and where a short incident pulse has a faithful replica as an echo.

**Scattering by surface irregularities** Irregularities, such as protuberances, corners, and edges, that have small radii of curvature compared with a wavelength, return sound by scattering rather than reflection. Most real objects possess many such irregularities on their surface, and the scattered return is composed of contributions from a large number of such scattering centers. When only a few scatterers on the underwater target are dominant, they form *highlights*, which may be observable in the echo envelope. Submarines, especially the older types, possess numerous scattering irregularities on the hull, such as the bow and stern planes, railings, periscopes; of these protuberances, the conning tower is likely to be a strong reflector or scatterer of sound.

**Penetration of sound into the target** Underwater targets seldom remain rigid under the impact of an incident sound wave, but move or deform in a complex manner. This reaction may be thought of as penetration of sound into the target and a complex deformation of the target by the exciting sound wave.

In solid metal spheres in water, Hampton and McKinney (27) found considerable experimental evidence that acoustic energy in the frequency range 50 to 150 kHz penetrated into solid spheres a few inches in diameter and thereby produced a complex echo envelope and a target strength which varied by as much as 30 dB with frequency. A theoretical study by Hickling (28) of hollow metal spheres in water demonstrated that part of the echo originates from a kind of flexural wave moving around the shell. Such surface waves were also observed experimentally by Barnard and McKinney (29) in a study of solid and air-filled cylinders in water. We have already described these kinds of deformation waves in Sec. 9.4.

Submarines are structurally much more complicated than the simple forms just mentioned. Figure 9.20 shows cross-sectional views of a fleet-type submarine of basically World War II construction. The hull is essentially a quasi-cylindrical pressure hull surrounded by a tank structure of thin steel. Penetration of sound into the tank structure is relatively easy, and a return of sound by corner reflectors should be expected. These internal reflections may be the cause of the enhanced target strength at about 20° off bow and stern in the butterfly pattern of Fig. 9.15. In addition, scattering and resonance effects in the tank structure are likely to be sources of the echo at off-beam aspects. Finally, the pressure hull itself may be expected to contribute a scattered return at some aspect angles.

Whenever a regular repeated structure or appendage exists on a target, an enhanced echo is likely to occur at the frequency and angle for which the scattered returns reinforce one another in a coherent manner. This is a diffraction-grating effect; it will occur when the projected distance between structural components is a half-wavelength or a multiple thereof. A regularly structured target appears to act like an array of radiating elements, and produces the same beam pattern in its echo as would a line of equally spaced elements at twice the spacing. This is an alternative explanation of the 20°

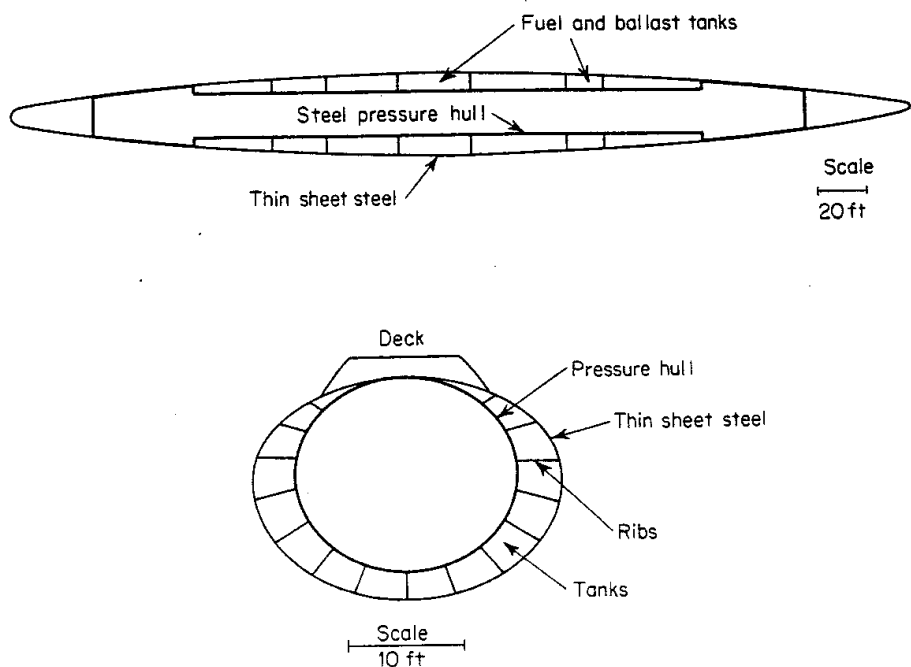


**fig. 9.20** Diagrammatic fore-and-aft and athwartship cross sections of a World War II U.S. fleet submarine.

"ears" of the butterfly pattern just mentioned; the tank structure, the framing of the hull, or some other regularly repeated structural component may provide the regularity needed for selective reinforcement of the echo.

**Resonant effects** Certain incident frequencies may correspond to various resonance frequencies of the underwater target. Such frequencies will excite different modes of oscillation or vibration of the target and give rise, in principle, to an enhanced target strength. Figure 9.21 is a pictorial description of a number of possible oscillatory modes of a compressible, flexible cigar-shaped object. When the sonar frequency is low enough, such modes may be excited by the incident sound wave and contribute to the target strength to an extent depending on the aspect and the  $Q$  or damping constant of the oscillatory mode. However, it should be pointed out that those modes which are good radiators of sound have a high damping constant because of radiation loading by the surrounding fluid, and as a result they would not necessarily give rise to a much greater target strength. Similarly, slightly damped modes of high  $Q$  might be poor reradiators of sound and thereby be poor contributors to the target strength. Such slightly damped modes would require a long sonar pulse of closely matched frequency for their excitation. It is even possible that resonant vibratory modes may be accompanied by a *lower* target strength if high internal losses in the target cause absorption of the incident energy, or if the mode is such that sound is reradiated, at resonance, into directions other than into the specular direction.

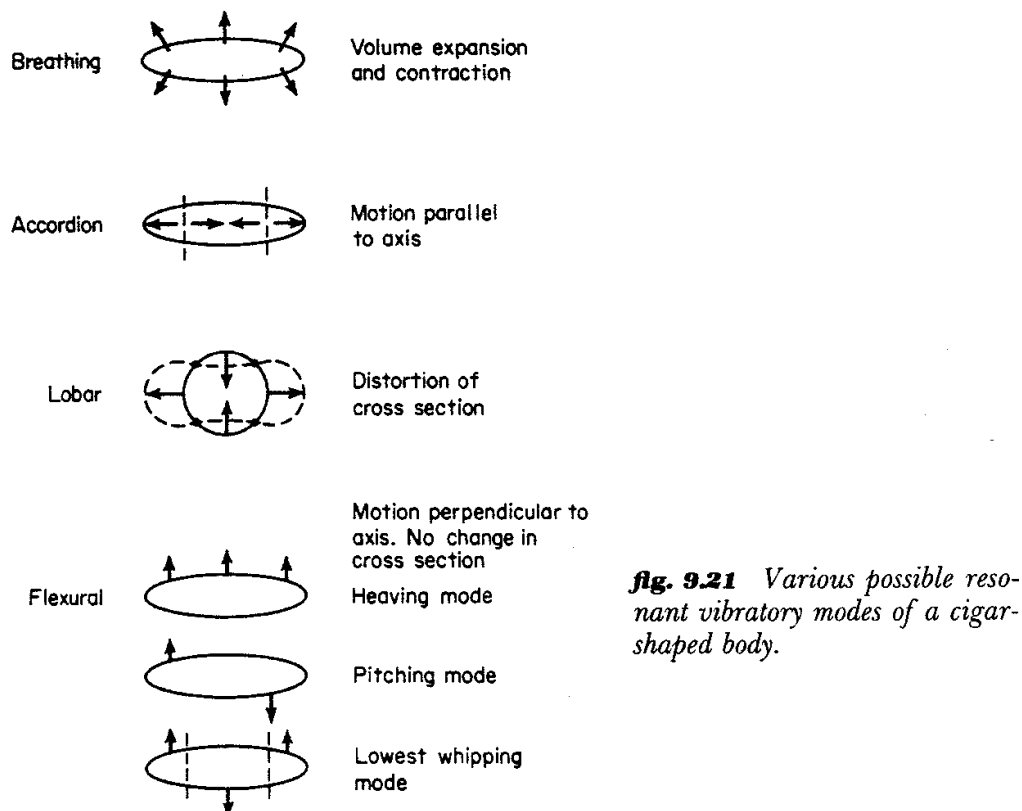


**fig. 9.21** Various possible resonant vibratory modes of a cigar-shaped body.

A resonance of an entirely different type is the flexural resonance of the plates of which an underwater target like a submarine is composed. At certain angles a steel plate has been shown by the work of Finney (30) to be transparent to sound because of coupling between shear waves in the plate and sound waves in the surrounding water.

### 9.15 Reduction of Target Strength

It is sometimes desired to do something to a target, other than make major structural and compositional changes to it, for the purpose of reducing its target strength. This kind of acoustic camouflage can be achieved in a variety of ways. These are listed in Table 9.2.

**table 9.2 Methods of Target Strength Reduction**

Wavelength Large: <sup>*</sup>	Low frequencies
	Volume reduction
Wavelength Small: <sup>*</sup>	High frequencies
	Body shaping
	Anechoic coatings
	Viscous absorbers
	Gradual-transition coatings
	Cancellation coatings
	Quarter-wave layer
	Active cancellation

\* Compared to all dimensions of the body.

At low frequencies, where the wavelength is large compared to all dimensions of the object, the only recourse is to reduce the *volume* of the target. This follows because, as we have seen, the target strength of a small sphere (Sec. 9.3) or of any small smooth object (Table 9.1) depends only on its volume at a fixed frequency. It follows that no alteration of body shape or application of a coating will be effective on a body that is small compared to a wavelength.

However, at high frequencies and short wavelengths, a variety of techniques are applicable, at least in principle. One is to *change the shape* of the body, if it is possible to do so, in such a way as to make the two principal radii of curvature ( $R_1 R_2$ , Sec. 9.2) everywhere small, avoiding in particular the infinities characteristic of flat plates and cylinders. The body shape should be smooth, without protuberances, holes, and cavities that act as scatterers of sound. In radar, a shape that has received much attention for missile applications is a cone with hemispherical base; this presents a particularly low target strength when viewed in the direction toward the conical tip. In radar, the radar cross section of the body need be minimized only in one (the forward) direction, whereas in sonar, a reduction usually must be achieved in many or all directions. For this reason, other shapes will be useful for sonar applications.

*Anechoic coatings* are materials that are cemented or attached to the body in order to reduce its acoustic return. The most important of these are various *viscous absorbing coatings* which attenuate the sound reaching, and returning from, the target by the process of viscous conversion to heat. Metal-loaded rubbers are an example of this kind of coating (31); here the tiny air cavities accompanying the metal particles cause a shear deformation of the rubber and a loss of sound to heat. Much larger air cavities causing shear deformation in rubber were employed in the Alberich coating used by the German Navy in World War II (32). This coating comprised a sheet of rubber 4 mm thick containing cylindrical holes 2 and 5 mm in diameter, with an overlying thin sheet of solid rubber to keep water out of the holes. This particular coating was effective in the octave 9 to 18 kHz; a number of German submarines were coated with it during the latter part of the war. A *gradual transition coating* consists of wedges or cones of lossy material with their apex pointing toward the incident sound. An example of this is a mixture of sawdust material called "insulkrete," described by Darner (33) for lining a tank to make it anechoic. This particular type of coating is massive and relatively fragile in construction for use on sonar targets.

A *cancellation coating* consists of alternate layers of acoustically hard and soft materials that reflect sound with opposite phase angles, so that no sound is returned from the target. Unfortunately, the cancellation occurs only at normal incidence, and there is little or no effect in other directions. A *quarter-wave layer* is a coating  $\lambda/4$  in thickness having an acoustic impedance ( $\rho c$ ) equal to the geometric mean between the materials on either side, as, for example water and steel (34). Theory shows that under these conditions the layer is a perfect impedance match between the two materials, and no sound is reflected. But, because it is effective only at a single frequency (plus odd

multiples thereof) and then only at normal incidence, the quarter-wave coating is of no value for practical sonar applications. Finally, we can mention the principle of *active cancellation*, wherein the incoming sound is monitored on the target and an identical signal is generated 180° out of phase to it by a small sound source. This technique has been used for reducing reflections in a tube for transducer calibrations (35), but requires expensive instrumentation; in any case, it would have little value for reducing reflections from the large complex targets of sonar.

### 9.16 Echo Characteristics

Echoes from most underwater objects differ from the incident pulse in a number of ways other than intensity, as described by the parameter target strength. The reflecting object imparts its own characteristics to the echo; it interacts with the incident sound wave to produce an echo that is, in general, different in wave shape and other characteristics from the incident pulse. These differences are useful to the sonar engineer in two ways: they may be employed as an aid in *detection*, as in filtering with narrow-band filters to enhance an echo buried in reverberation; they may be utilized to assist in target *classification* to distinguish one type of target from another, as in distinguishing a submarine from a school of fish.

Some distinguishing characteristics of echoes are:

**Doppler shift** Echoes from a moving target are shifted in frequency by the familiar doppler effect (36) by an amount equal to

$$\Delta f = \frac{2v}{c} f$$

where  $v$  = relative velocity or range rate between source and target

$c$  = velocity of sound (in same units as  $v$ )

$f$  = operating frequency of transmitter

In practical terms, and for a sound velocity of 4,900 ft/s,

$\Delta f = \pm 0.69 \text{ Hz/(knot)(kHz)}$

where the range rate is in units of knots and the sonar frequency is in kilohertz. An echo from an approaching target with a 10-knot relative velocity and a frequency of 10 kHz would thus be shifted higher in frequency by 69 Hz. The  $\pm$  sign indicates that an approaching target produces an echo of higher frequency ("up-doppler"), and a receding target one of lower frequency ("down-doppler").

**Extended duration** Echoes are lengthened by the extension in range of the target. Whenever an underwater target is such that sound is returned by scatterers and reflectors distributed all along the target, the entire area or volume of the target contributes to the echo. For a target of length  $L$  at an aspect angle  $\theta$ , the incident pulse is lengthened in duration by the time interval

$$\frac{2L \cos \theta}{c}$$

for the monostatic case, and by

$$\frac{L}{c} (\cos \theta_i + \cos \theta_r)$$

for the bistatic case with incidence at aspect angle  $\theta_i$ , and an echo return at angle  $\theta_r$ . This time elongation of the echo is most noticeable when short sonar pulses are employed. It occurs only for complex targets composed of numerous distributed scatterers and is negligible when specular reflection is the most important process of echo formation. Most sonar echoes are elongated, however, and so provide a clue concerning the size, and therefore the nature, of the echoing object.

Some actual measured data on the duration of echoes from a submarine target as a function of aspect angle are shown in Fig. 9.22. In this plot, each

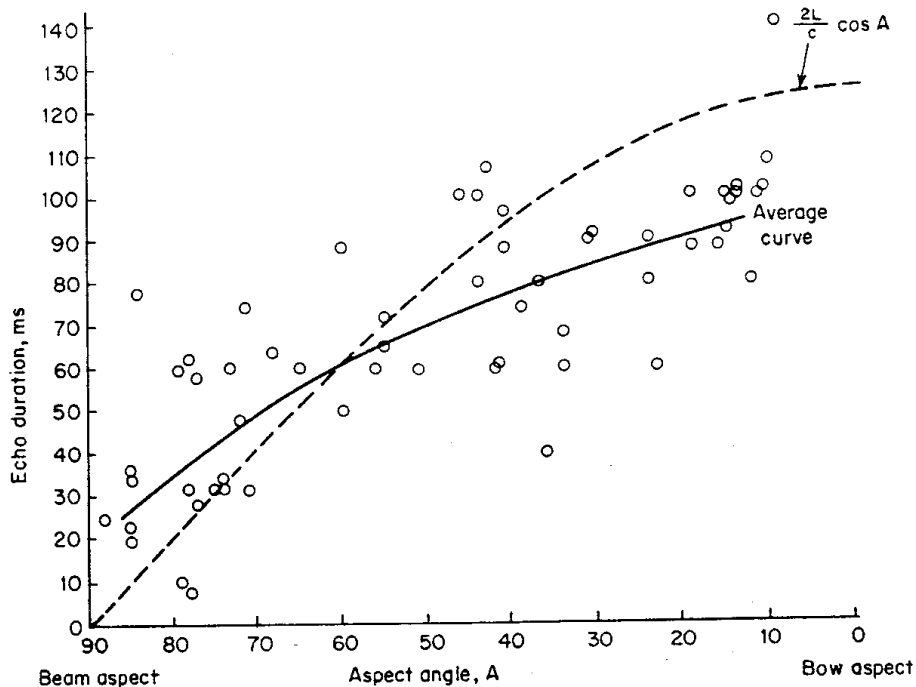


Fig. 9.22 Echo duration at different aspect angles of a submarine target. Each point represents a single echo from an explosive source.

point represents the time duration of an explosive echo at the particular aspect angle at which it occurred. We observe that the theoretical relationship  $t = 2(L/c) \cos A$  is only a rough approximation to the observations summarized by the average curve. The echoes are longer than they should be near beam aspect, probably because of multipath transmission (more particularly, the surface reflected path) from source to target and back again; the echoes are shorter than they should be near bow aspect, probably because of shadowing of the stern portions of the hull by the bow.

**Irregular envelope** The echo envelope is irregular, especially where specular reflection is not important. This irregularity arises from acoustic interference between the scatterers of the target. For some targets, individual highlights in the echo may be identified as arising from individual strong echoing portions of the target; for example, the conning tower of a submarine may yield a recognizable strong return of its own as part of the echo. Most often, however, the sonar echo from a sinusoidal ping is an irregular blob, without distinguishing features, that varies in envelope shape from echo to echo as the changing phase relationships among the scatterers and the propagation paths to and from the target take effect. Figure 9.23 is a sequence of three echoes from a short-range oblique-aspect submarine taken at intervals one second apart using a sonar with a pinglength of 15 ms. From this sequence we should note the rapid variability of the complex structure of the echo envelope and its extended duration relative to the 15-ms outgoing pulse.

**table 9.3 Nominal Values of Target Strength**

Target	Aspect	TS, dB
Submarines	Beam	+25
	Bow-stern	+10
	Intermediate	+15
Surface ships	Beam	+25 (highly uncertain)
	Off-beam	+15 (highly uncertain)
Mines	Beam	+10
	Off-beam	+10 to -25
Torpedoes	Bow	-20
Fish of length $L$ , in.	Dorsal view	$19 \log L - 54$ (approx.)
Unsuited swimmers	Any	-15
Seamounts	Any	+30 to +60

**Modulation effects** At stern aspects on propeller-driven targets, the propeller may amplitude-modulate the echo in the same way that the propeller of an aircraft is known (37) to modulate a radar echo. The propeller thus produces a cyclic variation in the scattering cross section of the target. Another possible form of modulation can arise from interaction between the echo from a moving vessel and the echo from its wake. The difference in frequency between the two may appear as beats, or amplitude variations, in the envelope of the combined echo from the hull and wake at certain aspect angles.

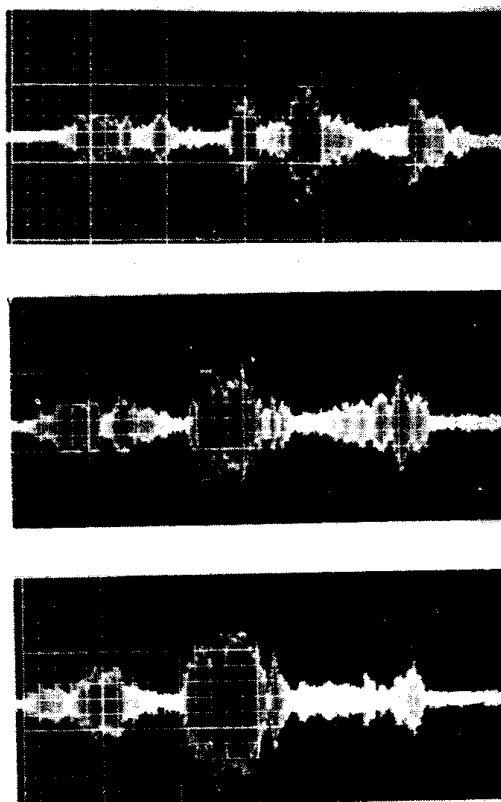


**Fig. 9.23** Photographs of three submarine echoes taken one second apart. The width of the horizontal scale is 120 ms; the sonar pinglength was 15 ms.

### 9.17 Summary of Numerical Values

Table 9.3 is a summary of target-strength values for the underwater targets described in this chapter, plus two others. As previously mentioned, these are subject to considerable variation in individual measurements on targets of the same type, and the target-strength values given are to be regarded only as nominal values useful for first-cut problem solving.

### REFERENCES

1. Kerr, D. E. (ed.): "Propagation of Short Radio Waves," M.I.T. Radiation Laboratory Series vol. 13, pp. 445-481, McGraw-Hill Book Company, New York, 1951.
2. Freedman, A.: Recent Approaches to Echo-Structure Theory, *J. Acoust. Soc. Am.*, **36**:2000(A) (1964). Also, A Mechanism of Acoustic Echo Formation, *Acustica*, **12**:10 (1962)
3. Neubauer, W. G.: A Summation Formula for Use in Determining the Reflection of Irregular Bodies, *J. Acoust. Soc. Am.*, **35**:279 (1963).
4. Steinberger, R. L.: Theoretical Analysis of Echo Formation in the Fluctuation Environment of the Sea, *U.S. Nav. Res. Lab. Rep.* 5449, 1960.
5. Rayleigh, Lord: "Theory of Sound," vol. 2, p. 277, eqs. 26 and 27, Dover Publications, Inc., New York, 1945.
6. Rayleigh, Lord: "Theory of Sound," vol. 2, p. 24, eq. 13, Dover Publications, Inc., New York, 1945.

## **Radiated noise of ships, submarines, and torpedoes: radiated-noise levels**

Ships, submarines, and torpedoes are excellent sources of underwater sound. Being themselves machines of great complexity, they require numerous rotational and reciprocating machinery components for their propulsion, control, and habitability. This machinery generates vibration that appears as underwater sound at a distant hydrophone after transmission through the hull and through the sea. Of particular importance is the machinery component called the propeller, which serves to keep the vehicle in motion, and in doing so, generates sound through processes of its own.

Radiated noise is of particular importance for passive sonars, which are designed to exploit the peculiarities of this form of noise and to distinguish it from the background of self-noise or ambient noise in which it is normally observed.

In this chapter the principal characteristics of radiated noise will be discussed, and some data on the level of this noise for various vehicles will be presented. The discussion will be restricted to conventional designs and conventional propulsion systems, omitting any discussion of the noise of nuclear-propelled vessels or unusual propulsion methods. The word "vessel" will be used to refer to surface ships, submarines, or torpedoes indiscriminately when it is unnecessary to distinguish among them.

### **10.1 Source Level and Noise Spectra**

The parameter *source level* for radiated noise in the sonar equations is the intensity, in decibel units, of the

noise radiated to a distance by an underwater source, when measured at an arbitrary distance and reduced to 1 yd from the *acoustic center* of the source. By acoustic center is meant the point inside or outside the vessel from which the sound, as measured at a distance, *appears* to be radiated. Practically speaking, radiated-noise measurements must of necessity be made at a distance from the radiating vessel, typically 50 to 200 yd, and must be reduced to 1 yd by applying an appropriate spreading or distance correction. Source levels are specified in a 1-Hz band, and will be referred to a reference level of 1  $\mu\text{Pa}$ . The source levels for radiated noise are accordingly *spectrum* levels relative to the 1- $\mu\text{Pa}$  reference level.

When 1 meter is used as the reference distance instead of 1 yd, a correction of  $-0.78$  dB must be applied to source levels referred to 1 yd. This same correction is required for all the other range-dependent sonar parameters when using 1 meter instead of 1 yd as the unit of range.

Noise spectra are of two basically different types. One type is *broadband noise* having a continuous spectrum. By continuous is meant that the level is a continuous function of frequency. The other basic type of noise is *tonal noise* having a discontinuous spectrum. This form of noise consists of tones or sinusoidal components having a spectrum containing *line components* occurring at discrete frequencies. These two spectral types are illustrated diagrammatically in Fig. 10.1. The radiated noise of vessels consists of a mixture of these two types of noise over much of the frequency range and may be characterized as having a continuous spectrum containing superposed line components.

## 10.2 Methods of Measurement

The noise radiated by vessels is nearly always measured by running the vessel past a stationary distant measurement hydrophone. Various types of hydrophones and hydrophone arrays have been employed for this purpose. The simplest arrangement uses a single hydrophone hung from a small measurement vessel. More elaborate configurations involve an array of hydrophones, either strung in a line along the bottom in shallow water, or hung vertically in

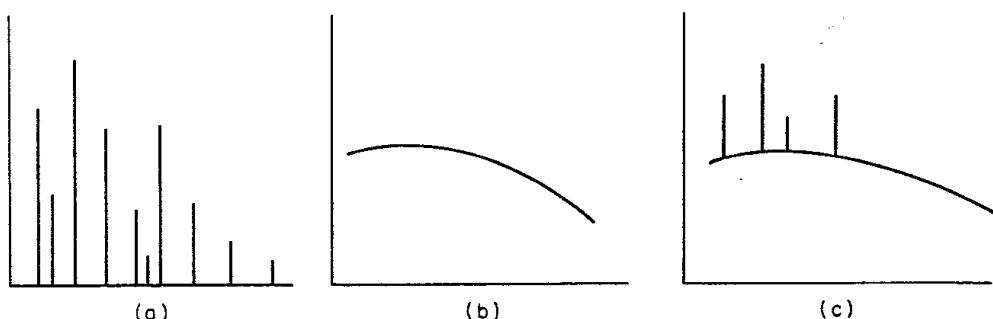


**fig. 10.1** Diagrams of (a) line-component spectrum, (b) continuous spectrum, and (c) composite spectrum obtained by superposing (a) and (b).

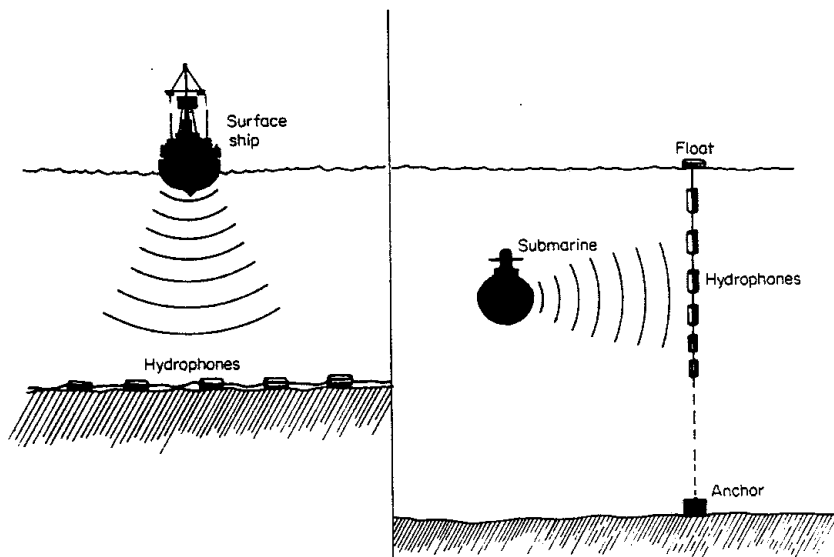


**fig. 10.2** Arrangements of hydrophones used at sound ranges for measuring radiated noise.

deep water, as illustrated in Fig. 10.2. The former arrangement is suitable for measuring the noise of surface ships, and the latter is useful for measuring the noise of submarines or torpedoes running at deep depths. In both cases the vessel under test is arranged to run at a constant speed and course so as to pass the measurement hydrophones at a known distance. Suitable techniques are used to determine the range of the vessel while its radiated-noise output is being measured. During the run, broadband tape recordings are made, and later subjected to analysis in different frequency bands.

Figure 10.3 shows the instrumentation employed at the Atlantic Undersea Test and Evaluation Center (AUTEC) for the measurement of the radiated noise of submarines. An elaborate system is used for tracking the submarine during its passage past the measurement hydrophones. This noise-measurement range is located in the "Tongue of the Ocean" east of the Bahama Islands.\*

Although radiated noise is commonly expressed as *spectrum levels*, that is, in 1-Hz bands, frequency analyses are often made in wider bands. The results are reduced to a band of 1 Hz by applying a bandwidth reduction factor equal to 10 times the logarithm of the bandwidth used. That is to say, if  $BL$  is the noise level measured in a band  $w$  hertz wide, the spectrum level in a 1-Hz band is  $BL - 10 \log w$  (Sec. 1.5). This reduction process is valid for continuous "white" noise having a flat spectrum; it can be shown to be also valid for noise having a continuous spectrum falling off at the rate of  $-6$  dB/octave, if the center frequency of the band is taken to be the geometric mean of the two

\* Five papers on AUTEC were presented at the 74th meeting of the Acoustical Society of America in 1967. Abstracts appear in *J. Acoust. Soc. Am.*, 42:1187 (1967).

ends of the frequency band. But for line-component noise containing one or several strong lines within the measurement bandwidth, this reduction process is not valid and yields spectrum levels lower than the level of the line component dominating the spectrum. In short, the nature of the spectrum must in principle be known before the reduction is made. Many old reported data are almost useless at low frequencies because an excessively broad frequency band had been employed in the original analysis.

Similarly, a correction for distance is required to reduce the measurements to the 1-*yd* reference distance. The ubiquitous spherical-spreading law is generally applied for this purpose. Several investigations have indicated that spherical or inverse-square spreading is a good rule of thumb for expressing the variation of ship noise with range at close distances, even for low frequencies in shallow water (1). In any case, in spite of the apparent artificiality of the reduction processes in many instances, the original levels can be recovered from the published reduced values if the reduction process, bandwidth, and measurement distance are stated.

Studies of the sources of noise under various operating conditions, as distinct from measurements of noise level alone, have employed various clever schemes to pinpoint the dominant sources of noise. For example, when ships and torpedoes are run very close to the measuring hydrophone, the principal source of noise—whether machinery noise originating amidships or propeller noise originating near the stern—can be identified by the correspondence between the peak of the noise and the closest part of the ship at that instant. Overseas surveys (2) of surface ships and submarines, in which a hydrophone

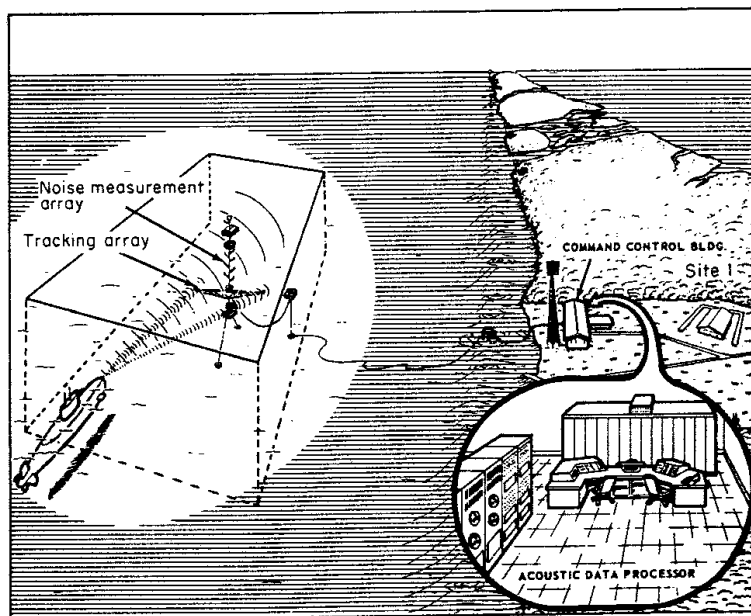


**fig. 10.3** Noise measurement range at the Atlantic Undersea Test and Evaluation Center (AUTEC).

is lowered over the side of the moored vessel, are sometimes made to measure the noise radiated into the water by different pieces of ship's machinery. Various modifications to a running vessel have been made to study their effect on the noise output; such modifications include towing a surface ship without its propeller and operating a torpedo in a "captive" condition alongside a measurement platform. The effect of a bubble screen has been simulated by turning a ship so as to cross its own wake and noting the effect on the self-noise and radiated noise. All these methods have contributed to our present knowledge of the sources of radiated noise.

### **10.3 Sources of Radiated Noise**

The sources of noise on ships, submarines, and torpedoes can be grouped into the three major classes listed in Table 10.1. *Machinery noise* comprises that part of the total noise of the vessel caused by the ship's machinery. *Propeller noise* is a hybrid form of noise having features and an origin common to both machinery and hydrodynamic noise. It is convenient to consider propeller noise separately because of its importance. *Hydrodynamic noise* is radiated noise originating in the irregular flow of water past the vessel moving through it and causing noise by a variety of hydrodynamic processes.

**table 10.1 Source of Radiated Noise  
(Diesel-Electric Propulsion)**

---

Machinery noise:

- Propulsion machinery (diesel engines, main motors, reduction gears)
- Auxiliary machinery (generators, pumps, air-conditioning equipment)

Propeller noise:

- Cavitation at or near the propeller
- Propeller-induced resonant hull excitation

Hydrodynamic noise:

- Radiated flow noise
  - Resonant excitation of cavities, plates, and appendages
  - Cavitation at struts and appendages
- 

**Machinery noise** Machinery noise originates as mechanical vibration of the many and diverse parts of a moving vessel. This vibration is coupled to the sea via the hull of the vessel. Various paths, such as the mounting of the machine, connect the vibrating member to the hull. Machine vibration can originate in the following ways:

1. Rotating unbalanced parts, such as out-of-round shafts or motor armatures
2. Repetitive discontinuities, such as gear teeth, armature slots, turbine blades
3. Reciprocating parts, such as the explosions in cylinders of reciprocating engines

4. Cavitation and turbulence in the fluid flow in pumps, pipes, valves, and condenser discharges

5. Mechanical friction, as in bearings and journals

The first three of these sources produce a *line-component spectrum* in which the noise is dominated by tonal components at the fundamental frequency and harmonics of the vibration-producing process; the other two give rise to noise having a *continuous spectrum* containing superposed line components when structural members are excited into resonant vibration. The machinery noise of a vessel may therefore be visualized as possessing a low-level continuous spectrum containing strong line components that originate in one or more of the repetitive vibration-producing processes listed above.

A diagrammatic view of the sources of machinery noise aboard a diesel-electric vessel is shown in Fig 10.4. Each piece of machinery produces periodic vibrational forces at the indicated fundamental frequency and thereby generates a series of line components at this frequency and at its harmonics. However, at a distance in the sea, the sound produced by these vibrational forces depends not only on their magnitude, but also on how such forces are transmitted to the hull and coupled to the water. A notable example is the resonant excitation of large sections of the hull by machinery vibration—called “hull drone”—such as that produced by the rotation of the massive propeller shaft, wherein certain frequencies of the excitation spectrum are reinforced by a short of sounding-board effect. The manner of mounting of the machine and the resulting vibration of the hull are determining factors in the radiation of sound. Another source of variability is in the propagation of different fre-

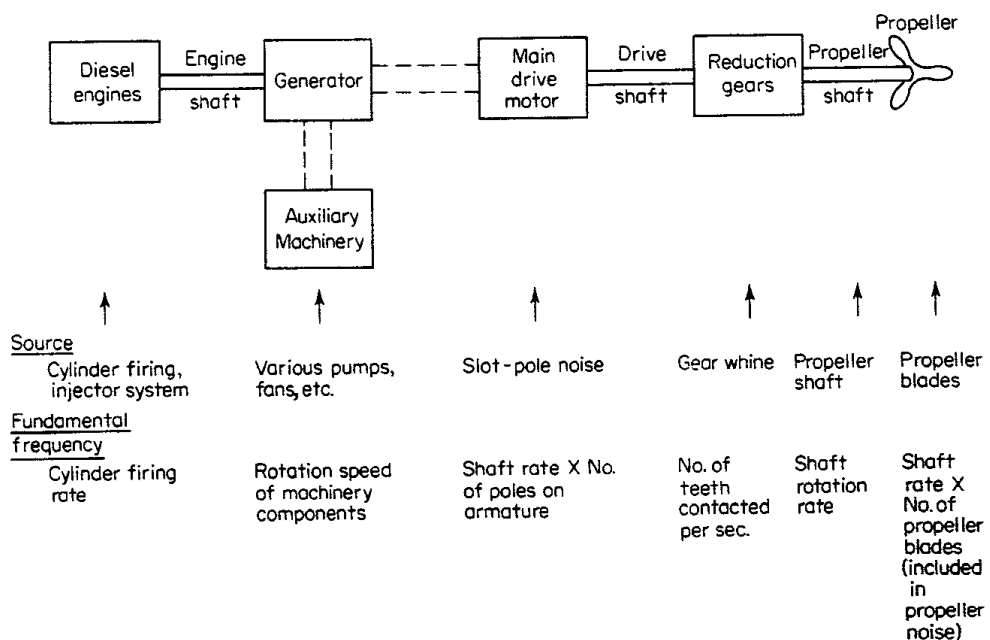


**fig. 10.4** Machinery components and noise sources on a diesel-electric vessel.

quencies to a distant point in the sea. Because of these various effects, the harmonic structure of radiated noise is complex, and the line-component series generated by even a single source of noise is irregular and variable. When many noise sources are present, as in a vessel under way, the machinery-noise spectrum contains line components of greatly different level and origin, and is, consequently, subject to variations of level and frequency with changing conditions of the vessel.

**Propeller noise** Even though the propeller is a part of the propulsion machinery of a vessel, the noise it generates has both a different origin and a different frequency spectrum from machinery noise. As just described, machinery noise originates *inside* the vessel and reaches the water by various processes of transmission and conduction through the hull. Propeller noise, on the other hand, originates *outside* the hull as a consequence of the propeller action and by virtue of the vessel's movement through the water. The location of the sources of noise along the hull is different as well. When a vessel passes close to a nearby hydrophone, it is observed that noises ascribable to the vessel's machinery reach a peak level *before* those originating at the propellers, in keeping with the place of origin aboard the noise-producing vessel.

The source of propeller noise is principally the noise of cavitation induced by the rotating propellers. When a propeller rotates in water, regions of low or negative pressure are created at the tips and on the surfaces of the propeller blades. If these negative (tensile) pressures become high enough, physical rupture of the water takes place and cavities in the form of minute bubbles begin to appear. These cavitation-produced bubbles collapse a short time later—either in the turbulent stream or up against the propeller itself—and in so doing emit a sharp pulse of sound. The noise produced by a great many of such collapsing bubbles is a loud “hiss” that usually dominates the high-frequency end of the spectrum of ship noise when it occurs. The production and collapse of cavities formed by the action of the propeller is called propeller cavitation.

Propeller cavitation may be subdivided into *tip-vortex cavitation*, in which the cavities are formed at the tips of the propeller blades and are intimately associated with the vortex stream left behind the rotating propeller, and *blade-surface cavitation*, where the generating area lies at front or back sides of the propeller blades. Of these two types of cavitation, the former has been found by laboratory measurements with model propellers and by analyses of field data (3) to be the more important noise source with propellers of conventional design.

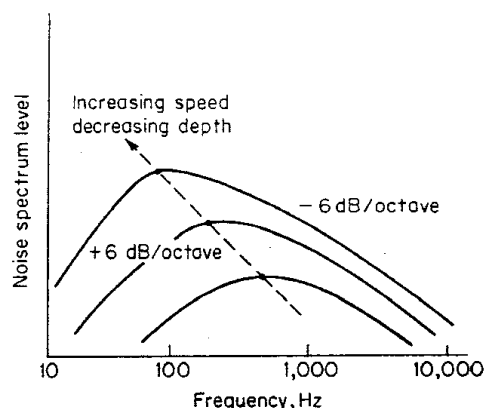
Because cavitation noise consists of a large number of random small bursts caused by bubble collapse, it has a continuous spectrum. At high frequencies, its spectrum level *decreases* with frequency at the rate of about 6 dB/octave, or about 20 dB/decade. At low frequencies, the spectrum level of cavitation noise

increases with frequency, although this reverse slope tends to be obscured in measured data by other sources of noise. There is, therefore, a peak in the spectrum of cavitation noise which, for ships and submarines, usually occurs within the frequency decade 100 to 1,000 Hz. The location of the peak in the spectrum shifts to lower frequencies at higher speeds and (in the case of submarines) at smaller depths. Figure 10.5 shows diagrammatic cavitation-noise spectra for three combinations of speed and depth for a hypothetical submarine. The behavior of the spectral peak is associated with the generation of larger cavitation bubbles at the greater speeds and the lesser depths and with the resulting production of a greater amount of low-frequency sound. On an actual submarine, the variation of propeller noise with speed at a constant depth and with depth at a constant speed is illustrated by the measured curves of Fig. 10.6, which were obtained with a hydrophone placed 4 ft from the propellers on the two submarines, "Hake" and "Hoe."

It has long been known that as the speed of the ship increases, there is a speed at which propeller cavitation begins and the high-frequency radiated noise of the vessel suddenly and dramatically increases. This speed has been called the *critical speed* of the vessel. The submarines measures during World War II were observed to have critical speeds between 3 and 5 knots when operating at periscope depth and to have well-developed propeller cavitation at 6 knots and beyond. At speeds well beyond the critical speed, the noise of cavitation increases more slowly with speed. The noise-speed curve of a cavitating vessel accordingly has a shape like the letter S, with an increase of 20 to 50 dB at high frequencies when the speed is a few knots beyond the critical speed and with a slower rise, at a rate of 1.5 to 2.0 dB/knot, beyond. Measured data illustrating the S-shape characteristics of the noise-speed curve for submarines are shown in Fig. 10.7. The flattening of the curve at high speeds may be surmised to be due to a self-quenching or an internal absorption effect of the cloud of cavitation bubbles. Surface ships do not exhibit the S-shape feature in their noise-speed curves, but show, instead, a more gradual, and nondescript, increase of level with speed.

Cavitation noise is suppressed, and the critical speed is increased, by sub-

**fig. 10.5** Variation of the spectrum of cavitation noise with speed and depth.



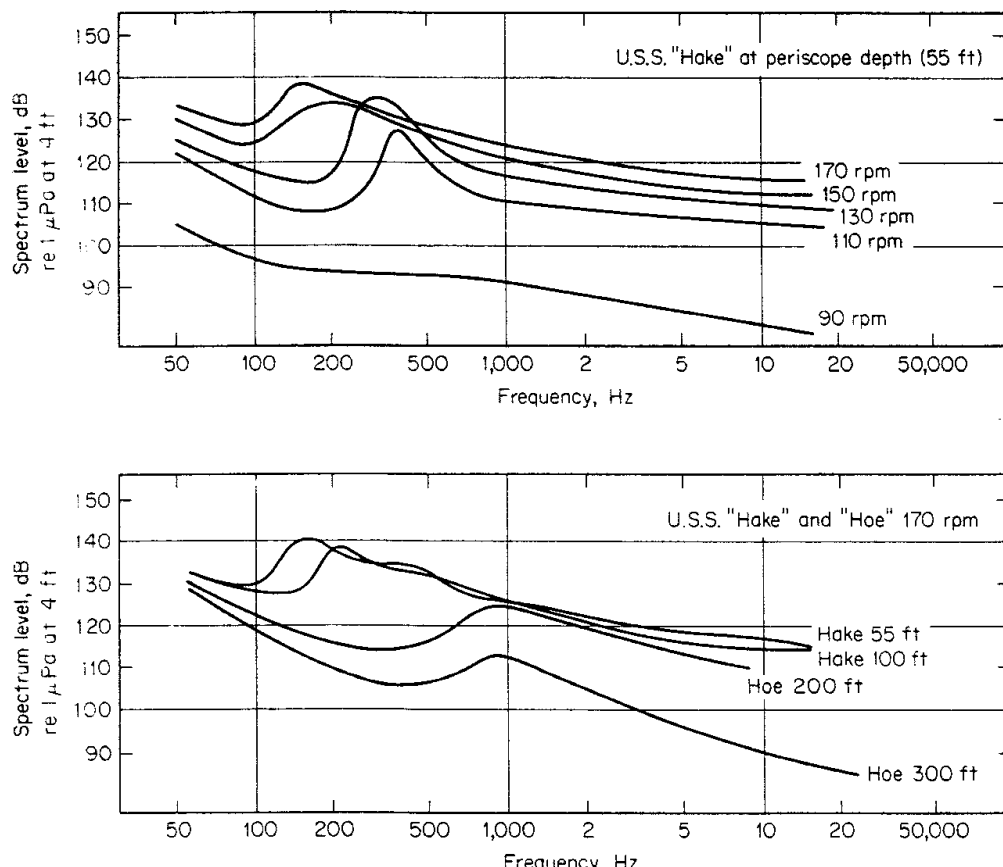


**fig. 10.6** Propeller noise as measured with a hydrophone located 4 ft from the tips of the propeller blades. World War II data on the submarines "Hake" and "Hoe." (Ref. 4.)

merging to a greater depth. This effect has long been well known to submariners as a means to avoid detection. By simple hydrodynamic theory, it is known that the intensity of tip-vortex cavitation is governed by the *cavitation index*, defined by

$$K_T = \frac{p_0 - p_v}{(\frac{1}{2})\rho v_T^2}$$

where  $p_0$  = static pressure at propellers

$p_v$  = vapor pressure of water

$\rho$  = density of water

$v_T$  = tip velocity of propeller blades

When  $K_T$  lies between 0.6 and 2.0, tip cavitation begins; when  $K_T$  is less than 0.2, the occurrence of cavitation is certain; when  $K_T$  is greater than 6.0, cavitation is unlikely. If it is assumed that cavitation begins at some fixed value of  $K_T$  and if  $p_v$  is neglected, we conclude that the critical speed must vary as the square root of the static pressure at the depth of the propellers. This is illustrated by the measurements on "Hake" and "Hoe" previously referred to.

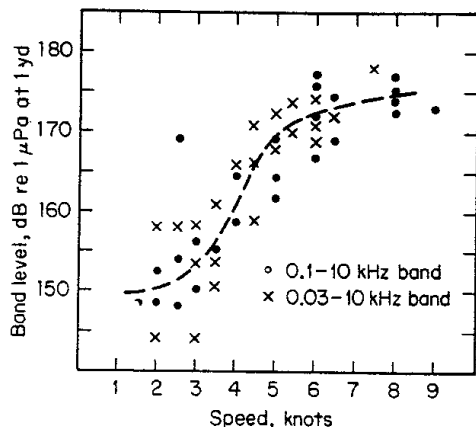


**fig. 10.7** Broadband measurements of the radiated noise of a number of World War II submarines operating at periscope depth. 200-yd data reduced to 1 yd. (Ref. 4.)

For these submarines, Fig. 10.8 shows noise levels in the 10- to 30-kHz band observed with a hydrophone mounted 4 ft from the propeller tips and normalized by dividing by the square root of the hydrostatic pressure at the operating depth.

Although the cavitation noise of submarines is suppressed by depth, the reduction of noise with depth does not occur uniformly. When strong cavitation at high speeds occurs, the radiated noise of submarines is observed to first increase as the submarine dives, before the onset of the normal suppression of noise with depth. Figure 10.9 illustrates the effect of depth on the cavitation noise of a German type XXI submarine. At 8 knots, for example, this particular submarine had to submerge to 150 ft before experiencing the beginning of lower noise levels. This has been called the *anomalous depth effect*, although the term is now a misnomer, since it can be accounted for by theoretical analysis of cavitation-noise formation.

Many factors other than speed and depth affect propeller noise. A damaged propeller makes more noise than an undamaged one. More noise is made during turns and accelerations in speed than during uniform cruising. Truly anomalous conditions are sometimes found. "Singing" propellers generate strong tones between 100 and 1,000 Hz as a result of resonant excitation of the propeller by vortex shedding. The sound made by a singing propeller is

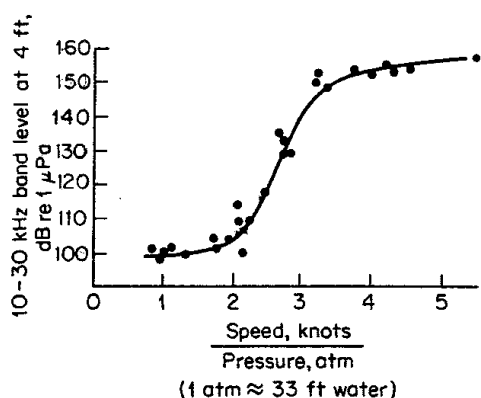


**fig. 10.8** Normalized curves of cavitation noise. (Ref. 4.)

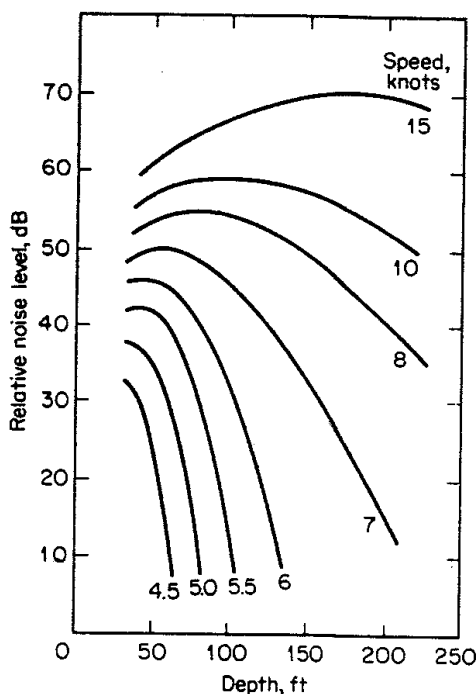


**fig. 10.9** The anomalous depth effect, illustrated by measured wartime data at audio frequencies on a type XXI German submarine. Relative levels only.

very intense and can be heard underwater at distances of many miles. When it occurs, it can readily be cured, either by using a propeller made of a high-damping alloy or more simply, by changing the shape of the tips of the propeller blades (6).

Propeller noise is not radiated uniformly in all directions, but has a characteristic directional pattern in the horizontal plane around the radiating vessel. Less noise is radiated in the fore-and-aft directions than abeam, probably because of screening by the hull in the forward direction and by the wake at the rear. The dips in the pattern generally occur within  $30^\circ$  of the fore-and-aft direction, with the bow dip a few decibels deeper than the dip at the stern. A directivity pattern in the 2.5- to 5-kHz band for a freighter traveling at 8 knots is given in Fig. 10.10, where the contours show the locations, relative to the ship, of equal sound intensity on the bottom in 40 ft of water.

Propeller noise has been known for many years to be amplitude-modulated and to contain "propeller beats," or periodic increases of amplitude, occurring at the rotation speed of the propeller shaft, or at the propeller blade frequency equal to the shaft frequency multiplied by the number of blades. Propeller beats have long been used by listening observers for target identification and for estimating target speed. They have been observed (9) to be present in the noise of torpedoes as well as in the noise of ships and submarines. Propeller beats are most pronounced at speeds just beyond the onset of cavitation and diminish in the great roar of steady cavitation noise at high speeds.

Propeller noise, with its origin in the flow of water about the propeller, creates tonal components in addition to the continuous spectrum of cavitation

noise. One tonal component is the "singing" tone of a vibrating singing propeller just mentioned. More normally, at the low-frequency end of the spectrum, propeller noise contains discrete spectral "blade-rate" components occurring at multiples of the rate at which any irregularity in the flow pattern into or about the propeller is intercepted by the propeller blades. The frequency of the blade-rate series of line components is given by the formula

$$f_m = mns$$

where  $f_m$  is the frequency, in hertz, of the  $m$ th harmonic of the blade-rate series of lines,  $n$  is the number of blades on the propeller, and  $s$  is the propeller rotation speed in number of turns per second. In one Russian experiment (10), these "blade" lines were observed with and without the emission of air bubbles around the propeller. At speeds when cavitation was well developed, they were found to be intimately associated with the cavitation process; in addition, line components not falling in the expected series were observed as well. Blade-rate line components were long ago observed (11) to be the dominant source of the noise of submarines in the 1- to 100-Hz region of the spectrum. It should be noted in passing that line components generated by the rotating propeller shaft—a form of machinery noise—fall in the same harmonic series as the blade-rate lines. Propeller noise, like machinery noise, can excite and be reinforced by the vibrational response of mechanical structures in the vicinity of the propeller.

The propellers of surface ships cavitate strongly at normal operating speeds. As a result, their low-frequency radiated noise spectrum is dominated by the blade-rate series of line components at the propeller blade frequency and its harmonics. Two examples of narrow-band spectra of surface ships—one a freighter, the other a supertanker—are shown in Fig. 10.11. The blade-rate series, with a fundamental frequency of about 8 Hz for both ships, is the principal feature of their radiation below about 50 Hz. The blade-rate series of

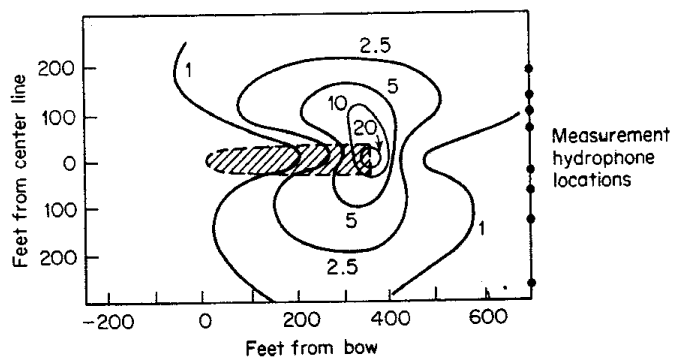


**fig. 10.10** Equal pressure contours on the bottom in 40 ft of water of a freighter at a speed of 8 knots. Contour values are pressures, in dynes per square centimeter in a 1-Hz band, at a point on the bottom, measured in the octave band, 2,500 to 5,000 Hz. (Ref. 8.)

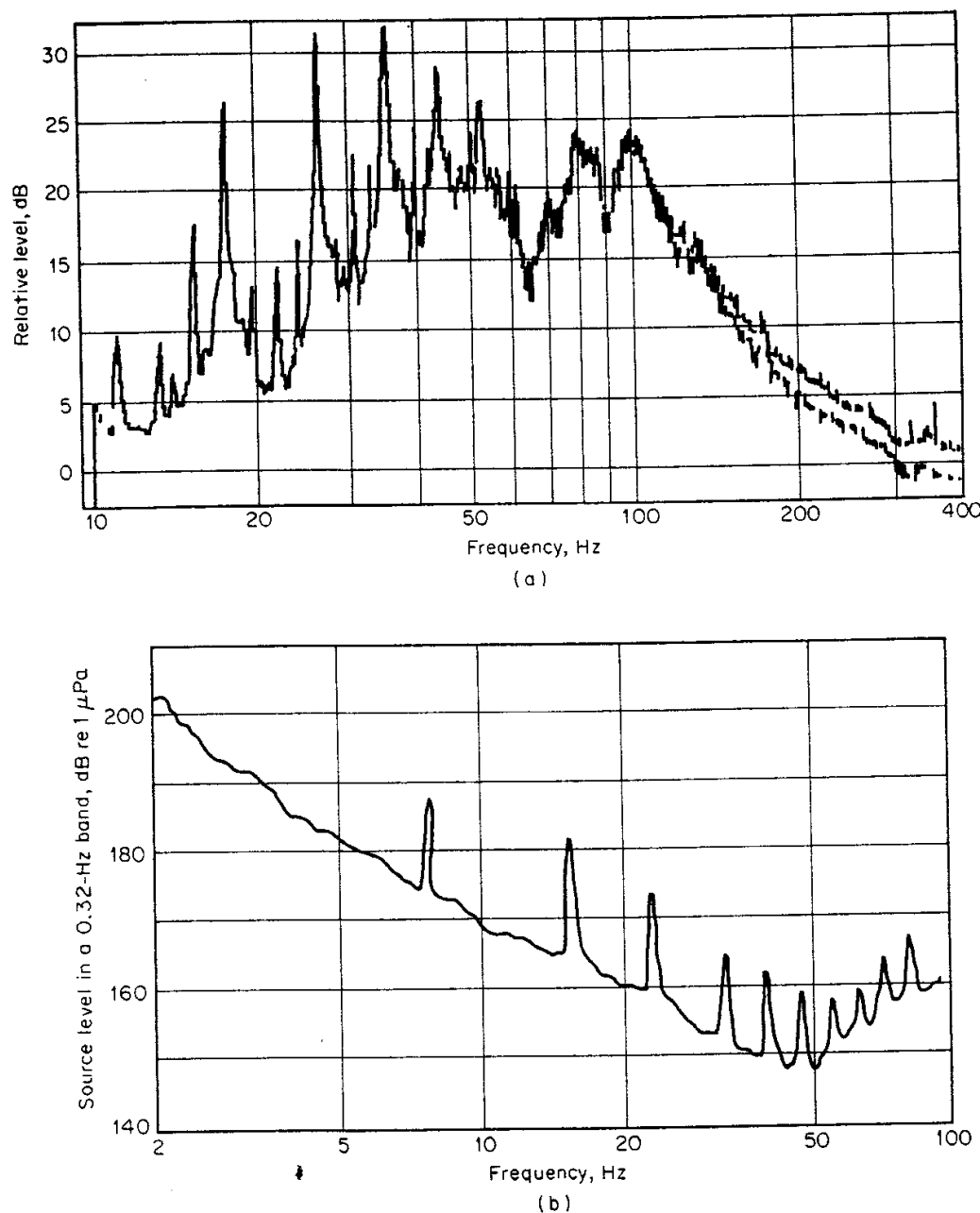


**fig. 10.11** Narrow-band spectra of two merchant ships. (a) A bulk cargo ship, dead-weight tons 12,200, speed 14.7 knots, analysis bandwidth 0.1 Hz. (b) A supertanker, "World Dignity," deadweight tons 271,000, speed 16 knots, shaft rate 1.44 rps, number of propeller blades 5, analysis bandwidth 0.32 Hz. (Ref. 7.)

line components are evenly spaced at 8-Hz intervals, although they do not appear to be so because of the logarithmic frequency scale.

The emission of air around the propeller is an effective practical way of reducing propeller noise. When cavitation occurs, air bubbles emitted in the neighborhood of the cavitating propeller replace the water-vapor bubbles created by the physical rupture of the water. The bubbles of air collapse with less force and thereby soften the effect of collapse caused by cavitation.

**Hydrodynamic noise** Hydrodynamic noise originates in the irregular and fluctuating flow of fluid past the moving vessel. The pressure fluctuations associated with the irregular flow may be radiated directly as sound to a distance, or, more importantly, may excite portions of the vessel into vibration. The noise created by the turbulent boundary layer is sometimes called "flow noise."

The excitation and reradiation of sound by various structures of the vessel are an important source of hydrodynamic noise. One kind of such noise is propeller singing, mentioned above. In addition, the flow of fluid may have an "aeolian harp" effect on other structures of the vessel, such as struts, and excite them into a vibrational resonance. Like Helmholtz resonators, cavities may be excited by the fluid flow across their openings, in the manner that a bottle can be made to "sing" by blowing over its opening. These resonant occurrences can sometimes be easily diagnosed and curative measures applied.

The form of hydrodynamic noise called *flow noise* is a normal characteristic of flow of a viscous fluid and occurs in connection with smooth bodies without protuberances or cavities. Flow noise can be radiated directly or indirectly as flow-induced vibrations of plates or portions of the body. The former—direct radiation to a distance—is an inefficient process not likely to be important at the low Mach numbers (ratio of speed of the vessel to the speed of sound in water) reached by vessels moving through water, since it is of quadrupole origin and is therefore not efficiently radiated to a distance. The latter process—flow excitation of a nonrigid body—depends on (1) the properties of the pressure fluctuation in the turbulent boundary layer, (2) the local response of the structure to these fluctuations, and (3) the radiation of sound by the vibrating portion. The response of plates to a random pressure field has been studied theoretically by Dyer (12). Flow noise is a more important contribution to self-noise than to radiated noise, and will be discussed more fully as a part of self-noise.

Other kinds of hydrodynamic noise are the roar of the breaking bow and stern waves of a moving vessel and the noise originating at the intake and exhaust of the main circulating water system.

Under normal circumstances, hydrodynamic noise is likely to be only a minor contributor to radiated noise, and is apt to be masked by machinery and propeller noises. However, under exceptional conditions, such as when a structural member or cavity is excited into a resonant source of line-component noise, hydrodynamic noise becomes a dominant noise source in the region of the spectrum in which it occurs.

#### **10.4 Summary of the Sources of Radiated Noise**

Of the three major classes of noise just described, machinery noise and propeller noise dominate the spectra of radiated noise under most conditions. The relative importance of the two depend upon frequency, speed, and depth.

This is illustrated by Fig. 10.12 which shows the characteristics of the spectrum of submarine noise at two speeds. Figure 10.12a is a diagrammatic spectrum at a speed when propeller cavitation has just begun to appear. The low-frequency end of the spectrum is dominated by machinery lines, together with the blade-rate lines of the propeller. These lines die away irregularly with increasing frequency and become submerged in the continuous spectrum of propeller noise. Sometimes, as indicated by the dotted line, an isolated high-frequency line or group of lines appear amid the continuous background of propeller noise. These high-frequency lines result from a singing propeller or from particularly noisy reduction gears, if the vessel is so equipped.

At a higher speed (Fig. 10.12b), the spectrum of propeller noise increases and shifts to lower frequencies. At the same time, some of the line components increase in both level and frequency, whereas others, notably those due to auxiliary machinery running at constant speed, remain unaffected by an increase in ship speed. Thus, at the higher speeds, the continuous spectrum of propeller cavitation overwhelms many of the line components and increases its dominance over the spectrum. A *decrease* in depth at a constant speed has, as indicated above, the same general effect on the propeller-noise spectrum as an *increase* in speed at constant depth.

For a given speed and depth, therefore, a "crossover" frequency may be said to exist, below which the spectrum is dominated by the line components of the ship's machinery plus its propeller, and above which the spectrum is in large part the continuous noise of the cavitating propeller. For ships and submarines, this frequency lies roughly between 100 and 1,000 Hz, depending on the individual ship and its speed and depth; for torpedoes, the crossover frequency is higher and the line components extend to higher frequencies because of the generally higher speeds of operation of torpedo machinery.

For illustrating the nature of ship spectra, a frequency-time analyzer, such as that used for speech analysis, is particularly convenient. This kind of analyzer, called a sound spectrograph, was first described by Koenig, Dunn, and

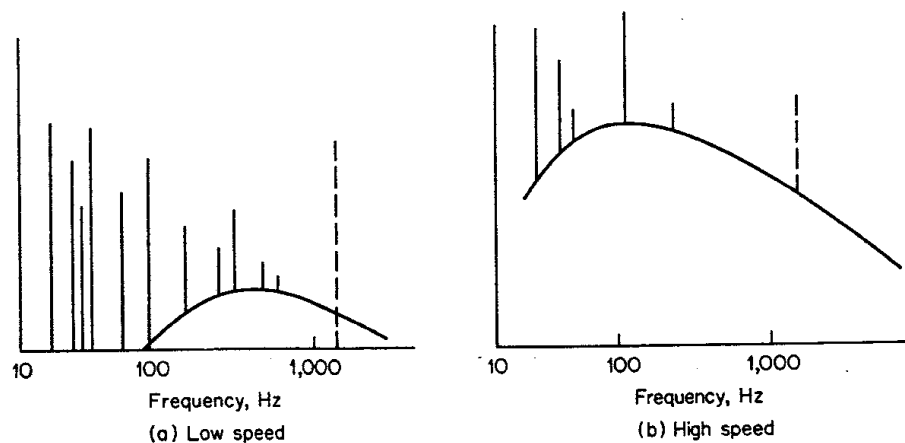


**fig. 10.12** Diagrammatic spectra of submarine noise at two speeds.

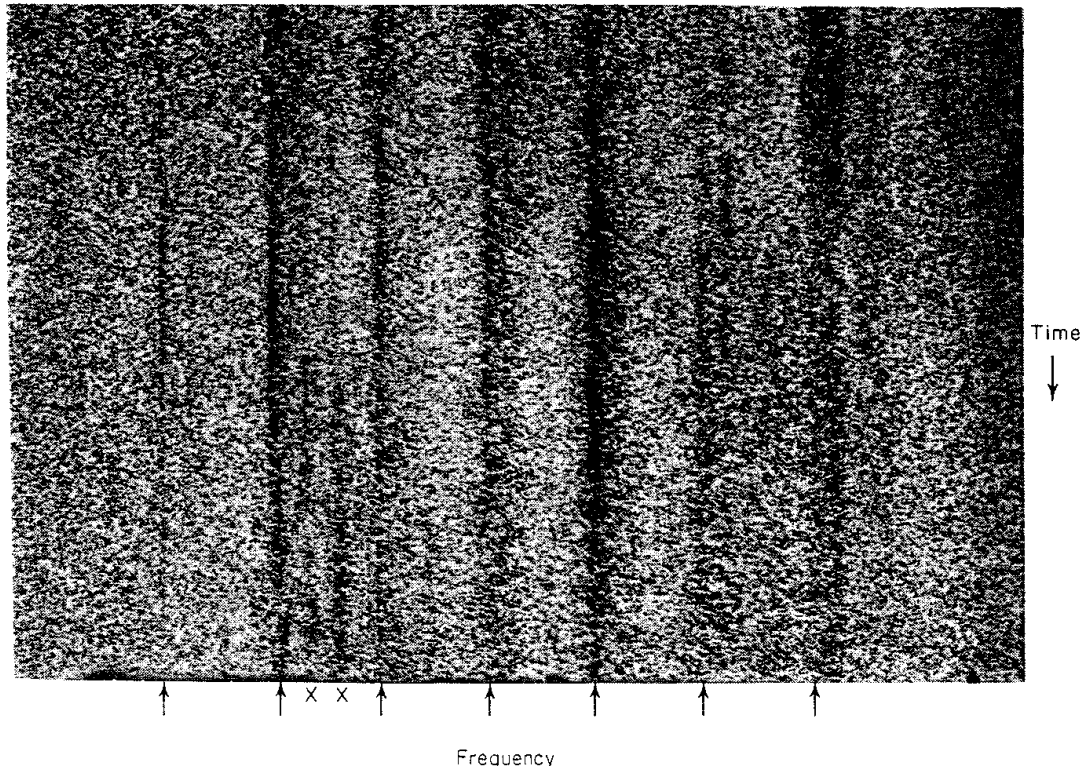


**Fig. 10.13** Sound spectrogram of a surface ship at a speed of 11 knots.

Lacy (13) and is widely used for the analysis of speech (14). It gives a plot of frequency against time and shows the intensity of the sound in the analysis bandwidth by a darkening of the record. Figure 10.13 is an example of a sound spectrogram of the noise of a large surface ship as it passed over a deep hydrophone. The frequency scale extends from 0 to 150 Hz, and the duration of the recording was approximately  $\frac{1}{2}$  hour. The harmonic series of line components marked by the arrows are blade-rate lines. The lines marked X are of unknown origin.

An interesting recent observation is that the noise spectrum of fishing boats, when trolling for fish at a speed of 10 to 12 knots, apparently influences the size of their catch of fish. Boats having spectral peaks above 1,500 Hz in their noise radiation were found to have an appreciably smaller catch of albacore than similar boats fishing at the same time and location, but having no strong high-frequency radiation, as if the high-frequency tones were scaring away, rather than luring, this particular species of fish (15).

### 10.5 Total Radiated Acoustic Power

It is of interest to determine how much total acoustic power is radiated by a moving vessel and how it compares with the power used by the vessel for propulsion through the water. This can easily be done by integration of the spectrum. When the spectrum is continuous and has a slope of  $-6$  dB/octave,

the intensity  $dI$  in a small frequency band  $df$  centered at frequency  $f$  can be written as

$$dI = \frac{A}{f^2} df$$

where  $1/f^2$  represents the  $-6$  dB/octave slope of the spectrum and  $A$  is a constant.

By integrating between any two frequencies  $f_1$  and  $f_2$ , the total intensity between  $f_1$  and  $f_2$  becomes

$$I_{(f_1, f_2)} = \int_{f_1}^{f_2} \frac{A}{f^2} df = A \left( \frac{1}{f_1} - \frac{1}{f_2} \right)$$

Letting  $f_2 \rightarrow \infty$ , we find that the total intensity for all frequencies above  $f_1$  is

$$I_{\text{tot}} = \frac{A}{f_1}$$

Recognizing that  $A/f_1^2$  is the intensity in a 1-Hz band centered at frequency  $f_1$ , we note that

$$I_{\text{tot}} = (I_{f_1})(f_1)$$

where  $10 \log I_{f_1}$  is the spectrum level at  $f_1$ .

As an example (Fig. 10.14), we take a spectrum having a spectrum level of 160 dB at 200 Hz with slope of  $1/f^2$  above this frequency. The total level of the radiated noise above 200 Hz becomes

$$\begin{aligned} 10 \log I_{\text{tot}} &= 10 \log I_{f_1} + 10 \log f_1 \\ &= 160 + 23 = 183 \text{ dB} \end{aligned}$$

The total acoustic power represented by this source level, if assumed to be radiated nondirectionally, amounts to 12 watts. It may be observed that if the continuous spectrum extended below 200 Hz to zero Hz at the constant level of 160 dB, as shown by the dashed line in Fig. 10.14, the total radiated power

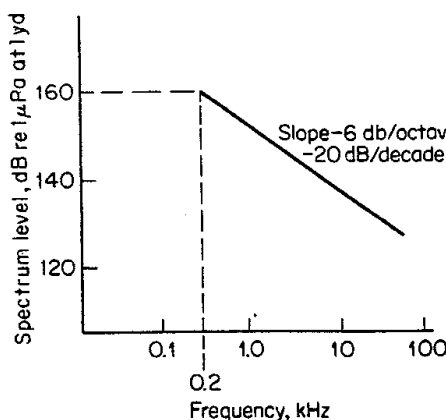


**fig. 10.14** Idealized spectrum integrated to obtain the total acoustic power radiated by a vessel.

at frequencies *below* 200 Hz would also be 12 watts, and the total radiation over the entire spectrum would become 24 watts.

If the vessel is regarded as a mechanical source of sound, this radiated power may be compared with the shaft horsepower developed by the radiating vessel. Let us assume that the selected spectrum corresponds to that of a destroyer at a speed of 20 knots. At this speed, an average destroyer is known to generate a shaft horsepower of approximately 14,000, or about  $10^7$  watts. Comparing this power with that radiated as sound in the continuous part of the spectrum, we observe that the efficiency of the vessel as a sound producer is only of the order of  $10^{-6}$ . Surface ships are therefore extremely inefficient radiators of sound in terms of the developed shaft power of their propulsion system, even when allowance is made for the power represented by the tonal components of the radiation.

### **10.6 Radiated-Noise Levels**

During World War II, the United States and Great Britain, motivated by the design needs of acoustic mines, made a great many measurements of the radiated noise of surface ships at a number of acoustic ranges. At locations such as Wolf Trap, Virginia; Treasure Island, California; Thames River, New London, Connecticut; Puget Sound, Washington; and Waipio Point, Honolulu, Hawaii, literally thousands of "runs" on hundreds of ships of all types were made. Far fewer wartime measurements were made on submarines and torpedoes. Although much of this old data is obsolete because many of the vessels measured are no longer in existence, the general run of sound levels and their variation with speed, frequency, and depth will still be pertinent to many presently existing vessels, if only as a guide for approximation.

In the following sections, a few extracts have been selected from this vast wartime literature to illustrate the main quantitative aspects of the subject. Particular attention is called to two excellent summaries on the radiated-noise levels of submarines (4) and surface ships (5) and to one of the NDRC Summary Technical Reports (17) on the radiated noise of torpedoes.

**Surface ships** Table 10.2 shows typical radiated source levels for various classes of ships current during World War II, as reduced to 1 yd from an original reference distance of 20 yd by the conventional assumption of spherical spreading.

In graphical form, Fig. 10.15 gives in the upper set of curves average spectrum levels at 5 kHz as a function of speed for a number of classes of surface ships. The lower curve is a relative spectrum for use in obtaining values at other frequencies. The standard deviation (in decibels) of individual measurements from the line drawn is indicated for each class of ships.

Empirical expressions also were devised to fit the mass of data. In terms of the propeller-tip speed  $V$  in feet per second, the displacement tonnage  $T$  of

**table 10.2 Typical Average Source Levels for Several Classes of Ships in dB vs. 1  $\mu$ Pa in a 1-Hz Band at 1 yd.\* (Ref. 5)**

Frequency	Freighter, 10 knots	Passenger, 15 knots	Battleship, 20 knots	Cruiser, 20 knots	Destroyer, 20 knots	Corvette, 15 knots
100 Hz	152	162	176	169	163	157
300 Hz	142	152	166	159	153	147
1 kHz	131	141	155	148	142	136
3 kHz	121	131	145	138	132	126
5 kHz	117	127	141	134	128	122
10 kHz	111	121	135	128	122	116
25 kHz	103	113	127	120	114	108

\* Originally reported at 20 yd.

the ship, the frequency  $F$  in kilohertz, and distance  $D$  in yards, the source level for the average radiated noise of large ships was found to be given by

$$SL = 51 \log V + 15 \log T - 20 \log F + 20 \log D - 13.5$$

This formula, based on 157 runs of 77 ships of 11 different classes (mostly freighters, tankers, and large warships), was found to fit individual measurements to a standard deviation of 5.4 dB. It is applicable only at frequencies above 1 kHz where propeller cavitation is the principal source of noise. A more convenient formula, in terms of the speed of the ship, for use when information concerning the propeller-tip speed is lacking, was found to be

$$SL = 60 \log K + 9 \log T - 20 \log F + 20 \log D + 35$$

In this formula  $K$  is the forward speed of the ship in knots. This expression was found to fit the measured levels of passenger ships, transports, and warships at a frequency of 5 kHz to a standard deviation of 5.5 dB, but to be unreliable for freighters and tankers.

Figure 10.16 shows the radiated noise of a postwar destroyer as a function of speed for three frequencies. World War II levels as read from Fig. 10.15 for 500 and 5,000 Hz are also plotted. The residual levels at speeds less than 10 knots are caused by auxiliary and other non-speed-dependent machinery aboard the vessel.

At the low-frequency end of the spectrum, Fig. 10.17 illustrates other measured data (1) on four destroyers measured in the frequency bands 2 to 17 Hz and 7 to 35 Hz. The levels shown are band levels giving the total intensity measured in each band. The levels of any individual line components in the spectrum would be an indefinite number of decibels higher than the level indicated, depending on the number and relative strengths of the lines occurring in each band.

The distribution of radiated levels in the octave 75 to 150 Hz, based on a large number of ship runs at a number of wartime acoustic ranges (18), is shown in Fig. 10.18. In terms of the spectrum level at 1 yd, the ordinate in this figure gives the percentage of runs in which the measured level exceeded that

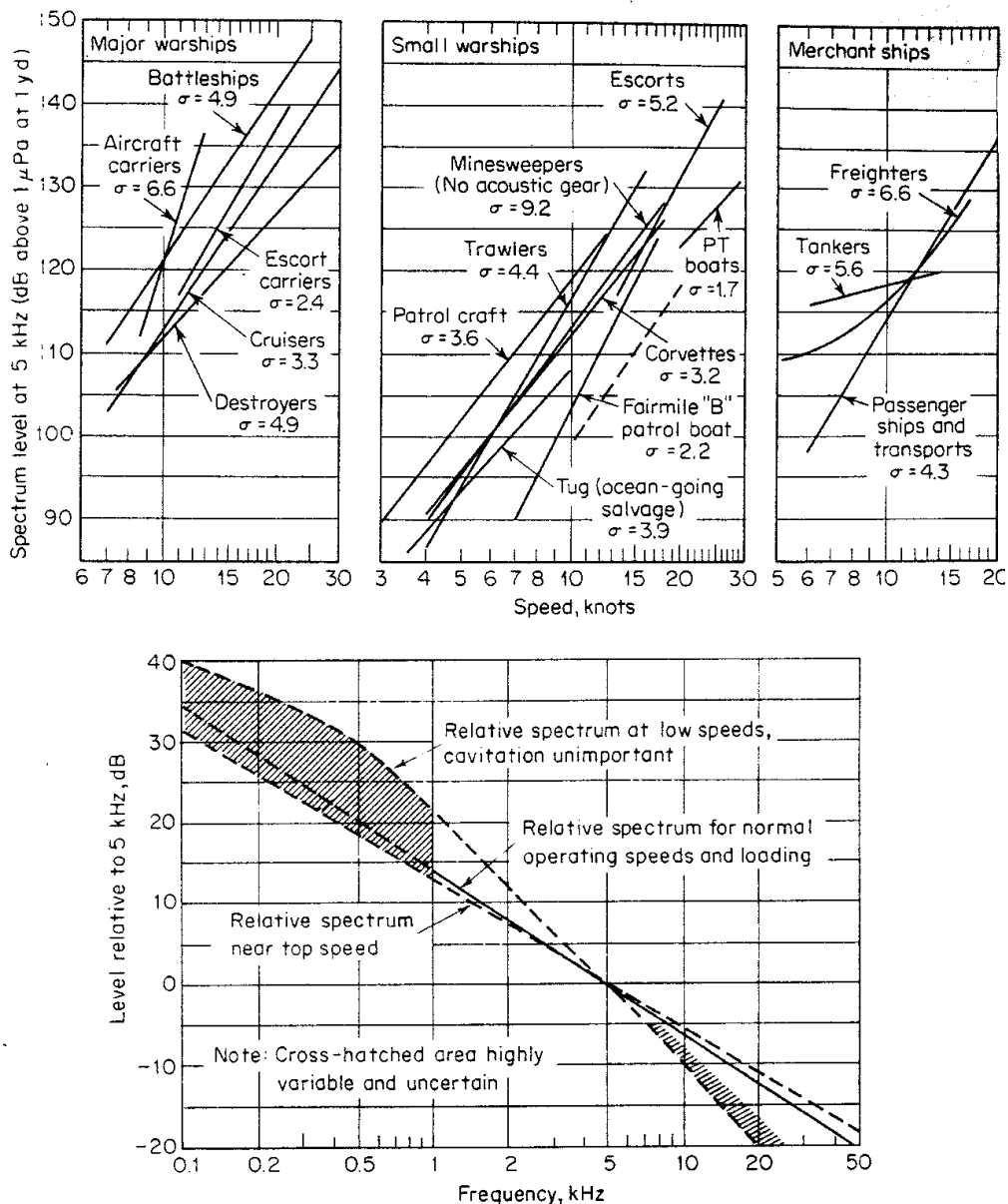


**Fig. 10.15** Average radiated spectrum levels for several classes of surface ships. (Ref. 5.)

shown on the horizontal scale. The levels have been reduced to spectrum levels at 1 yd from octave-band data given at a distance of 100 ft beneath the ship.

Regarding such averaged, reduced data, it should be borne in mind that individual ships occasionally deviate greatly from the average levels. Moreover, at low frequencies, the use of spectrum levels is questionable because of the likely tonal content of the radiated sound. Finally, the data are entirely based on measurements on the bottom in shallow water averaging 20 yd in depth, and do not necessarily indicate the levels that would be observed in deep water.

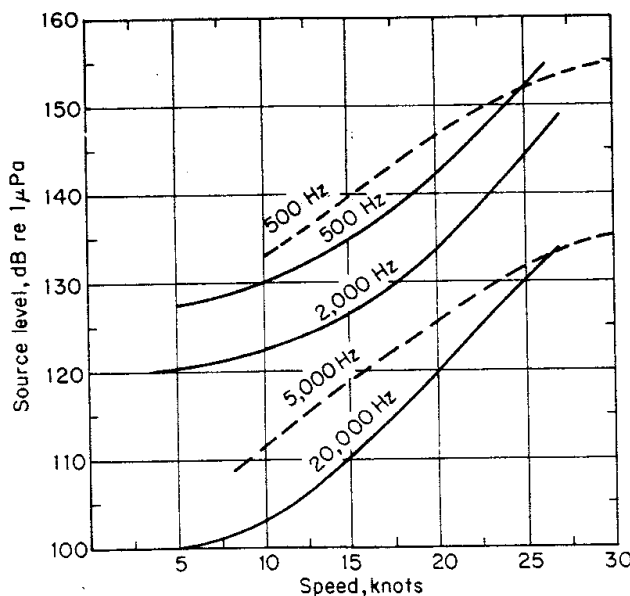


**fig. 10.16** Solid curves, noise level versus speed at 0.5, 2, and 20 kHz for a postwar destroyer. Dashed curves, noise level versus speed for World War II destroyers from Fig. 10.15.

A quantitative model for the radiation at the blade-rate fundamental frequency has been presented by Gray and Greeley (16). Based on this model, expressions for the source level at the design speed of the blade-rate radiation of merchant ships were found to be

$$\begin{aligned} \text{SL}_D &= 6 + 70 \log L \pm 11 \text{ dB} \\ &= 92 + 94 \log D \pm 8 \text{ dB} \end{aligned}$$

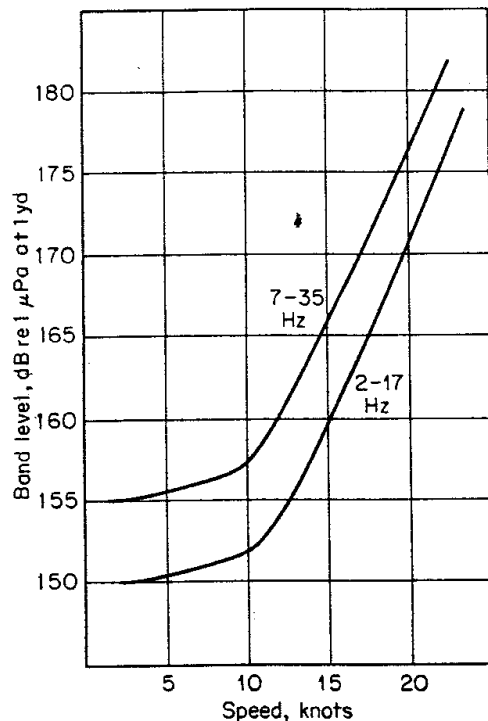
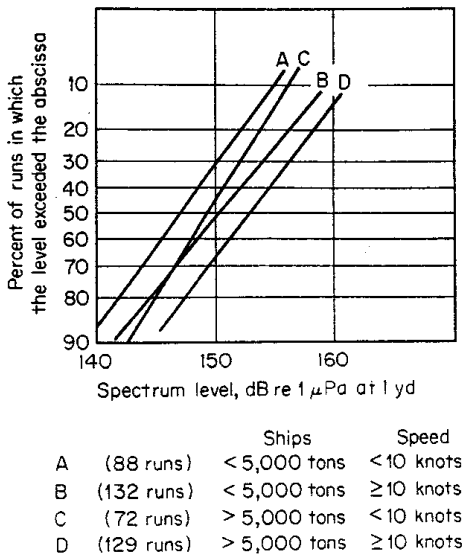


**fig. 10.17** Average levels on four destroyers in two frequency bands as measured on the bottom in 105 ft of water at the Puget Sound acoustic range. Values reduced from 105 ft to 1 yd. (Ref. 1.)

**fig. 10.18** Cumulative distribution curves of the radiated noise of surface ships in the octave 75 to 150 Hz. (Ref. 18.) Horizontal scale is spectrum level obtained from band levels by subtracting 10 log bandwidth and reduced from 100 ft to 1 yd by assuming spherical spreading.



where  $L$  and  $D$  are the ship length and propeller blade diameter, both in meters. The uncertainty values of 11 and 8 dB are the estimated standard deviation of a prediction based on these expressions, relative to calculated values based on the model and the known characteristics—such as ship length, draft, and propeller size—of merchant ships. The source level  $SL_D$  is the dipole source level at 1 meter. From it, the free-field source level can be found from

$$SL = SL_D + 6 + 20 \log kd$$

where  $k$  is the wave number  $2\pi/\lambda = 2\pi f/c$ , and where  $d$  is the operating depth of the propeller. For merchant ships the blade-rate fundamental frequency  $f$  falls largely in the range 6.7 to 10.0 Hz, and lies near 8 Hz for many ships. However, no data are available to compare the predictions based on this hydrodynamic model with noise measurements on actual ships under way at sea.

**Submarines** The available data on submarines are much less extensive and involve only a few submarines under limited operating conditions. Figure 10.19 shows average spectra for three World War II submarines at periscope depth (about 55 ft to the keel) and at the surface. Spectra appreciably higher, though similar in shape, were obtained for the single British submarine, HMS "Graph," as illustrated in Fig. 10.20.

The effect of depth on the radiated levels of submarines is illustrated in Fig. 10.21, which shows the reduction in noise involved in submerging from periscope depth to 200 ft. The effect of depth may also be determined from Fig. 10.8, given previously, in which the spectrum level was plotted as a function of speed divided by the square root and the hydrostatic pressure. These depth

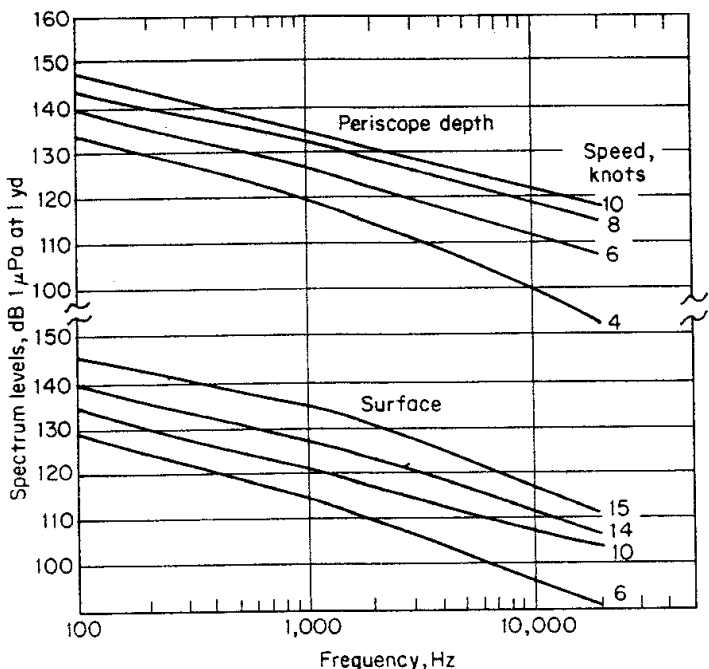


**fig. 10.19** Smoothed spectra of three submarines (USS S-48, "Hake," and "Runner") on electric drive. Levels, originally reported at 200 yd, reduced to 1 yd. (Ref. 4.)

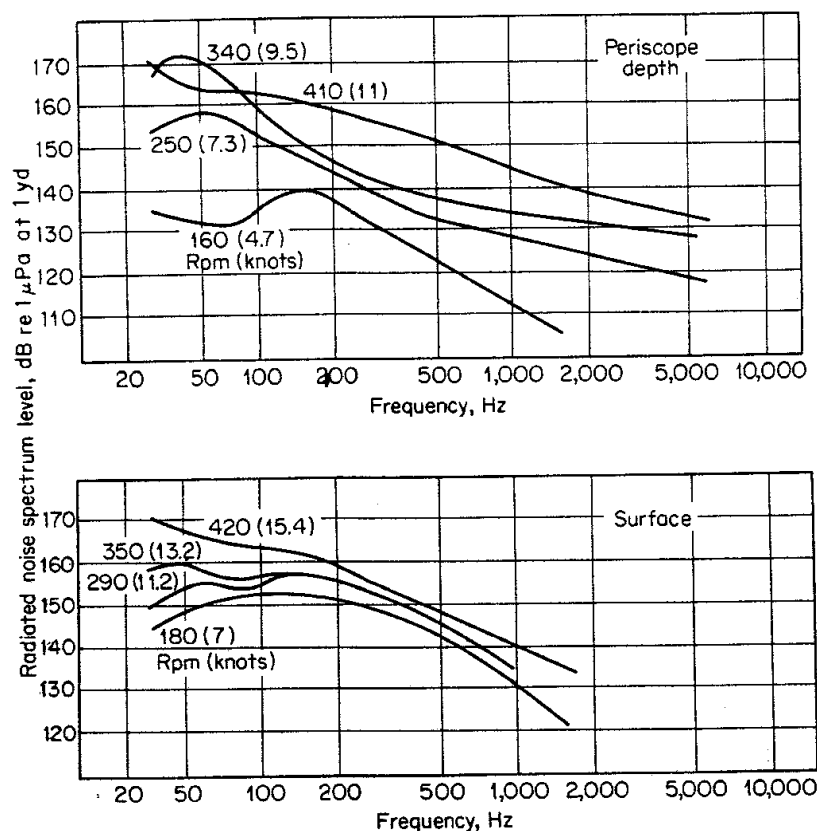


**fig. 10.20** Radiated-noise spectra of the British submarine HMS "Graph" at periscope depth and on the surface. 200-yd reported data reduced to 1 yd. (Ref. 4.)

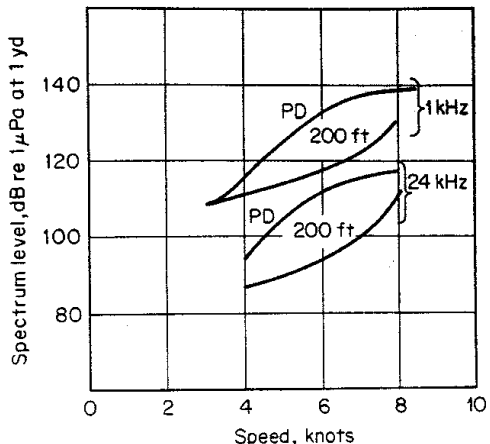


**fig. 10.21** Representative submarine-radiated-noise spectrum levels at two frequencies at periscope depth (PD) and at a depth of 200 ft on electric drive. (Ref. 19.)

effects occur only for the noise produced by the cavitating propeller; when machinery noise predominates, as at very low speeds or very low frequencies, little or no quieting on submergence to deep depths is expectable.

**Torpedoes** Figure 10.22 illustrates measured radiated-noise spectra over a wide frequency range for a variety of torpedoes running at different speeds, and Fig. 10.23 is a compilation of torpedo noise levels at 25 kHz as a function of speed. Although the torpedoes listed had a variety of propulsion systems, the noise radiated at kilohertz frequencies must be presumed to be dominated by propeller cavitation.

### 10.7 Cautionary Remark

The potential user of the numerical data presented in this chapter will discover that it represents, for the most part, World War II measurements on obsolete vessels. Although it may be useful for first-cut problem solving and for showing qualitative effects, it must be stressed that the source level data will be almost useless for practical work. The subject of the radiated noise of

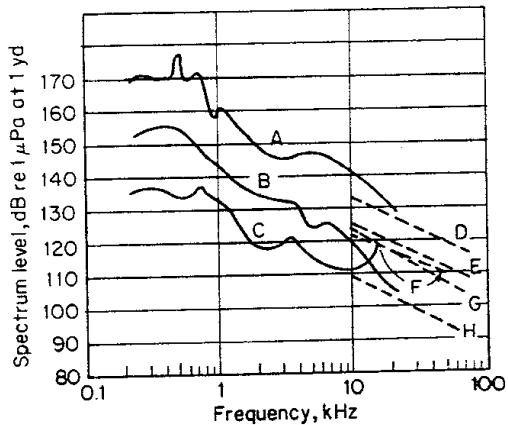


**fig. 10.22** Noise spectra of various World War II torpedoes running at shallow depths. [(A-C), Ref. 20; (D-H), Ref. 17.] (A) Highest measured values for several U.S. torpedoes. (B) Japanese Mark 91, 30 knots. (C) U.S. Mark 13, 30 knots. (D) U.S. Mark 14, 45 knots. (E) British Mark VIII, 37 knots. (F) U.S. Mark 18, 30 knots. (G) U.S. Mark 13, 33 knots. (H) British Mark VIII, 20 knots.

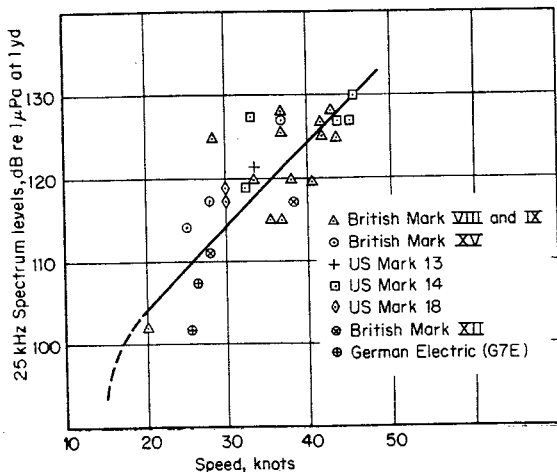


fig. 10.23 25-kHz spectrum levels of various torpedoes as a function of speed. The straight line has a slope of 1 dB/knot increase of speed. (Ref. 17.)

vessels is, and has long been, almost completely classified on security grounds, and the reader must resort to the classified literature for the information and data needed on modern existing vessels.

## REFERENCES

1. Pomerantz, J., and G. F. Swanson: Underwater Pressure Fields of Small Naval Vessels in the 2-17 and 7-35 cps Bands at the Puget Sound Acoustic Ranges, *U.S. Nav. Ord. Lab. Rep.* 1022, 1945.\*
2. Ship Acoustical Surveys, *U.S. Navy Bur. Ships Rep.* NAVSHIPS 250-371, no date.
3. Strasberg, M., and W. J. Sette: Measurements of Propeller Noise on Three Submarines of the SS212 Class, *David Taylor Model Basin Rep.* R-205, 1944.\*
4. Knudsen, V. O., R. S. Alford, and J. W. Emling: Survey of Underwater Sound No. 2: Sounds from Submarines, *Nat. Def. Res. Comm. Div. 6 sec. 6.1*-NDRC-1306, 1943.\*
5. Dow, M. T., J. W. Emling, and V. O. Knudsen: Survey of Underwater Sound No. 4: Sounds from Surface Ships, *Nat. Def. Res. Comm. Div. 6 sec. 6.1*-NDRC-2124, 1945.\*
6. Ross, D.: "Mechanics of Underwater Noise," Sec. 9.5, Pergamon Press, New York, 1976.
7. Cybulski, C. J.: Probable Origin of Measured Supertanker Noise Spectra, *Conf. Proc. OCEANS '77*, October 1977.
8. Pomerantz, J.: An Analysis of Data in the 2500-10,000 cps Region Obtained at the Wolf Trap Range, *U.S. Nav. Ord. Lab. Rep.* 733, 1943.\*
9. Irish, G.: "Low Frequency Modulation of the Supersonic Pressure Field of Torpedoes," U.S. Naval Ordnance Laboratory unpublished memorandum, 1944.\*
10. Aleksandrov, I. A.: Physical Nature of the Rotation Noise of Ship Propellers in the Presence of Cavitation, *Sov. Phys. Acoust.*, 8(1):23 (July-September 1962).
11. Jaques, A. T.: Subsonic Pressure Variations Produced by Submarines, *U.S. Nav. Ord. Lab. Rep.* 744, 1943.\*
12. Dyer, I.: Response of Plates to a Decaying and Convecting Random Pressure Field, *J. Acoust. Soc. Am.*, 31:922 (1959).

## **design and prediction in sonar systems**

### **13.1 Sonar Design**

The various applications of the sonar equations fall into two general classes. One involves *sonar design*, where a sonar system is to be devised to accomplish a particular purpose. In a sonar design problem, a set of sonar parameters that will provide the desired performance must be found. This can usually be expressed in terms of *range*, through its counterpart, by some assumed propagation condition, the parameter *transmission loss*.

This selection of parameters in sonar design is beset with difficulties arising from constraints that are of economic, mechanical, or electrical origin. Sonar systems must often be primarily inexpensive, as in expendable units such as sonobuoys. Sometimes they must fit in a confined space, as in a torpedo, where the maximum size of the transducer to be used is dictated by dimensions over which the design engineer has no control. Sonar systems may also have to be designed to consume only a limited amount of electric power, as in a battery-powered underwater acoustic beacon, where a limitation is placed on the available acoustic power output and the pulse length. Generally speaking, one or more of the parameters related to the system itself, such as directivity index or source level, may be fixed or limited by practical considerations not under the designer's control. The final design is achieved by "trade offs" and compromises between performance and achievable values of the equipment parameters. It

is reached by what amounts to repeated solutions of the sonar equations—by a trial-and-error process wherein successive adjustments of parameters and performance are made until a reasonably satisfactory compromise is reached. Complications arise when the desired performance involves two or more of the variables. For example, a certain search rate, or area searched for a target in a given time, may be desired; this is a function of both range and beam width. In such problems, a number of trial solutions of the sonar equations will be needed to give a “feel” for the best set of conditions.

Sometimes the fortunate design engineer has a free choice of the operating frequency, or the operating frequency band, of the sonar under design. Then the choice will be influenced by the optimum frequency appropriate to the desired maximum range of the sonar. This choice will be considered in a section to follow.

In an active-sonar design problem, the design will depend in part on whether the echoes occur in a background of noise or reverberation. In active-sonar systems, the range increases with acoustic power output until the echoes begin to occur in a reverberation background. When this happens, the range is said to be *reverberation-limited*. Beyond this value of output power, no increase of range is available, since both echo level and reverberation increase together with increasing power. It follows, as a precept in active-sonar design, that the acoustic output power should be increased until the *reverberation level is equal to the level of the noise background at the maximum useful range of the system*. Unfortunately, although this is a useful general rule, it cannot always be followed because of limitations imposed by the amount of available power or because of interaction effects and cavitation at the sonar projector.

### 13.2 Sonar Prediction

The other broad class of problems has to do with *performance prediction*. Here the sonar system is of fixed design—and, indeed, may already be in operational use—and it is desired to predict its performance under a variety of conditions. Alternatively, if field trials of a system have already been made, it may be necessary to account for the performance that has been achieved—a kind of “postdiction,” in which a numerical explanation is required for the results obtained. This class of problems normally requires solving the appropriate form of the sonar equation for the parameter containing the range. The passive-sonar equation may be written

$$\begin{aligned} \text{TL} &= \text{SL} - \text{NL} + \text{DI} - \text{DT} \\ &= \text{FM} \end{aligned}$$

where the sum of the parameters on the right is called (Table 2.2) the *figure of merit* FM for the particular target referred to in the parameter SL. Similarly,

the active-sonar equation for a noise background may be written as

$$\begin{aligned} 2(TL) &= SL + TS - NL + DI - DT \\ &= FM \end{aligned}$$

where FM is the figure of merit for the target implied by the value used for the parameter TS. The prediction of range requires the conversion into range of the value of transmission loss that is equal to the figure of merit. The conversion demands a specification of the propagation conditions, such as layer depth and propagation path, under which the equipment will be, or has been, used. With reverberation backgrounds, the transmission loss is usually the same for both the target and reverberation, and the range occurs implicitly in the terms  $10 \log A$  or  $10 \log V$ , representing in decibel units the reverberating area or volume, respectively.

### **13.3 The Optimum Sonar Frequency**

**Existence of an optimum frequency** When range calculations at different frequencies are made for a sonar set of a particular design and for some specified propagation and target conditions, it is often found that the range has a maximum at some particular frequency. This frequency is the *optimum frequency* for the particular equipment and target characteristics being considered. At the optimum frequency, a minimum figure of merit is required to reach a given range. Hence, the optimum frequency is a function of the detection range as well as the specified set of medium, target, and equipment parameters. If the operating frequency is made much higher than optimum, the absorption of sound in the sea reduces the range; if the operating frequency is made much lower than optimum, a number of other parameters become unfavorable and act to reduce the range. Examples of such parameters are the directivity index, background noise, and detection threshold (through a necessarily smaller bandwidth at the lower frequencies), all of which conspire to reduce the system figure of merit at low frequencies.

Curve AA of Fig. 13.1 shows a range-versus-frequency plot for a hypothetical sonar. If, by some means, the figure of merit of this sonar is raised by an amount that is the same for all frequencies, the range-frequency curve is shifted to BB. Although the range is increased at all frequencies, the optimum frequency, at which the maximum range occurs, has become lower. The locus of the peak values of a series of such curves gives the best frequency to use to obtain a desired range. Its shape and position depend on the system figure of merit and on the transmission loss and, more importantly, on how both vary with frequency.

**Illustrative example** The determination of the optimum frequency can best be illustrated by an example. Consider a passive listening system that employs a line hydrophone 5 ft long. It is desired to find the optimum frequency for

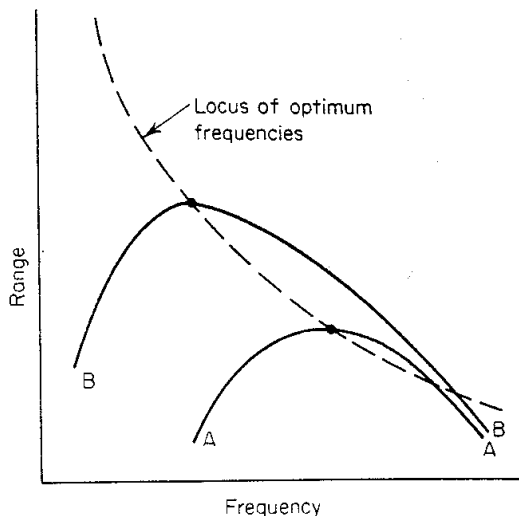


**Fig. 13.1** Range as a function of frequency for two sonar systems of different figures of merit.

the detection of a freighter traveling at a speed of 10 knots. The noise background is taken to be the ambient noise of the sea in sea state 3 (wind speed 11 to 16 knots), and the detection threshold is zero decibels. Let the transmission loss be determined by spherical spreading plus absorption according to the relationship  $TL = 20 \log r + 0.01f^2r \times 10^{-3}$ , where  $f$  is the frequency in kilohertz and  $r$  is the range in yards. Based on this expression, Fig. 13.2 shows curves of TL as a function of frequency for a number of different ranges. Superposed on the same plot is the line AA, equal to FM at different frequencies for the particular problem at hand, using appropriate values of the parameters.\* At any frequency, the detection range is that for which  $TL = FM$ . This range has a maximum, for the curve AA, of 6,000 yd and occurs at 5 kHz. This is the optimum frequency for the assumed conditions. At this frequency, the slopes of the line AA and of an interpolated member of the family of TL curves are equal. At frequencies different from 5 kHz, the range is less, becoming reduced to 5,000 yd at both 2 and 10 kHz. If, by redesigning the system, the FM is increased by an amount that is constant with frequency, the line AA might be shifted to BB; the range will be increased to 19,500 yd and the optimum frequency lowered to 1.7 kHz. If the redesign is such as to change the slope of the FM curve, an altogether new optimum frequency will be obtained.

**Analytic method** When, as in the example just given, the transmission loss can be expressed as a particular function of range for the conditions of interest, the optimum frequency can be found analytically. In the equality  $TL = FM$ , the maximum (or minimum) range is obtained by differentiating both sides with respect to frequency and setting  $dr/df$  equal to zero. With the preceding expression for TL, we would have

$$TL = 20 \log r + 0.01f^2r \times 10^{-3} = FM$$

\* SL: Table 10.2; NL: Fig. 7.5; DI: Fig. 3.6; DT = 0.

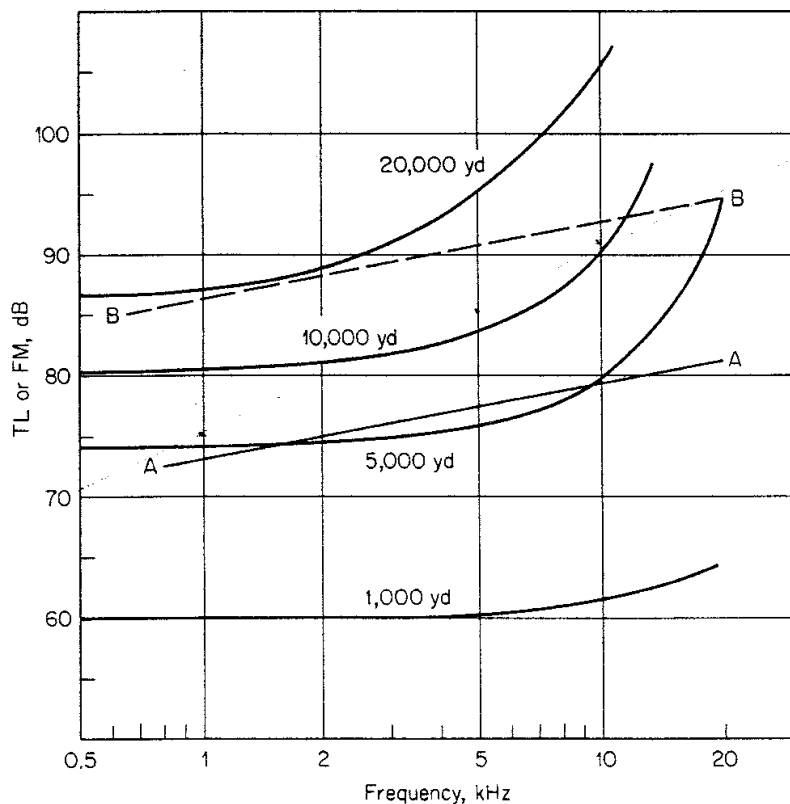


**fig. 13.2** Curves of transmission loss and figure of merit as a function of frequency.

On differentiating and placing  $dr/df = 0$ , we obtain

$$0.02f_0 r_0 \times 10^{-3} = \frac{d(\text{FM})}{df}$$

where  $f_0$  = optimum frequency

$r_0$  = maximum range

$d(\text{FM})/df$  = rate of change of FM with frequency, dB/kHz

In terms of the more conventional unit of decibels per octave of frequency, we can write

$$\left. \frac{d(\text{FM})}{df} \right|_{\text{db/octave}} = \frac{f_0}{\sqrt{2}} \left. \frac{d(\text{FM})}{df} \right|_{\text{db/kHz}}$$

since the octave whose geometric mean frequency is  $f_0$  is  $f_0/\sqrt{2}$  Hz wide. It therefore follows that

$$\frac{0.02}{\sqrt{2}} f_0^2 r_0 = \frac{d(\text{FM})}{df}$$

and the optimum frequency becomes

$$f_0 = \left[ \frac{70.7}{r_0} \frac{d(\text{FM})}{df} \right]^{1/2}$$

where  $d(\text{FM})/df$  is the rate of change of FM with frequency in units of decibels per octave, and  $f_0$  and  $r_0$  are in units of kilohertz and kiloyards, respectively. Since for a passive system

$$\text{FM} = \text{SL} - \text{NL} + \text{DI} - \text{DT}$$

it follows that

$$\frac{d(\text{FM})}{df} = \frac{d(\text{SL})}{df} - \frac{d(\text{NL})}{df} + \frac{d(\text{DI})}{df} - \frac{d(\text{DT})}{df}$$

so that the quantity  $d(\text{FM})/df$  is the sum, with due regard for sign, of the rates of change with frequency of the sonar parameters of which it is composed. Considering the example given above (Fig. 13.2),  $d(\text{FM})/df$  would be found to be approximately equal to  $-6 + 5 + 3 + 0 = +2$  dB/octave. On substituting in the above expression for  $f_0$  and taking  $r_0 = 6,000$  yd,  $f_0$  becomes equal to 5.3 kHz. In echo ranging, where the two-way transmission loss is involved, the expression for  $f_0$  becomes

$$f_0 = \left[ \frac{35.4}{r_0} \frac{d(\text{FM})}{df} \right]^{1/2}$$

The optimum frequency accordingly depends upon the frequency variation of all the sonar parameters and is especially sensitive to the frequency variation of the absorption coefficient. It is not sharply defined, but is the peak of a broad maximum extending over a frequency range of several octaves. The optimum frequency may be defined in terms other than range, as, for example, search rate or processing time, as discussed by Stewart, Westerfield, and Brandon (1). For reverberation backgrounds, the figure of merit is itself a function of range, and the optimum frequency is not as easily determined. Normally, an optimum frequency does not exist in reverberation-limited systems since the frequency-dependent absorption coefficient is ordinarily the same for the echo and for the reverberation background.

An extended discussion of the subject is given by Horton (2), who can be credited with having first recognized the existence of optimum frequencies in sonar applications. More recently, Stewart, Westerfield, and Brandon (3) have published curves of optimum frequency versus maximum range for active sonar detection using more recent expressions for attenuation as a function of frequency.

### 13.4 Applications of the Sonar Equations

#### Sonar Problem Solving

The following are some examples of how the sonar equations may be used to solve problems in a number of different applications of sonar. The examples given and the conditions assumed do not necessarily have any practical significance, but are selected more or less at random to illustrate how the equations

are used in some specific problems concerning the many modern uses of sonar.

The approach to problem solving by means of the sonar equations is to select the equation appropriate to a particular problem and then to solve it for the unknown parameter in terms of the other parameters which are either specifiable or can be selected, with more or less uncertainty, from specified conditions on which they depend. Typical values for nearly all conditions of interest can be found in curves or tables given in earlier chapters.

In an actual design problem the usually straightforward computation should be accompanied by a plot of echo or signal level, together with the reverberation and noise masking levels, as a function of range. Such a plot will indicate most strikingly how the range, determined by intersection of the curves of signal and background, will vary with changes in level. This plot will lend confidence to the numerical computations. Once the range is determined, other quantities of perhaps greater significance, such as area searched per unit time, can be readily computed.

#### **Active Submarine Detection**

**PROBLEM:** An echo-ranging sonar mounted on a destroyer has a power output of 1,000 watts at a frequency of 8 kHz. Its DI is 20 dB and it uses a pulse length of 0.1 second, with a receiving bandwidth of 500 Hz. Find the range at which it can detect a beam-aspect submarine at a depth of 250 ft in a mixed layer 100 ft thick when the ship is traveling at a speed of 15 knots. Detection is required 50 percent of the time, using incoherent processing, with a probability of 0.01 percent of occurrence of a false alarm during the echo duration.

**SOLUTION:** The active-sonar equation, solved for TL, is

$$TL = \frac{1}{2}(SL + TS - NL + DI - DT)$$

SL is given by Fig. 4.4, using  $DI_T = 20$  dB, as 221; by Table 9.3,  $TS = 25$ ; by Fig. 11.11 and reducing from 25 kHz by assuming  $-6$  dB/octave spectral slope,  $NL = +53 + 20 \log(25/8) = +63$ ;  $DI = +20$ ; by Fig. 12.6,  $d = 15$  and  $DT = 5 \log(15 \times 500/0.1) = +24$ . Therefore  $TL = \frac{1}{2}(179) = 90$ . Referring to Fig. 6.7b, for a layer depth of 100 ft, and assuming that the transmission is the same as that for a source depth of 50 ft, the range corresponding to this value of TL is 5,500 yd.

#### **Passive Submarine Detection**

**PROBLEM:** A submarine radiating a 500-Hz line component at a source level 160 dB crosses a convergence zone. Another submarine, located 30 miles away, listens with a nondirectional hydrophone. Assuming a noise background equivalent to that of the deep sea in sea state 3, how long an observation time will the second submarine need to detect the first if it uses incoherent (energy) processing in a receiver band 100 Hz wide and if a detection probability of 50 percent, with a 1 percent false-alarm probability, is satisfactory?

**SOLUTION:** When solved for the parameter of interest, the passive-sonar equation is

$$DT = SL - TL - NL + DI$$

SL is given as 160; TL is taken as being equal to spherical spreading to 30 miles plus a convergence gain of 10 dB, or  $TL = 20 \log(30 \times 2,000) - 10 = +86$ ; by Fig. 7.5, NL = 66; DI = 0 for a nondirectional hydrophone. Therefore DT = +8. By the formula,  $DT = 5 \log(dw/t)$ , with  $w = 100$  (given) and  $d = 6$  (Fig. 12.7), we find an observation time of  $t = 15$  seconds. The signal energy must therefore be integrated for this length of time in order for detection to occur at the required probability levels.

### Minesweeping

**PROBLEM:** A minesweeper tows behind it, for the purpose of sweeping acoustic mines, a broadband sound source having a source spectrum level of 150 dB in a 1-Hz band. The mines to be swept are sensitive to noise in the band 100 to 300 Hz, and are suspected to be set to be actuated when the level of noise in this frequency band is 40 dB above the spectrum level of the ambient-noise background in coastal waters at a wind speed of 30 to 40 knots. If spherical spreading describes the transmission loss, at what range will the minesweeper sweep (actuate) these mines?

**SOLUTION:** Solving the passive equation for TL, we have

$$TL = SL - NL + DI - DT$$

Since the spectrum of the broadband source is 150 dB, the level in the sensitive frequency band of the mines is  $SL = 150 + 10 \log 200 = 173$ ; by Fig. 7.8, NL = +84; DI = 0 is implied by the nature of the problem; DT = 40 is given. Therefore,  $TL = 49$ . For spherical spreading, this corresponds to a swept range of 280 yd.

### Depth Sounding

**PROBLEM:** A fathometer transducer is mounted on the keel of a destroyer and is pointed vertically downward. It has a DI of 15 dB with a source level of 200 dB at a frequency of 12 kHz. Assuming that reflection takes place at the sea bottom with a reflection loss of 20 dB, at what speed of the destroyer will the echo from the bottom in 15,000 ft of water be equal to the self-noise level of the ship in the 500-Hz receiving bandwidth of the fathometer receiver?

**SOLUTION:** Because reflection at the sea bottom has been postulated, the actual source can be replaced by an image source in the bottom at a range equal to twice the water depth. The transmission loss then will be

$$TL = 20 \log 2d + 2\alpha d \times 10^{-3} + 20$$

where  $d$  is the water depth in yards. With  $d = 5,000$  yd and  $\alpha$  taken at 1 dB/kyd,  $TL = 110$  dB. The appropriate form of the sonar equation is

$$SL - TL = NL + 10 \log w - DI$$

where  $NL + 10 \log w$  is the noise level in the bandwidth  $w$  of the receiver. Solving for the unknown parameter,

$$NL = SL - TL - 10 \log w + DI$$

With  $SL = 200$  dB (given),  $10 \log w = 10 \log 500 = 27$  dB,  $DI = 15$  dB, we find  $NL = 78$  dB at 12 kHz. This would correspond at 25 kHz to a value of  $NL = 78 - 20 \log(25/12) = 72$  dB. Referring to Fig. 11.13, the ship speed at which the 25-kHz isotropic self-noise level is 72 dB is 25 knots.

### Mine Hunting

**PROBLEM:** A mine of average aspect lies on a sand bottom. It is desired to detect the mine at a slant range of 100 yd by means of an active sonar located 20 yd from the bottom. If a pulse length of 10 ms is used, what horizontal beam width will be required if detection can be achieved at a detection threshold of zero decibels?

**SOLUTION:** The sonar equations for a reverberation background are

$$\begin{aligned} SL - 2TL + TS &= RL + DT \\ RL &= SL - 2TL + S_s + 10 \log A \\ A &= \Phi r \frac{ct}{2} \end{aligned}$$

Solving for  $A$  and eliminating common terms from the first two expressions, we obtain

$$10 \log A = TS - S_s - DT$$

By Table 9.3, we estimate  $TS = -17$  dB; by Fig. 8.27 and estimating for a grazing angle equal to  $\sin^{-1}(20/100) = 12^\circ$ ,  $S_s = -37$  dB;  $DT$  is given as zero. Therefore  $10 \log A = 20$  dB and  $A = 100$  yd $^2$ . Solving the third equation for  $\Phi$ , with  $A = 100$ ,  $r = 100$ , and  $ct/2 = 1,600 \times 0.01/2 = 8$  yd, we find  $\Phi = 1/8$  rad =  $7.2^\circ$ . By Table 8.1, this would require a horizontal line transducer 11 wavelengths long.

### Explosive Echo Ranging

**PROBLEM:** A 1-lb charge is used as a sound source for echo ranging on a submarine. Find the detection range of a bow-stern aspect submarine target in a background of deep-sea ambient noise in sea state 6. Detection is required 90 percent of the time with a 0.01 percent chance of a false alarm in the echo duration of 0.1 second. A nondirectional hydrophone with a 1-kHz bandwidth centered at 5 kHz is used for reception. Let the source and receiver depths be 50 ft in a mixed layer 100 ft thick, and let the target depth be 500 ft.

**SOLUTION:** For short transient sources, the source level is

$$SL = 10 \log E - 10 \log t_e$$

where  $E$  = source level in terms of energy density

$t_e$  = echo duration

Solving the active sonar equation for  $TL$ , we obtain

$$TL = \frac{1}{2}(10 \log E - 10 \log t_e + TS - NL + DI - DT)$$

The quantities  $t_e$  and  $DI$  are given in the problem statement. Since the source is broadband, and using Fig. 4.19 at 5 kHz,  $E = 180 + 10 \log 1,000 = 210$  dB in the 1-kHz receiver bandwidth; by Table 9.3,  $TS = 10$  dB; by Fig. 7.5,  $NL = 57$  dB; by formula,  $DT = 5 \log(dw/t)$ , using  $d = 25$  (Fig. 12.7),  $w = 1,000$  and  $t = 0.1$ ,  $DT = 27$ .  $DI = 0$  (given). With these values  $TL$  is found to be 73 dB. By Fig. 6.6c, the range is 2,600 yd at 2 kHz; by Fig. 6.7c, the range is 2,200 yd at 8 kHz; on interpolating for 5 kHz, the estimated range becomes 2,400 yd. However, it should be remarked that in this problem the range is likely to be reverberation-limited instead of noise-limited.

### Torpedo Homing

**PROBLEM:** In an active homing torpedo, a detection range of 3,000 yd is required on an average-aspect submarine. A detection threshold of 30 dB is needed to

cause the torpedo to "home" on its target. If the torpedo transducer is a plane-piston array restricted to a diameter of 15 in., how much acoustic power output is needed at an operating frequency of 40 kHz? The transmission loss is assumed to be adequately described by spherical spreading and absorption at a temperature of 60°F, and the self-noise is to be taken equal to the ambient noise of the deep sea in sea state 6.

**SOLUTION:** Solving the active-sonar equation for SL, we obtain

$$SL = 2TL - TS + NL - DI + DT$$

From Fig. 5.8, TL = 95 dB; by Table 9.3, TS = 15 dB; by Fig. 7.5, NL = 41 dB; by Fig. 3.6, DI = 30 dB; DT = 30, given. We therefore find SL = 216 dB, and by Fig. 4.4, with  $DI_T = 30$ , the required power output is found to be 30 watts.

### Fish Finding

**PROBLEM:** A compact school of fish containing 1,000 members, each averaging 20 in. in length, lies 100 yd from a fishing boat equipped with a fish-finding sonar. What will be the level of the echo from this school of fish at a frequency of 60 kHz, assuming that the transducer has a beam pattern broad enough to contain the entire school? The sonar projector radiates 100 acoustic watts of power and is a circular plane array 10 in. in diameter.

**SOLUTION:** The echo level is the left-hand side of the active-sonar equation and is equal to  $SL - 2TL + TS$ . By Fig. 3.6, DI = 30 dB; by Fig. 4.4, SL = 221 dB; with spherical spreading and absorption, using  $\alpha = 19 \text{ dB/kyd}$  (Fig. 5.5), TL = 42 dB; by Fig. 9.19, TS =  $-31$  for a single fish 20 in. long; and for 1,000 fish, TS =  $-31 + 10 \log 1,000 = -1$  dB. The echo level becomes 136 dB re 1  $\mu\text{Pa}$ . If the transducer has a receiving sensitivity of  $-170$  dB, the echo would appear as a voltage equal to  $136 - 170 = -34$  dB re 1 volt across the transducer terminals.

### Communication

**PROBLEM:** In the sofar method of aviation rescue, a downed aviator drops a 4-lb explosive charge set to detonate on the axis of the deep sound channel. How far away can the detonation be heard by a nondirectional hydrophone, also located on the axis of the deep sound channel, at a location of moderate shipping in sea state 3? The receiving system uses a frequency band centered at 150 Hz and squares and integrates the received signals for an interval of 2 seconds—an interval estimated to be sufficiently long to accommodate all the energy of the signal. A signal-to-noise ratio of 10 dB is required for detection.

**SOLUTION:** Solving the passive equation for TL, we obtain  $TL = SL - NL + DI - DT$ . Recognizing the existence of severe signal distortion, we convert to energy-density and obtain  $TL = 10 \log E_0 - (NL + 10 \log t) + DI - DT$ , where  $E_0$  is the source energy-density and  $t$  is the integration time. From Fig. 4.19,  $10 \log E_0$  for a 4-lb charge at 150 Hz = 207 dB; by Fig. 7.5, NL = 68; DI = 0 dB, DT = 10 dB, and  $10 \log t = 3$  dB are given in the problem statement. Therefore, TL = 126 dB. To convert to range, we write (Sec. 6.2)  $TL = 10 \log r + 10 \log r_0 + \alpha r \times 10^{-3}$ . Assume that  $r_0 = 10,000$  yd. Using the formula (Sec. 5.3)  $\alpha = 0.1f^2/(1 + f^2)$ , where  $f$  is in kilohertz, we find that  $\alpha = 0.00225 \text{ dB/kyd}$ . Drawing a curve of TL against  $r$ , we read off, for TL = 126, the value of  $r = 8,000$  kyd, or 4,000 miles.

### An Echo Repeater

**PROBLEM:** It is desired to build an echo repeater which when suitably triggered will return a simulated echo to a range of 1,000 yd equal in level to the echo from a beam-aspect submarine at the same range. The echo that it must simulate is obtained with a sonar having a source level of 210 dB re 1  $\mu\text{Pa}$ . How much acoustic power should it radiate? How much electric power will be needed to drive it if its projector has an efficiency of 50 percent? How much power should it radiate at 100 yd? Assume spherical spreading plus absorption at the rate of 3 dB/kyd.

**SOLUTION:** The echo level is  $EL = SL - 2(TL) + TS = 210 - 2(20 \log 1,000 + 3) + 25 = 109$  dB re 1  $\mu\text{Pa}$ , where 25 is the target strength of the submarine (Table 9.3). The simulated echo level is  $SL' - TL = SL' - (20 \log 1,000 + 3) = SL' - 63$ . Equating the two levels, we find  $SL' = 172$ . By the relation  $SL' = 171.5 + 10 \log P + DI_T$ , we find  $10 \log P = \frac{1}{2}$ ; hence,  $P = 1$  watt, if  $DI_T = 0$ . At 50 percent efficiency, 2 electric watts will be needed to drive it. At 100 yd, the acoustic power rises to 220 watts! *Note:* A practical echo repeater would simulate much more than the level of the echo; its echoes would have a doppler shift and other realistic echo characteristics.

### 13.5 Concluding Remarks

A few words of caution must be said regarding the “pat” solutions of the problems just given. Everything depends upon the values of parameters assumed in their solution. These values are always accompanied by uncertainties arising from two sources: first, uncertainty that the conditions assumed are really those of actual interest and importance; and second, uncertainty that, under these conditions, the chosen values of the parameters are valid.

The first of these two sources of uncertainty involves the specification of the conditions, some natural, some of human origin, that the engineer feels will be representative of the environment and the target in and against which the system must operate. Here extreme cases will often need to be worked out in the hope that conditions beyond the selected limits will not be of practical significance. The second uncertainty arises from the presently crude state of underwater sound as a body of quantitative knowledge. Even when all the necessary nature and target conditions are specified, the associated acoustic parameter is likely to be uncertain by several decibels or more, simply because of insufficient quantitative information.

### REFERENCES

1. Stewart, J. L., E. C. Westerfield, and M. K. Brandon: Optimum Frequencies for Sonar Detection, *J. Acoust. Soc. Am.*, **33**:1216 (1961).
2. Horton, J. W.: Fundamentals of Sonar, *U.S. Nav. Inst.*, art. 7C-3, 1957.
3. Stewart, J. L., E. C. Westerfield, and M. K. Brandon: Optimum Frequencies for Noise Limited Active Sonar Detection, *J. Acoust. Soc. Am.*, **70**:1336 (1981).

## ***self-noise of ships, submarines, and torpedoes: self-noise levels***

Self-noise differs from radiated noise in that the measurement hydrophone is located on board the noise-making vessel and travels with it, instead of being fixed in the sea at a location some distance away. Although the fundamental causes of noise are the same, the relative importance of the various noise sources is different. Moreover, in self-noise, the paths by which the noise reaches the hydrophone are many and varied and play a dominant role in affecting the magnitude and kind of noise received by the hydrophone on the moving vessel.

In the sonar equations, radiated noise occurs as the parameter *source level* SL, where it is the level of the source of sound used by passive sonar systems. By contrast, self-noise is a particular kind of background noise occurring in sonars installed on a noisy vehicle; in the sonar equations, self-noise occurs quantitatively as the *noise level* NL. Self-noise exists in fixed hydrophones as well, whenever the manner of mounting or suspension creates noise of its own.

Self-noise is one of many different kinds of undesired sound in sonar and originates in a variety of ways. Figure 11.1 illustrates the interrelationships of the various kinds of sonar backgrounds. Self-noise refers to those noise sources between the dashed lines.

Self-noise depends greatly upon the directivity of the hydrophone, its mounting, and its location on the vehicle. On surface ships, the sonar transducer is located in a streamlined dome projecting below the keel of the ship. On older submarines, the principal passive

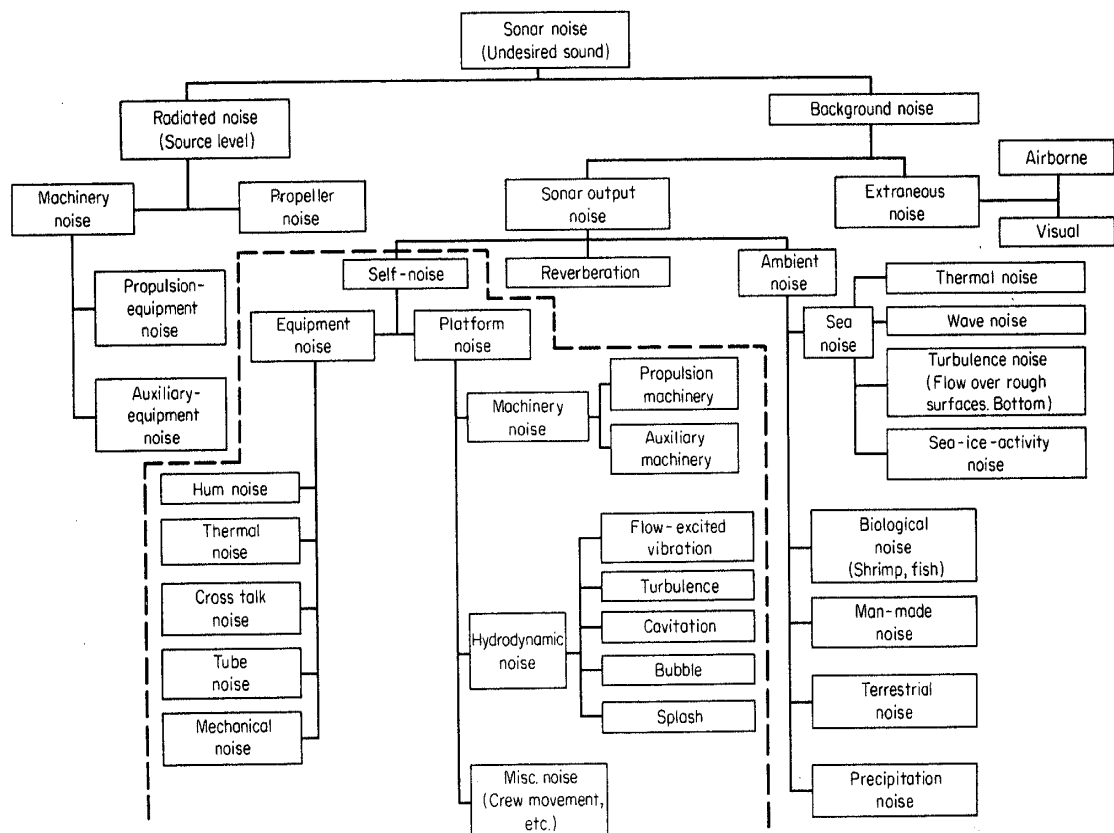


**fig. 11.1** Interrelationships of various sonar noise sources. (Ref. I.)

sonars were the JT and JP sonars, having horizontal line transducers placed topside toward the bow of the vessel; on modern submarines, a large portion of the bow of the vessel is taken over by the sonar transducer. Acoustic homing torpedoes often have their transducers in the nose of the torpedo and face forward in the direction of travel. On all these vessels, the sonar transducer is placed as far forward on the vessel as is practicable, so as to be removed as much as possible from the propulsion machinery and the propeller noises of the vessel. Figure 11.2 is a pictorial view of the location of the sonar transducer on these three kinds of vessels.

### 11.1 Self-Noise Measurements and Reduction

Self-noise measurements on these vehicles have been made in the past with sonar hydrophones of varying sizes and shapes and hence of differing directivity. In order to make these various measurements compatible with one another, and at the same time make them useful for other directional sonars, it is convenient to express self-noise levels as *equivalent isotropic levels*. The equivalent isotropic self-noise level is the level that would be indicated by a nondirectional hydrophone of sensitivity equal to that of the directional transducer with which the self-noise measurements were made. If the noise level measured with a directional hydrophone is  $NL'$ , the equivalent isotropic level is

$$NL = NL' + DI$$

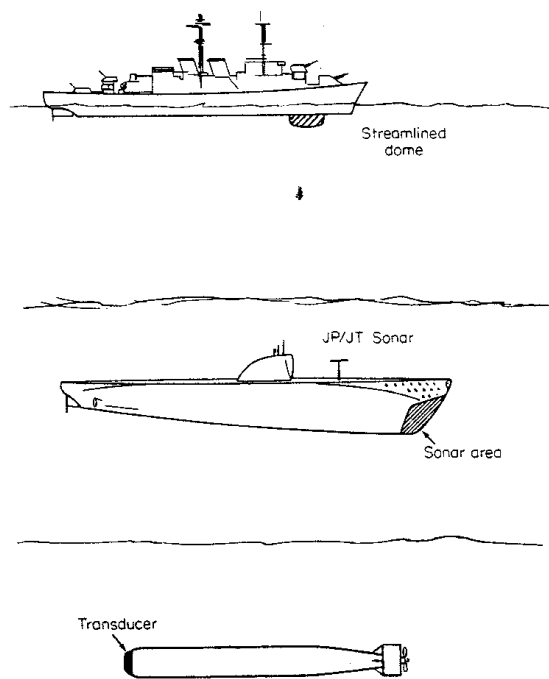


**fig. 11.2** Locations of the sonar transducer aboard surface ships, submarines, and torpedoes.

In converting to equivalent isotropic levels, therefore, the measured levels  $NL'$  are corrected for directivity by applying the directivity index of the measurement hydrophone. The isotropic level  $NL$  is the level required for use in the sonar equations previously written.

Although this convention serves to bring self-noise measurements made on the same kind of vessel with different transducers into some degree of agreement, some hesitancy must be felt when applying self-noise data obtained with one sonar to a sonar of different design, directivity, mounting, and location on the same vehicle. Self-noise, like ambient noise, is seldom isotropic in its directional and coherence characteristics, and the DI is not always a satisfactory measure of the discrimination of transducers against it. Often noise coming from a single direction will predominate, and the DI will be almost meaningless as a measure of the discrimination against noise. In torpedoes, for example, it has been found that the front-to-back ratio of the transducer beam pattern—defined as the difference in response between the forward and backward directions—is a more useful measure of the discrimination against self-noise than the directivity index. In general, it is necessary to understand the sources and paths of the prevailing kind of noise before transferring self-noise data from one sonar to another. When this knowledge is lacking, the equivalent isotropic self-noise level must be used in the sonar equations, with recognition of its crude nature and of the likelihood that large errors may occur in some circumstances.

## **11.2 Sources and Paths of Self-Noise**

The three major classes of noise—*machinery noise*, *propeller noise*, and *hydrodynamic noise*—apply for self-noise as well as for radiated noise. The sound and vibration generated by each kind of noise reach the sonar hydrophone through a variety of different acoustic paths.

Figure 11.3 shows a surface ship and the paths in the ship and through the sea by which sound generated at the propeller and in the machinery spaces of the ship can reach the sonar hydrophone. Path A is an all-hull path by which the vibration produced by the machinery, the propeller shaft, and the propeller itself reach the vicinity of the sonar array at a forward location. Here it may be reradiated by the hull or, more importantly, cause vibration of the wall of the streamlined dome and the mounting of the hydrophone array. Path B is an all-water path leading directly from the ship's propellers to the hydrophone. Path C shows propeller noise backscattered by volume scatterers located in the volume of the sea. In general, these scatterers are the same as those causing volume reverberation. Path D is the bottom-reflected or scattered path by which propeller noise can reach the vicinity of the hydrophone. This path is likely to be a major contributor to self-noise on surface ships operating in shallow water.

For submarines and torpedoes, the upward analog of Path D—reflection and scattering from the sea surface—is, similarly, an important acoustic path

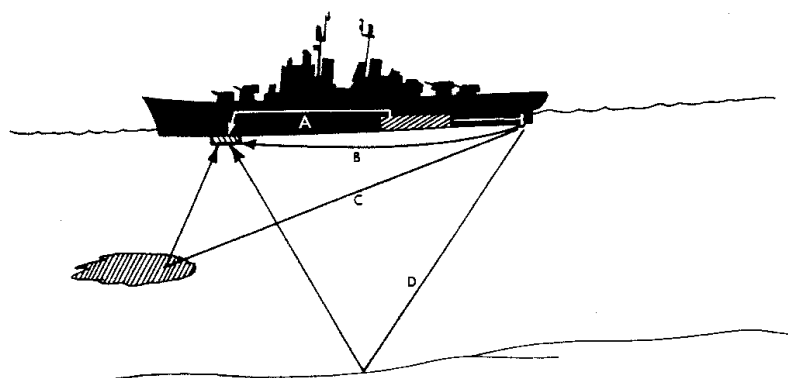


**fig. 11.3** Paths of self-noise on a surface ship.

when the vehicle is running at a shallow depth. An example of this kind of path is shown in Fig. 11.4. This is an artist's conception of a torpedo with three areas of forward and side scattering on the surface by which sound from the propellers can reach hydrophones located near the nose. Of all the vessels of interest, the self-noise of torpedoes long ago received a considerable amount of analytical attention, probably because of the relative ease of performing experiments upon them. For example, torpedoes were "run" with and without propellers, in water and in air, and with various modifications, all during the World War II years (2).

Both machinery noise and propeller noise are prominent contributors to self-noise. The self-noise contribution of the vessel's machinery occurs principally at low frequencies as tonal components in the overall noise. Unlike other kinds of noise, machinery noise tends to be relatively independent of speed,

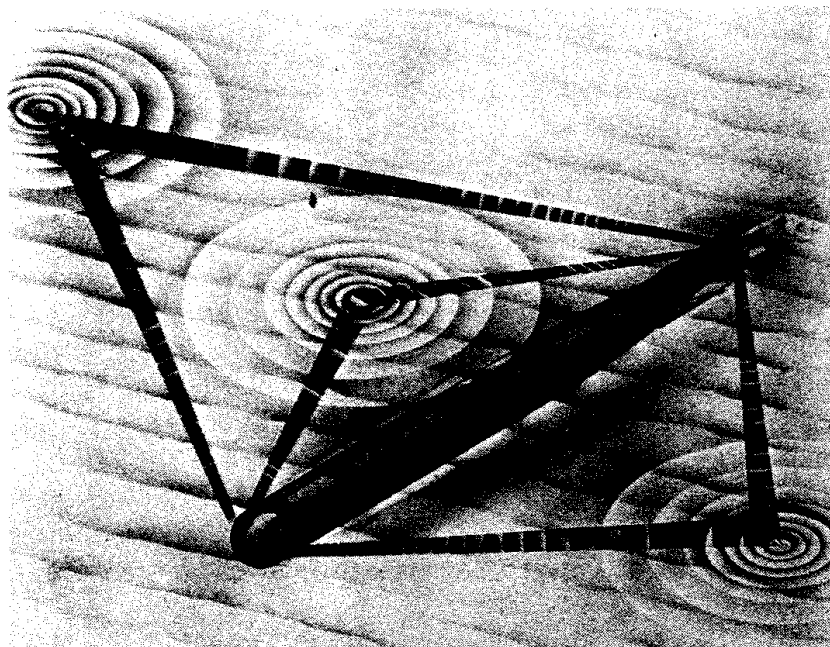


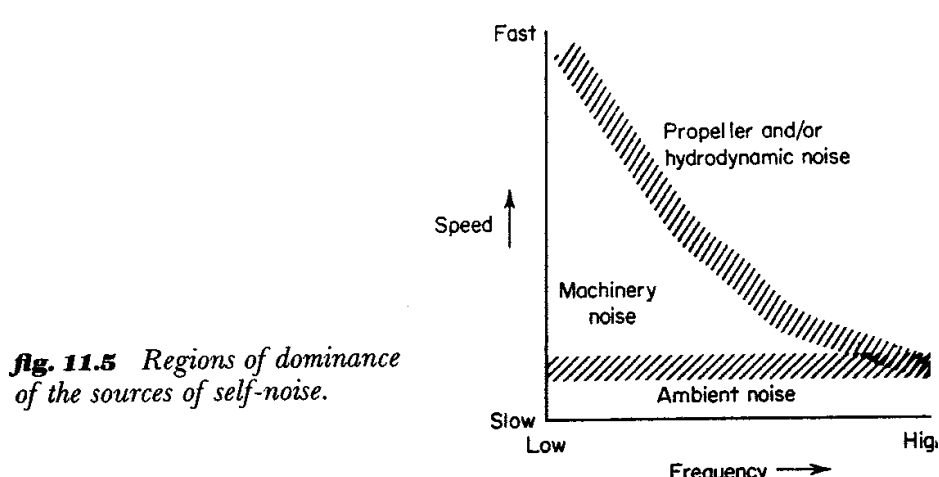
**fig. 11.4** Surface-reflected paths of torpedo self-noise.

since much of it originates in the constant-speed auxiliary machinery of the vessel. Hence, at slow speeds, where other kinds of noise are of low level, the noise of the vessel's auxiliary machinery is often a troublesome source of self-noise. In the wartime JP equipment on submarines operating below 5 knots, it was observed that listening was affected by power operation of the bow and stern planes, the steering machinery, and certain rotating equipment aboard the submarine. At higher speeds, propeller noise becomes the dominant contributor to self-noise under conditions of high frequencies, shallow water depths, and stern bearings. At high speeds also, the many and diverse forms of hydrodynamic noise become important.

Hydrodynamic noise includes all those sources of noise resulting from the flow of water past the hydrophone and its support and the outer hull structure of the vessel. It includes the turbulent pressures produced upon the hydrophone face in the turbulent boundary layer of the flow (flow noise), rattles and vibration induced by the flow in the hull plating, cavitation around appendages, and the noise radiated to a distance by distant vortices in the flow. Hydrodynamic noise increases strongly with speed, and because the origin of this noise lies close to the hydrophone, it is the principal source of noise at high speeds whenever the noise of propeller cavitation—itself a form of hydrodynamic noise—is insignificant.

The relative importance of the sources of self-noise can be illustrated by showing their areas of dominance on a plot having vessel speed and frequency as the two coordinates (Fig. 11.5). At very low speeds, the hydrophone "sees" the ambient noise of the sea itself. With increasing speed, machinery noise tends to dominate the low-frequency end of the spectrum, and a combination of propeller and hydrodynamic noise becomes important at high frequencies. The scales and the crosshatched regions separating the noise sources in Fig. 11.5 vary with the kind of vessel and with the directivity, location, and mounting arrangement of the measuring hydrophone.

Hydrodynamic noise occurs in stationary hydrophones as well as in those on moving vessels. Around the case of an acoustic mine on a rocky bottom, for example, a swift tidal current was found (3) to produce pressures of 1,000



dyn/cm<sup>2</sup> in the 1- to 4-Hz band and 50 dyn/cm<sup>2</sup> in the 5- to 32-Hz band on the crystal hydrophone of the mine.

Electrical noise is occasionally bothersome in sonar sets as a form of self-noise. However, its existence indicates a pathological condition whose cure is normally obvious. Except under exceptionally quiet conditions, as at times in the Arctic under a uniform ice cover, electrical noise is not a serious problem in well-designed sonars.

### 11.3 Flow Noise

A particular kind of hydrodynamic noise has been called *flow noise*. Because it is amenable to theoretical and experimental study and has an urgent application to the reduction of cabin noise inside aircraft, it has received relatively abundant attention in the literature. Flow noise, in actual practice, may be said to be what is "left over" after all other sources of hydrodynamic noise aboard the vessel have been accounted for or removed.

Flow noise consists of the pressures impinging upon the hydrophone face created by turbulent flow in the turbulent boundary layer about the hydrophone. Figure 11.6 illustrates a rigid, flat boundary containing a flush-mounted pressure hydrophone, above which a viscous fluid is flowing. Between the free stream and the boundary lies a turbulent boundary layer within which fluctuating pressures are created and are transmitted to the hydrophone in the boundary. Although these turbulent pressures are not true sound, in that they are not propagated to a distance, they form what has been termed "pseudosound" (4) and give rise to a fluctuating noise voltage at the output of the pressure hydrophone. In the following sections, some of the salient characteristics of flow noise will be briefly summarized. The interested reader is referred to the quoted literature for more detailed information; a good tutorial paper on the subject has been published by Haddle and Skudrzyk (5).

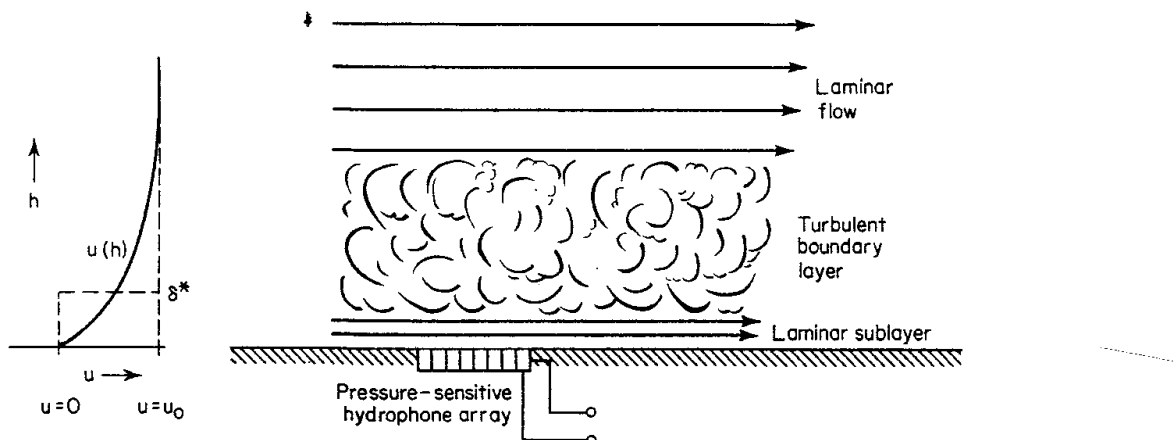


**fig. 11.6** Flow structure in a fluid moving over a stationary surface. The diagram at the left shows the variation of flow velocity with height above the boundary.

**Total fluctuating pressure** The rms pressure  $p_{\text{rms}}$  on the boundary due to the turbulent flow is related to the free-stream dynamic pressure by

$$\frac{p_{\text{rms}}}{\frac{1}{2} \rho u_0^2} = 3 \times 10^{-3} \alpha$$

where  $\rho$  = fluid density

$u_0$  = free-stream flow velocity

$\alpha$  is a constant, called the Kraichman constant after a pioneering investigator of turbulent flow, ranging from 0.6 to 4 in different measurements using different data (6), but centering roughly about unity. In any one series of measurements,  $\alpha$  is found to be a constant over a wide range of flow velocities.

**Spectrum of flow noise** The power spectrum of flow noise, or the distribution in frequency of the mean-squared pressure, is found to be flat at low frequencies and to slope strongly downward at high frequencies at the rate of  $f^{-3}$ , or as -9 dB/octave, as shown by the flow-noise spectra observed with a flush-mounted hydrophone  $\frac{1}{2}$  in. in diameter inside a rotating cylinder (6). The transition frequency  $f_0$  between the flat and the sloping portions of the spectrum is given by

$$f_0 = \frac{u_0}{\delta}$$

where  $\delta$  is the thickness of the boundary layer. Since the flow velocity is a continuous function of distance away from the wall (Fig. 11.6), the boundary-layer thickness is more exactly expressed by the "displacement thickness"  $\delta^*$  such that

$$\delta^* u_0 = \int_0^\infty u(h) dh$$

where  $u(h)$  is the flow velocity at a distance  $h$  normal to the wall. The actual boundary layer is thus replaced by an equivalent layer (in the above sense) of zero velocity (that is, the layer is attached to the wall) and of thickness  $\delta^*$ . It is found that  $\delta = 5\delta^*$ , approximately. In experiments of Skudrzyk and Haddle (6),  $\delta^*$  was found to be 0.153 in. at a speed  $u_0$  of 20 ft/s and 0.135 in. at 60 ft/s.

**Variation with speed** At frequencies less than  $f_0$ , the spectrum level of flow noise varies as the cube of the speed  $u_0$ ; at frequencies appreciably greater than  $f_0$ , it varies as the sixth power of the speed. The latter rate of increase amounts to 18 dB per speed doubled. This is equivalent to a straight-line rate-of-rise of 1.8 dB/knot in the speed range 10 to 20 knots, in approximate agreement with observations of self-noise on large naval surface ships over this range of speed.

A practical way to measure flow noise without the contaminating effects of machinery noise is to use a sinking streamlined body as a test vehicle or,

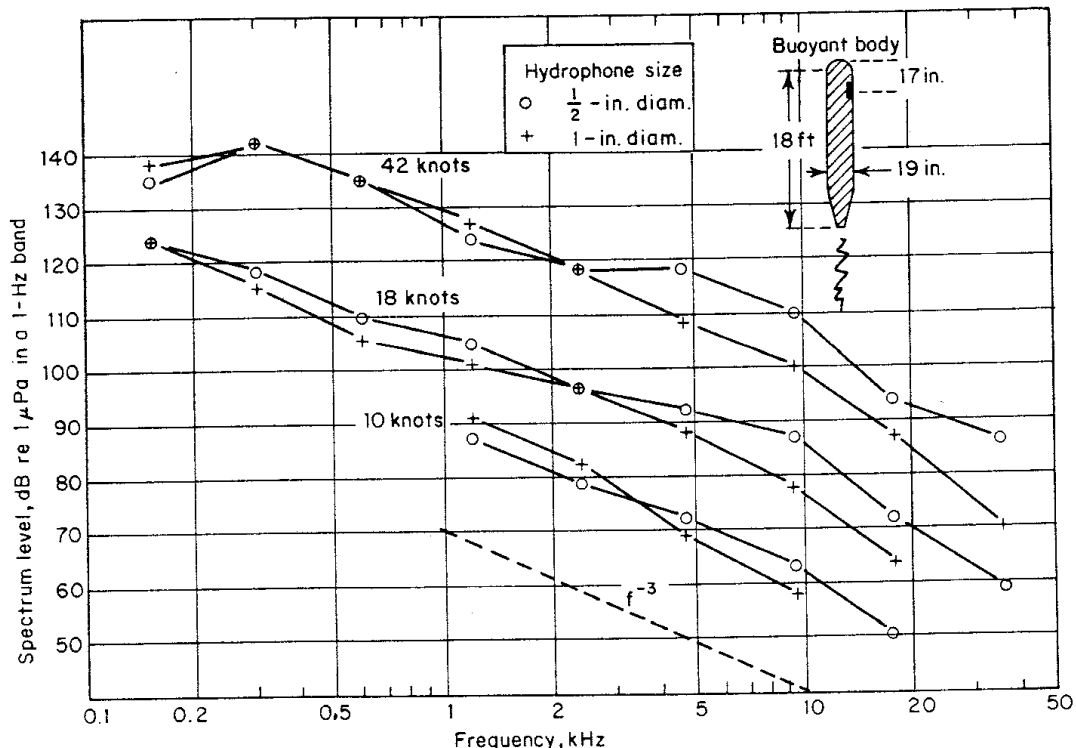


**fig. 11.7** Flow-noise levels on a buoyant body at different speeds for two hydrophone diameters. (Ref. 5.)

alternatively, to use a buoyant body rising under its own buoyancy from a depth in the sea. Examples of measurements by Haddle and Skudrzyk (5) on a buoyant streamlined body are shown in Fig. 11.7. The data shown here were obtained with two hydrophones of different sizes placed 17 in. behind the nose of the body 18 ft long. The results roughly confirm the 18-dB increase per speed doubled just described, as well as the  $f^{-3}$  variation with frequency. It will be noted that doubling the hydrophone diameter from  $\frac{1}{2}$  to 1 in. decreased the flow-noise level by some 5 to 10 dB near the high-frequency end of the spectrum.

**Effect of surface roughness** Flow noise across a rough surface has been studied by Skudrzyk and Haddle (6) using a rotating cylinder having different degrees of surface roughness obtained by cementing grit of various sizes to the outside. It was found that at 24 kHz the noise produced by the roughnesses became equal to the flow noise across the perfectly smooth surface when the height of the roughness was such that

$$h = \frac{0.06}{u'}$$

where  $u'$  = flow velocity, knots

$h$  = roughness height, in.

Surfaces need not be optically smooth to be considered "smooth" for flow noise, but must be free of roughnesses high enough to extend above the laminar boundary layer (Fig. 11.6) and affect the turbulent flow.

**Coherence of turbulent pressures** Measurements of the longitudinal and transverse correlation of the pressures due to the flow have been made with small hydrophones in the walls of tubes and pipes (7, 8). In a frequency band  $w$  hertz wide centered at frequency  $f$ , the crosscorrelation coefficient of the pressure measured at two points along the walls at distance  $d$  apart has been found (7) to be

$$\rho(d, w) = \rho(s) \frac{\sin(\pi wd/u_c)}{\pi wd/u_c} \cos 2\pi s$$

where  $s$  is the (nondimensional) Strouhal number defined as

$$s = \frac{fd}{u_c}$$

in which  $u_c$  is the "convection velocity" equal to the velocity at which turbulent patches are carried past the hydrophone by the flow.  $u_c$  is somewhat smaller than the free-stream velocity  $u_0$  and varies from  $0.6u_0$  to  $1.0u_0$ , depending on the frequency  $f$ . The correlation function  $\rho(s)$  has been found experimentally to be

$$\rho_L(s) = e^{-0.7|s|}$$

for longitudinal separations  $d$  parallel to the flow (7), and

$$\rho_T(s) = e^{-5|s|}$$

for transverse separations at right angles to the flow (8).

**Discrimination against flow noise** A pressure hydrophone of finite size, that is, an array, will discriminate against flow noise to an extent determined by the spatial correlation coefficients  $\rho_L$  and  $\rho_T$  described above. The magnitude of this discrimination  $\beta$  is defined as

$$\beta = \frac{R'}{R}$$

where  $R'$  is the mean-square voltage output of an array placed in a flow noise field, and  $R$  is the mean-square voltage output of a very small pressure hydrophone placed in the same noise field and having a sensitivity equal to the plane-wave axial sensitivity of the array. The quantity  $10 \log(1/\beta)$  is equivalent to the *array gain for flow noise*; the ratio  $\beta$  measures the reduction of flow noise experienced by an array of pressure-sensitive elements relative to the noise pickup of a single small element. The magnitude of the discrimination factor  $\beta$  has been worked out by Corcos (8) for circular and square arrays, on

the assumption that the correlation function in oblique directions to the flow is given by the product of the two principal components  $\rho_L$  and  $\rho_T$ . White (9) has extended this work by means of a unified theory and has carried out computations for rectangular arrays with long side parallel to and perpendicular to the direction of flow. Figure 11.8 shows the quantity  $\beta$  as defined above for a rectangular array (after White) and for a circular array (after Corcos). For a large square hydrophone of side equal to  $L$ , Corcos shows that

$$\beta = \frac{0.659}{\gamma^2}$$

where  $\gamma = 2\pi f L/u_c$ , and for a circular hydrophone of radius  $r$ ,

$$\beta = \frac{0.207}{\gamma^2}$$

where  $\gamma = 2\pi f r/u_c$ . In both cases,  $\gamma$  must be much greater than unity.

**Comparison with an isotropic sound field** If now we define a *convection wavelength*  $\lambda_c$  such that

$$\lambda_c = \frac{u_c}{f}$$

in analogy with acoustic wavelength

$$\lambda_s = \frac{c}{f}$$

where  $c$  is the velocity of sound, the expression for the discrimination factor of a circular hydrophone becomes

$$\beta = 0.207 \left( \frac{\lambda_c}{2\pi r} \right)^2$$

For isotropic noise, the corresponding expression is (Table 3.2)

$$\beta_{iso} = \left( \frac{\lambda_s}{2\pi r} \right)^2$$

where  $10 \log (1/\beta_{iso})$  is the ordinary directivity index of the circular array. Comparing the two expressions, we observe that  $\beta = 0.207 \beta_{iso}$  when the appropriate wavelength is used for the two types of noise. But  $\lambda_c$  is far smaller than  $\lambda_s$  for vehicles traveling in the sea; the ratio  $\lambda_c/\lambda_s$  is approximately equal to the Mach number of the vessel, or the ratio of its speed to the speed of sound in the sea. Since  $M$  is a small quantity, it follows that the discrimination against flow noise for a large array of a given size is much greater than it is for isotropic noise. In terms of the Mach number  $M$ ,

$$\frac{\beta}{\beta_{iso}} = 0.207 M^2$$

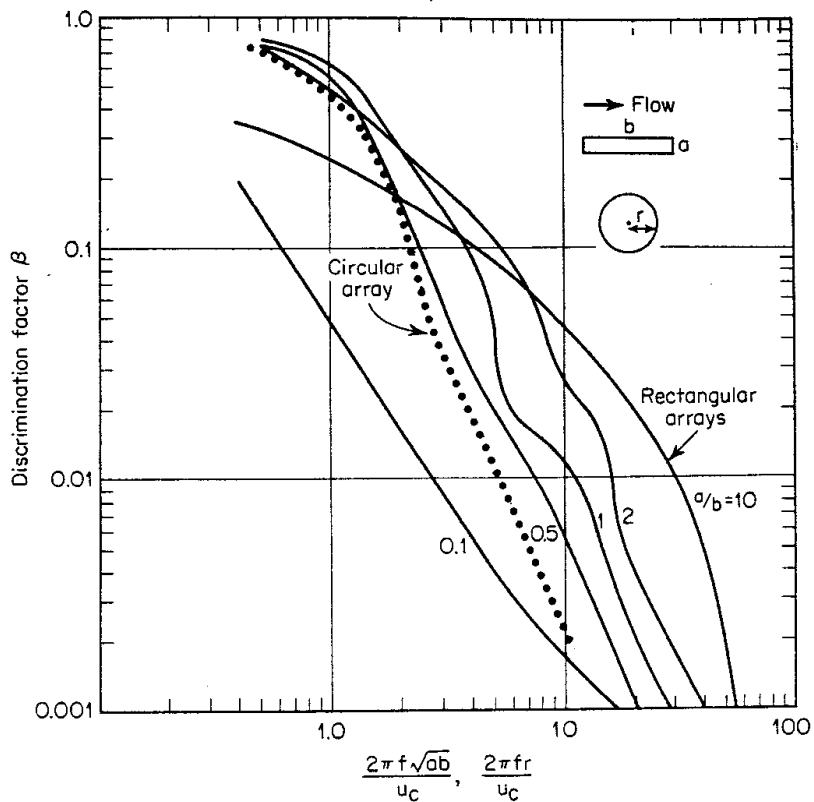


**Fig. 11.8** Discrimination of rectangular and circular arrays against flow noise. The sides  $a$  and  $b$  of the rectangular array are oriented perpendicular and parallel to the direction of flow, respectively. [After White (9) and Corcos (8).]

As an example, at a speed of 2.0 knots,  $M = 7 \times 10^{-4}$ , and the quantity  $10 \log (\beta/\beta_{iso})$  becomes  $-70$  dB. In actual practice on a moving vessel, however, such great benefits of large arrays for reducing noise are not likely to be observed because of the existence of sources of noise other than the turbulent-flow pressures on the rigid wall. If the wall is not rigid, resonant wall vibration as well as the radiated noise of distant turbulence are likely to overwhelm the ideal flow-noise pressures picked up by a large array.

#### 11.4 Flow-Noise Reduction

For a well-streamlined body with a minimum of vanes, fins, and appendages, various techniques can be used to reduce the sensitivity to flow noise of a hydrophone located on it. Some of these are:

1. *Make the hydrophone larger.* The effect of a larger hydrophone size is to cause the turbulent flow-noise pressures to average out as a result of their small correlation distance. In wind and water tunnels, reductions of 40 dB or more can be obtained in this way, but on moving bodies such great reductions

cannot be achieved, as mentioned above, because of effects such as shell vibration and the flow-excited radiated noise of fins and other appendages.

2. *Move the hydrophone forward.* A forward location is quieter than one toward the tail of the body because of a thinner boundary layer and a greater distance from the noise-producing surfaces at the rear of the body. The quietest place of all is right at the nose itself in the region of the "stagnation point" where the flow separates; here the boundary layer is absent, and flow noise is received only by radiation and diffraction around the front of the body. Figure 11.9 shows diagrammatically the output of a hydrophone at a forward location and one toward the stern of a streamlined body in the turbulent boundary layer. A hydrophone located at the nose of a blunt-nose body picks up the radiated noise of the turbulence by diffraction around the nose, as shown by the experimental work of Lauchle in a water tunnel (10).

3. *Remove the hydrophone from the turbulent boundary layer.* This can be done by placing it in a cavity or in a recess in the wall. The effect here is to allow the positive and negative pressures to cancel out, in much the same way as with a hydrophone of larger size.

4. *Eject polymer fluids.* The ejection of very small amounts of polymers consisting of long-chain unbranched molecules of high molecular weight (about  $10^6$ ) has been found effective in the reducing fluid drag in pipes and on moving bodies. The drag-reduction process appears to be one of thickening the laminar sublayer (Fig. 11.6) and thereby reducing self-noise by separating the hydrophone from the turbulent boundary layer, as in technique 3 above. The concentration of polymer found to be effective is very low (100 parts per million or less), and, on a moving body, ejection can be achieved through holes in the nose. Long-chain polymers are viscoelastic fluids that cause the solution to be non-Newtonian: that is, they cause the shear stress to be no longer linearly proportional to the rate of shear. Just how their effect on

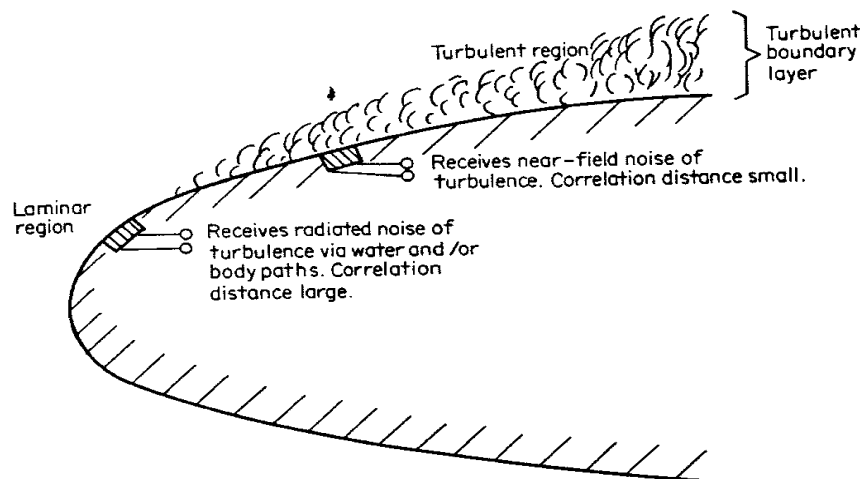


**fig. 11.9** Response of a hydrophone on a streamlined body in the laminar and turbulent regions of the flow.

the boundary layer occurs is uncertain; one idea is that the long-chain molecules tend to align themselves parallel to the wall and thereby inhibit the formation of stress differences normal to the wall that result in the formation of turbulence. On a self-propelled body like a torpedo, polymer ejection has an added beneficial effect on self-noise in that, by reducing drag, the propulsive power needed to achieve a given speed is less; in other words, the machinery and propeller contributions to self-noise are lower. The hydrodynamic effects of polymer ejection have received much attention in the literature, and an excellent review paper by Hoyt (11) containing many references has been published.

### **11.5 Domes**

It was observed many years ago that large reductions of what is now known as hydrodynamic noise could be achieved on surface ships by surrounding the sonar transducer by a streamlined housing. Such housings are called *sonar domes*. They reduce self-noise by minimizing turbulent flow, by delaying the onset of cavitation, and by transferring the source of flow noise to a distance from the transducer. Sonar domes were originally spherical in shape but were soon streamlined into a teardrop shape to prevent the occurrence of cavitation at high speeds. Some examples of domes used during World War II are shown in Fig. 11.10. The domes in this figure are of all-metal construction and have a thin stainless steel window to permit the ready exit and entrance of sound out of and into the transducer inside. Modern domes are constructed of rubber reinforced with thin steel ribs. Many have baffles, such as those seen in Fig. 11.10a and 11.10c, to reduce machinery and propeller noises coming from the rear.

The acoustic and mechanical requirements of dome design are severe. The dome must be acoustically transparent, so as to introduce only a small transmission loss and produce no large side lobes in the directivity pattern of the enclosed transducer. The latter requirement means the absence of internal specular reflection from the dome walls. At the same time the dome should be sufficiently streamlined to delay the onset of cavitation on its surface beyond the highest speed reached by the vessel and should be of sufficient mechanical strength to resist the hydrodynamic stresses upon it when under way. These requirements are to a large extent mutually incompatible.

Expressions have been obtained theoretically (12, 13) and generally verified experimentally for the transmission loss and the specular reflection produced by a dome of a given material and wall thickness on a transducer of given frequency, directivity, and position in the dome. Both the transmission loss and reflectivity of the dome increase with frequency and with the thickness and density of the dome walls. Internal reflections in domes can be greatly reduced by increasing the horizontal, and particularly the vertical, curvature of the dome walls. Hence, for both acoustic and hydrodynamic reasons, sonar domes employ materials as thin and light as possible formed into curved

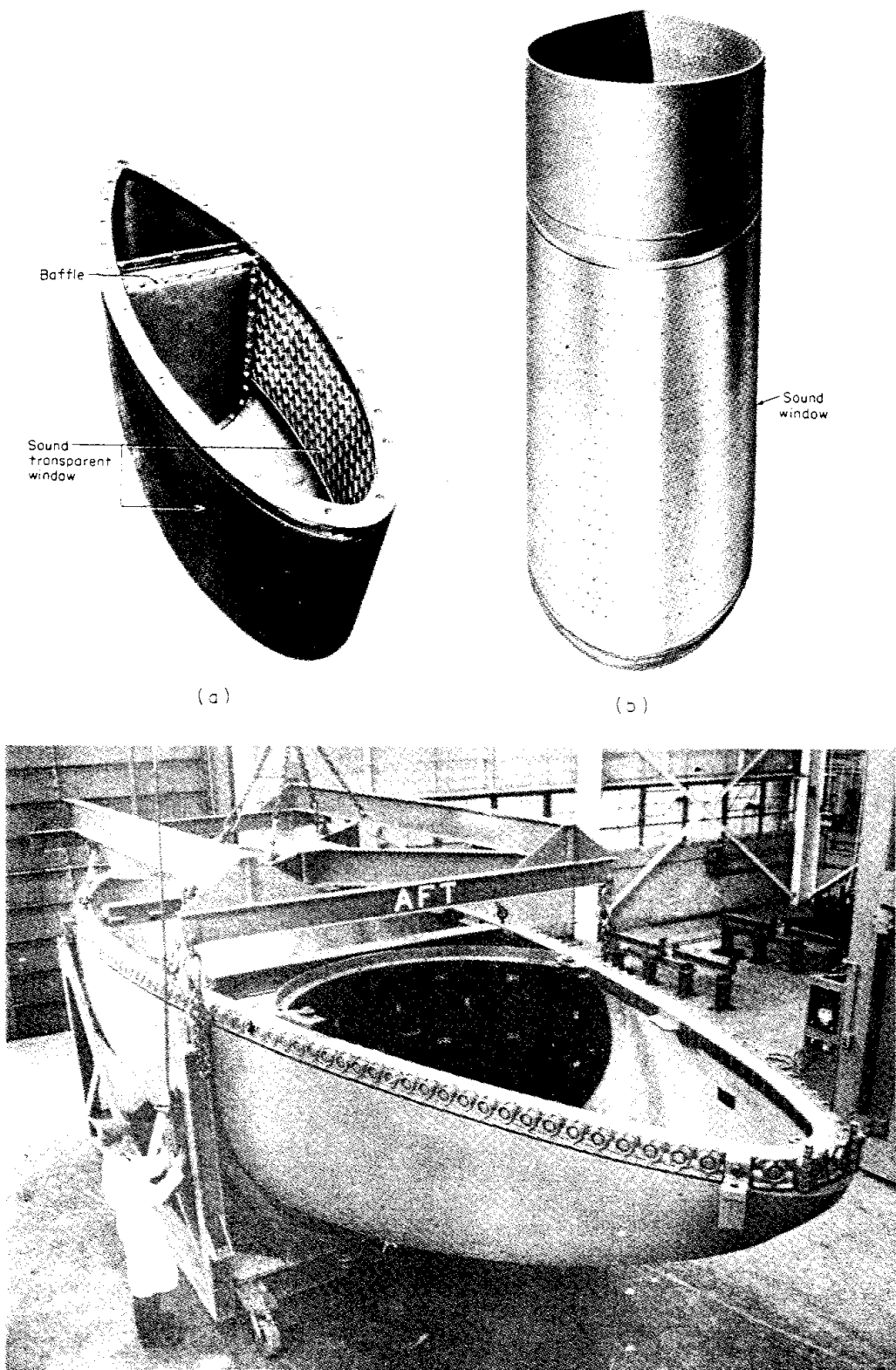


**fig. 11.10** Photographs of streamlined domes. (a) QBF dome. (b) QGA dome. (c) A modern surface ship dome; note the curved baffle in this dome. (a, b, from Ref. 14; c, courtesy B. F. Goodrich Co., Akron, Ohio.)

streamlined shapes. The acoustic windows of sonar domes used during World War II, like those of Fig. 11.10, ranged from 0.020 to 0.060 in. in thickness (14).

For low self-noise, sonar domes must be kept undamaged and free of marine fouling. A dome with a rough exterior surface will produce a higher flow noise, as well as noise caused by local cavitation at "hot spots" on its surface at the higher speeds of the vessel on which it is mounted.

For many years the sonar domes of surface ships were located aft of the bow, and were retractable for use in shallow water and for ease of dry docking. However, the recent trend toward lower frequencies, higher powers, and larger sizes of modern sonars has required a shift in location and an abandonment of the retractable feature of sonar domes. The dome of the A/N-SQS 26 sonar is located just at the bow and is bulbous in shape to accommodate the tremendous size of the transducer (Fig. 11.11). It is about 50 ft long, 10 ft high, and 18 ft wide, and weighs some 40 tons. Compared to older installations, the location and size of this dome has both benefits and disadvantages. It is as far removed from the propellers as is possible with a hull installation,

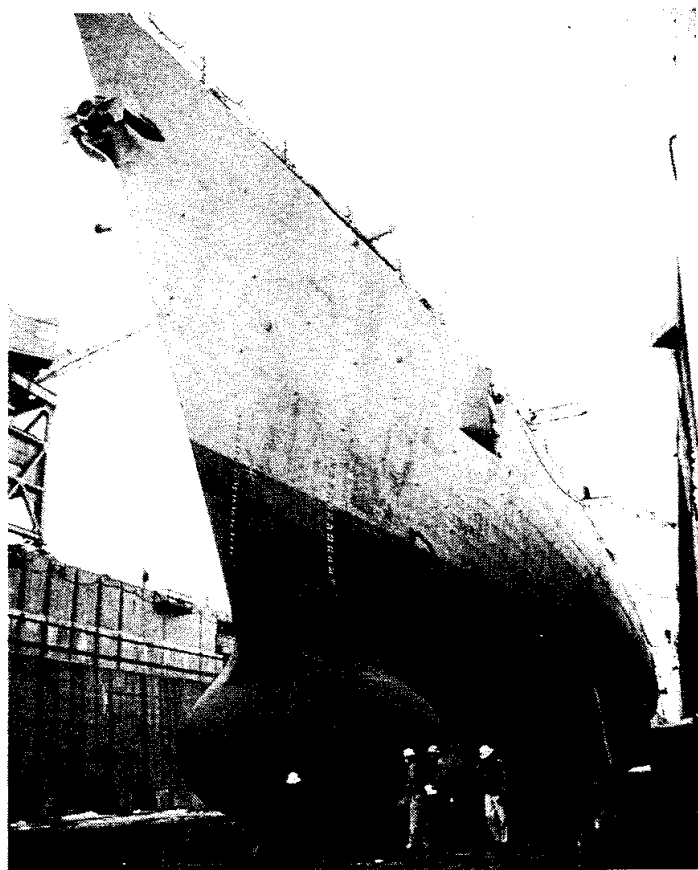


**fig. 11.11** The A/N-SQS 26 pressurized sonar dome with rubber window on the USS "Willis A. Lee" (DL-4) in drydock. (Photo courtesy of B. F. Goodrich Company.)

and so experiences a lower level of propeller noise. The bulbous shape of the bow reduces—rather than increases—the drag of hull in its motion through the water, and is said to reduce pitching of the ship as well. On the other hand, the draft of the vessel is increased, and the drydocking operation is made more complicated. The alternative to such a large dome is to use the sides and length of the vessel to provide the necessary surface area for efficient power radiation and directivity, but the problems of element phasing and interaction in this kind of array are formidable.

### **11.6 Self-Noise of Cable-Suspended and Bottomed Hydrophones**

Hydrophones that are hung from the end of a cable are likely to suffer from a peculiar kind of noise called *strumming* or *flutter* noise. This form of self-noise occurs in a current of water, and is the result of cable vibration induced by the eddies or vortices shed by the cable. This is the “aeolian harp” effect, or the singing of telephone wires in a wind, that has long been known in air acoustics (15). The frequency of vortex shedding is given by the simple expression  $f = Sv/d$ , where  $S$  is the dimensionless “Strouhal number,”  $v$  is the water current speed, and  $d$  is the cable diameter in the units of length of  $v$ . The Strouhal number happens to be a constant equal to 0.18 over much of the range of current speeds and cable sizes occurring in practice. Thus, with a 1-cm-diameter cable in a 1-knot current (51.5 cm/s), the strumming frequency will be 9 Hz. Strumming noise can be readily alleviated by a number of means, including using a faired cable, keeping the natural frequency of cable vibration well separated from the strumming frequency, isolating the hydrophone from the cable (as by such simple means as suspending it from the cable by rubber bands), and employing a hydrophone having an acceleration canceling design.

Another malady of cables is *triboelectric noise* or the spurious voltages resulting from friction (“tribo”) between the cable conductor and the shield. Any motion of the cable tends to produce varying frictional charges in the cable dielectric; these appear as voltages at the end of the cable. They occur in voids or gaps between the conductor and the dielectric that act as variable air capacitors. Triboelectric noise exists whenever the cable is bent or altered in shape; it enhances the effect of cable strumming. It can be alleviated by coating the dielectric with graphite (Aquadag) or by binding the dielectric material tightly to the conductors. This kind of noise has been investigated empirically with various kinds of cables subjected to different kinds of deformation (16), and a number of low-noise cables are commercially available.

Hydrophones resting on the ocean floor are susceptible to the motional effects of water currents flowing past, and around, the hydrophone and its mounting. Strasberg (17) has discussed and made quantitative estimates of the apparent noise caused by the impingement of the turbulent and thermal microstructure carried along by a current and striking a hydrophone. Vorti-

ces and turbulences shed by the hydrophone and its structure are also a form of low frequency nonacoustic noise, as shown by laboratory measurements of McGrath et al. (18). These current-produced pseudonoises make difficult valid measurements of the infrasonic ambient background of the sea, especially in shallow water, and require careful design of the hydrophone structure, as well as a thermal shield around the hydrophone for quiet operation at frequencies below 20 Hz.

### **11.7 Self-Noise of Towed Sonars**

A sonar housed in a streamlined body and towed at a depth behind a surface craft (see Fig. 1.2) is subject to a wide variety of self-noise sources. These range from "pure" flow noise—the pressure fluctuations of the boundary layer adjacent to the hydrophone—to vibrations of the towing cable.

Some direct field trials of the noise of hydrophones inside a towed streamlined body of revolution have been made by Nishi, Stockhausen, and Evensen (19). The body they used was 6 ft long and 1½ ft in maximum diameter. A number of small hydrophones 0.07 in. in diameter were placed on it for self-noise measurements at various places along its length. Towing was done by a hydrofoil craft at speeds up to 30 knots. It was found during the field trials that a hydrophone along the side of the body, where the turbulent boundary layer was well developed, picked up mainly flow noise at frequencies above 1 kHz; its levels were not greatly different from those of the buoyant body shown in Fig. 11.7, when allowance is made for hydrophone size. A hydrophone at the nose was found to be quieter than the one located along the side of the body. This sensor picked up the radiated noise of the towing craft, together with the wall vibrations caused by vibrations of the tow cable and the tail-fin structure of the body.

Another kind of towed sonar is a *flexible-line hydrophone array* towed at a considerable distance (up to several miles) behind a surface craft to reduce pickup of the noise from the towing vessel. This is the successor of the "eel" worked on the World War I (Sec. 1.1); more recently towed lines have been extensively used in waterborne seismic prospecting for oil (20). Typically, a seismic "streamer" consists of 24 or more hydrophone groups, each up to several hundred feet long, and having an overall length of about 8,000 feet (21, 22). The hydrophones are placed inside a thin-walled flexible plastic jacket, typically 2½ in. in diameter, filled with a fluid of low specific gravity so as to be nearly neutrally buoyant. In the shallow water of waterborne prospecting, a constant depth is maintained by dynamic controllers or "birds," which themselves are a source of noise for hydrophones near them. Fig. 11.12 shows smoothed measured spectra of a hydrophone group in a streamer towed at two speeds a distance of 1,000 feet behind the towing vessel in sea states 0 to 1. Added for comparison is an average curve of the ambient noise level for a wind speed of 6 knots at seven Pacific Ocean locations, due to Wenz (Fig. 7.8).

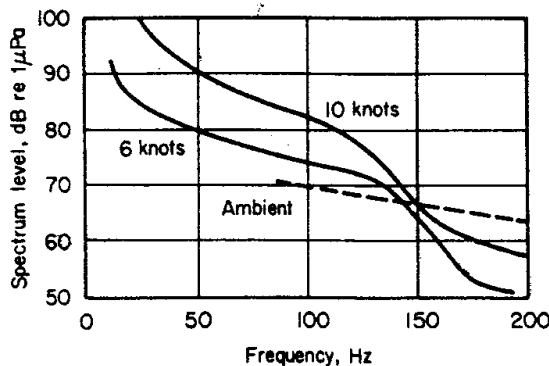


**fig. 11.12** Seismic streamer self-noise spectrum levels at two towing speeds, and the ambient-noise spectrum for a wind speed of 6 knots in shallow water as given by Wenz (Fig. 7.8). (After Ref. 22.)

Although towed arrays do reduce greatly the radiated noise of the ship by means of their distance and directivity, they are subject to various motional effects and to various forms of hydrodynamic noise, including "pure" flow noise. Especially deleterious are the results of vibration induced by towing, which causes effects such as acceleration response in the array hydrophones, hydrostatic pressure changes due to the vertical motion of the array, changing pressures in the oil filling of the flexible hose, and vortex shedding by the vibrating tow cable. Nevertheless, flexible towed-line arrays make possible the rapid exploration for oil in coastal areas and, as passive sonars, provide a capability for listening from surface ships to low frequencies and in stern directions—something that hull-mounted sonars do not possess.

### 11.8 Self-Noise Levels

Figure 11.13 shows equivalent isotropic self-noise levels at 25 kHz on a number of World War II American and British destroyers. These data, taken from

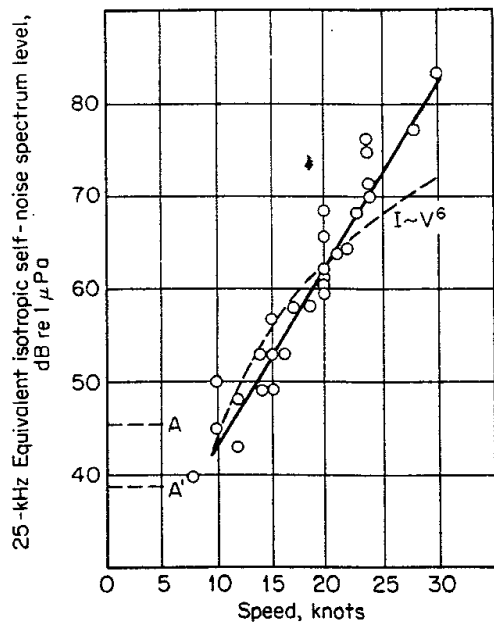


**fig. 11.13** Equivalent isotropic spectrum levels at 25 kHz on destroyers (Ref. 23). The levels A and A' are deep-sea ambient levels at sea states 3 and 6. The dashed curve shows the theoretical variation with speed of flow noise.

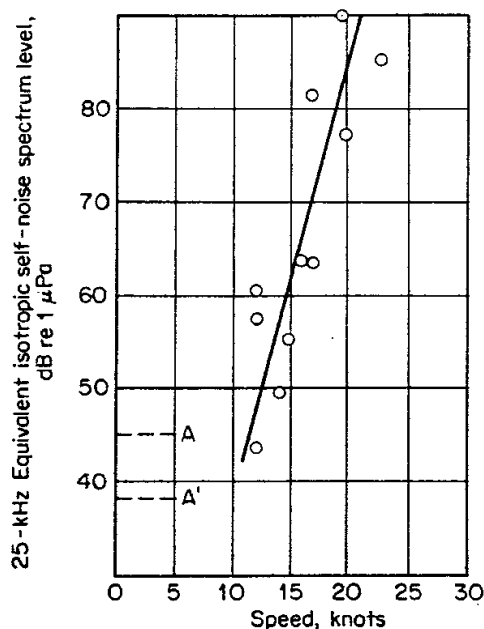
a wartime study of Primakoff and Klein (23), were obtained with various sonar transducers of differing directivity, and have been corrected to equivalent isotropic levels, as discussed above, by allowing for (adding) the directivity index of the transducer. The curved line shows an increase of self-noise intensity as the sixth power of the speed, in agreement with theoretical expectations for the speed variation of flow noise. Although higher noise levels are observed at high speeds, probably because of dome cavitation and other sources of noise, the general agreement suggests the dominance of some form of flow noise in these data at moderate speeds.

Figure 11.14 is a similar plot for small warships of the PC and SC classes and for British DE-type ships and frigates. Here the increase of noise with speed is much more rapid and suggests the dominance of propeller cavitation noise in these smaller ships, on which the sonar dome, its distance from the propellers, and the amount of screening by the hull are all much smaller than on destroyers.

The levels of Figs. 11.13 and 11.14 apply for forward bearings, when the directional transducer in its dome is trained in a forward direction. When it is trained toward the stern of the ship, higher levels are observed, particularly on small ships, due to the noise of the cavitating propeller.

At the lower frequencies more typical of modern destroyers, the same sort of behavior with speed as that shown in Fig. 11.13 is observed. Figure 11.15 is representative of modern destroyer sonars operating at frequencies of 10 kHz and below. At very slow speeds, or when lying to, the sonar self-noise level is close to the ambient background level of the sea in the prevailing sea state. At speeds between 15 and 25 knots the self-noise level increases sharply with speed at the rate of about 1½ dB/knot, and represents the domi-

**fig. 11.14** Equivalent isotropic spectrum levels at 25 kHz on American PC and SC class ships and on British DE types and frigates. A and A' are ambient levels at sea states 3 and 6. (Ref. 23.)



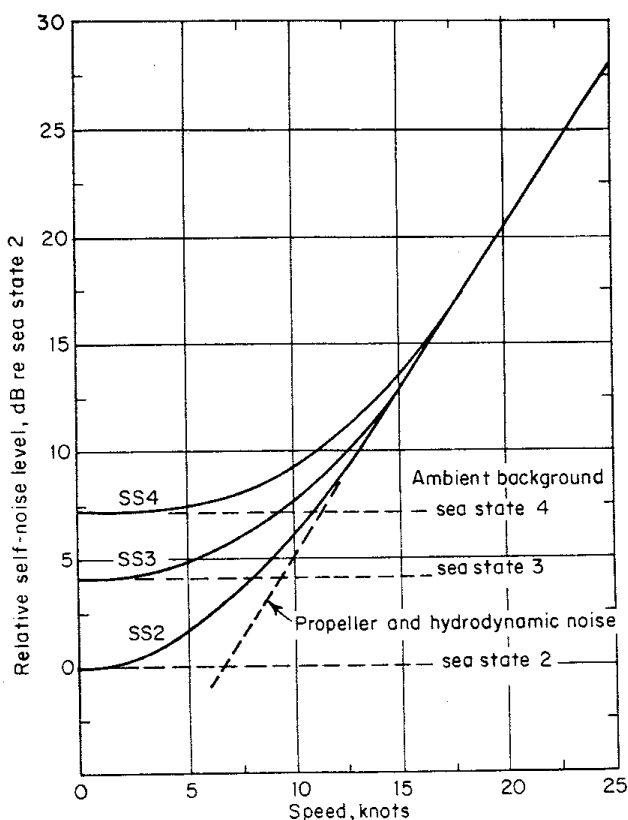


**fig. 11.15** Self-noise levels versus speed on a modern destroyer.

nant contributions of hydrodynamic and propeller noise to the total noise level.

Self-noise levels on submarines are illustrated in Fig. 11.16 *a* and *b*. These show average spectra and the increase of noise with speed measured during World War II with the JP-1 listening equipment. The JP sonar had a 3-ft horizontal line hydrophone mounted on the deck of the submarine forward of the conning tower and could be trained manually so as to listen in different directions. The spectra of Fig. 11.16 *a* are for noisy, average, and quiet installations at a speed of 2 knots. They approximate the levels of deep-water ambient noise at the high-frequency end, but rise more rapidly with decreasing frequency, probably as a result of machinery-noise contributions. The extremely rapid rise with speed suggests the influence of propeller cavitation as the speed increases, as does the fact that the self-noise of the JP-1 sonar decreased with increasing depth of submergence (24). In other submarine sonars, less exposed to cavitation noise, the effect of speed is less marked and approximates the rate of rise of 1½ to 2 dB/knot found on destroyer-like surface ships (Fig. 11.13).

Just as for destroyers, the self-noise of submarines observed with the JP-1 sonar was found to be independent of bearing on forward bearings but to increase sharply as the hydrophone was trained toward the stern. Examples of the "directivity pattern" of self-noise at several speeds are given in Fig. 11.17.

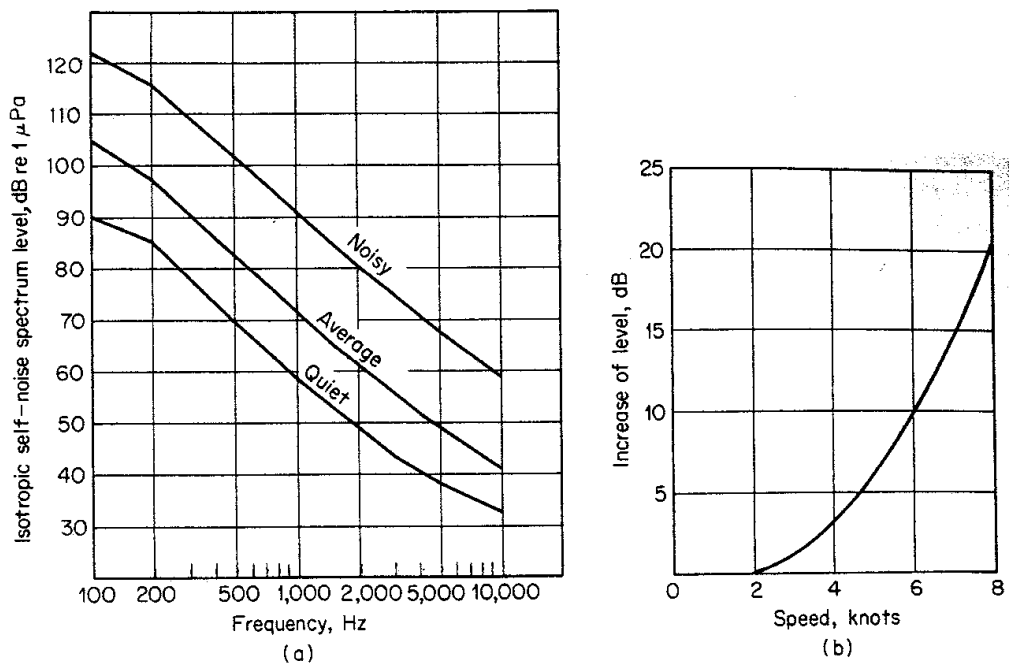


**Fig. 11.16** Average self-noise spectra on submarines: (a) JP-1 data, forward bearings, speed 2 knots, periscope depth. (b) Increase of noise level with speed relative to 2 knots. (Ref. 25, figs. 9 and 10.)

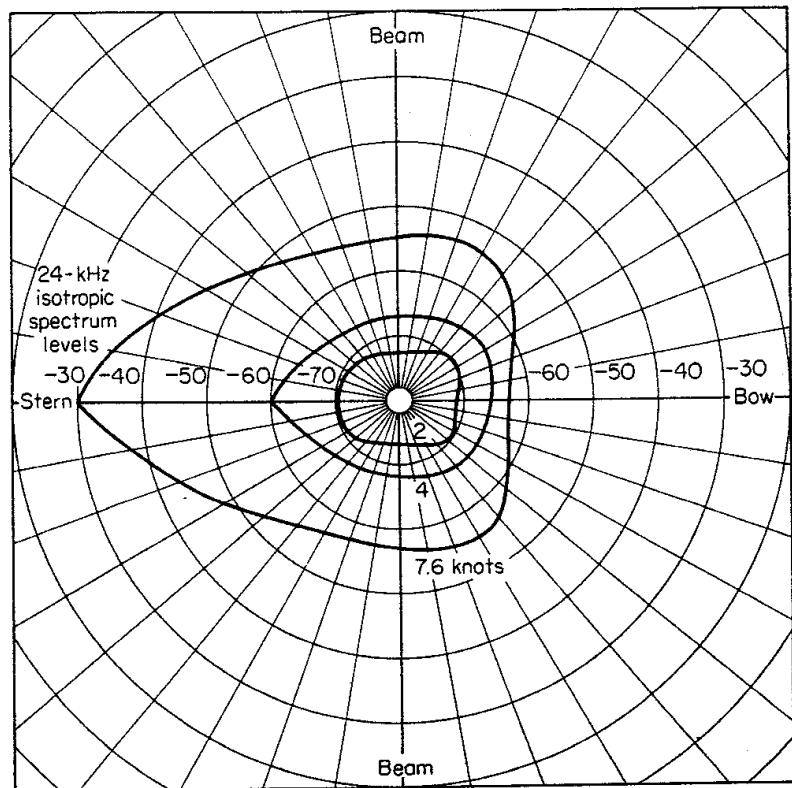


**Fig. 11.17** Directionality of high-frequency self-noise at various speeds. Hydrophone directivity index assumed to be 20 dB. (Ref. 24.)